



PB95-183612

# The John A. Blume Earthquake Engineering Center

Department of Civil Engineering  
Stanford University

---

---

## REGIONAL SEISMIC HAZARD AND RISK ANALYSIS THROUGH GEOGRAPHIC INFORMATION SYSTEMS

by  
**Stephanie A. King**  
and  
**Anne S. Kiremidjian**

This research was partially supported by

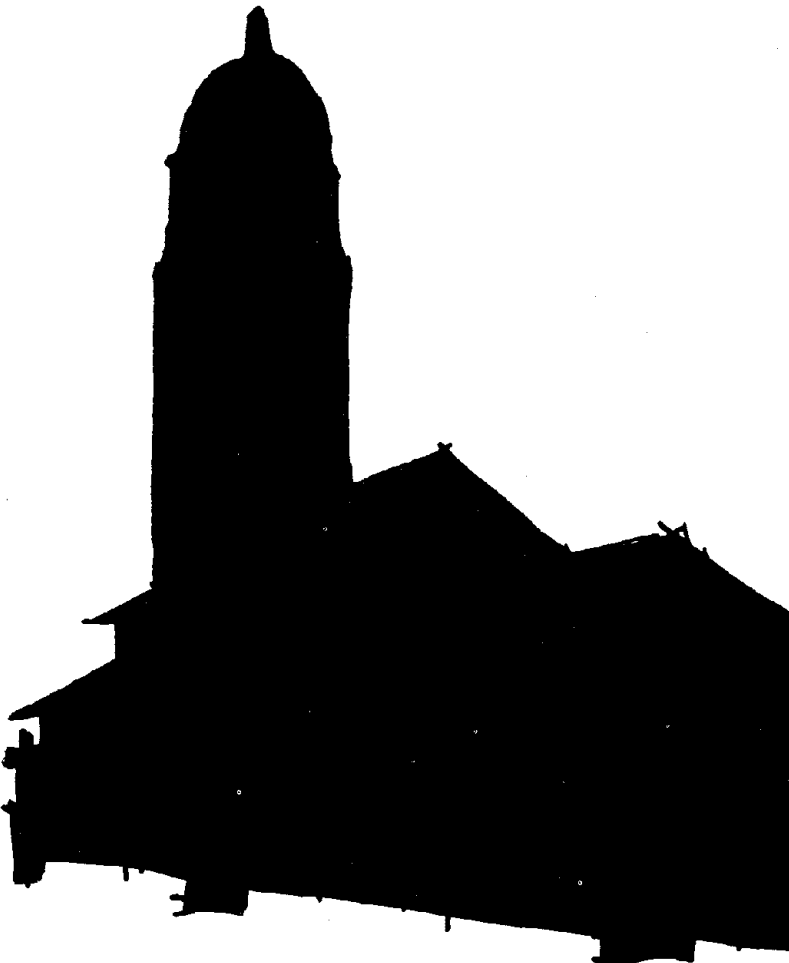
The National Science Foundation  
Grant No. EID-9024032

and

The John A. Blume Earthquake  
Engineering Center  
Stanford, CA

Report No. 111

June 1994



*The John A. Blume Earthquake Engineering Center* was established to promote research and education in earthquake engineering. Through its activities our understanding of earthquakes and their effects on mankind's facilities and structures is improving. The Center conducts research, provides instruction, publishes reports and articles, conducts seminars and conferences, and provides financial support for students. The Center is named for Dr. John A. Blume, a well-known consulting engineer and Stanford alumnus.

*Address*

The John A. Blume Earthquake Engineering Center  
Department of Civil Engineering  
Stanford University  
Stanford, California 94305

BIBLIOGRAPHIC INFORMATION

PB95-183612

Report Nos:

Title: Regional Seismic Hazard and Risk Analysis through Geographic Information Systems.

Date: Jun 94

Authors: S. A. King and A. S. Kiremidjian.

Performing Organization: Stanford Univ., CA. John A. Blume Earthquake Engineering Center.

Sponsoring Organization: \*National Science Foundation, Arlington, VA.

Contract Nos: NSF-EID-9024032

Supplemental Notes: Also pub. as Stanford Univ., CA. John A. Blume Earthquake Engineering Center rept. no. REPT-111.

NTIS Field/Group Codes: 48F (Geology & Geophysics), 48I (Cartography), 89D (Structural Analyses)

Price: PC A09/MF A02

Availability: Available from the National Technical Information Service, Springfield, VA. 22161

Number of Pages: 188p

Keywords: \*Geographic information systems, \*Risk analysis, \*Ground motion, \*Earthquakes, \*Site characterization, Seismic effects, Seismic waves, Earthquake damage, Seismicity, Soil structure interactions, Structural analysis, Computerized simulation, Mathematical models, Case studies, \*Seismic hazards.

Abstract: A geographic information system (GIS) provides the ideal environment for conducting a comprehensive regional seismic hazard and risk analysis. This dissertation describes in detail the current GIS technology and the various steps in a regional seismic hazard and risk analysis. An overview of the different models for estimating the effects of local site conditions is presented. This research includes the development and example illustration of a GIS-based methodology for quantifying and combining the hazards associated with these secondary site effects. The methodology to combine the various hazards is based on a weighted average approach that utilizes the knowledge of local experts. This dissertation also covers the estimation of regional earthquake damage and loss, including the development of a methodology for compiling a comprehensive inventory of structures in a large region.





PB95-183612

**REGIONAL SEISMIC HAZARD  
AND RISK ANALYSIS THROUGH  
GEOGRAPHIC INFORMATION SYSTEMS**

**by**

**Stephanie A. King and Anne S. Kiremidjian**

**This research was partially supported**

**by**

**The National Science Foundation**

**Grant No. EID-9024032**

**and**

**The John A. Blume**

**Earthquake Engineering Center**

**Report No. 111**

**June 1994**





## ABSTRACT

---

A geographic information system (GIS) provides the ideal environment for conducting a comprehensive regional seismic hazard and risk analysis. A GIS has the ability to store, manipulate, analyze, and display the large amount of required spatial and tabular data. The system can typically be linked to external computational programs, high level database management systems, and knowledge-based expert systems. The objective of this research is the development of a methodology for using geographic information system technology to conduct a regional multi-hazard seismic risk analysis. The term multi-hazard refers to the consideration of ground shaking and the secondary site effects of soil amplification, liquefaction, landslide, and surface fault rupture. The methodology involves a modular framework that allows new models and database information to be included as the technology advances.

This dissertation describes in detail the current GIS technology and the various steps in a regional seismic hazard and risk analysis. An overview of the different models for estimating the effects of local site conditions is presented. This research includes the development and example illustration of a GIS-based methodology for quantifying and combining the hazards associated with these secondary site effects. The methodology to combine the various hazards is based on a weighted average approach that utilizes the knowledge of local experts. This dissertation also covers the estimation of regional earthquake damage and loss, including the development of a methodology for compiling a comprehensive inventory of structures in a large region.

A substantial part of this dissertation is devoted to a case study that illustrates the ideas and methodologies developed in this research. The case study is an earthquake damage and loss study for a magnitude 7.5 event on the Wasatch fault in Salt Lake County, Utah. The various seismic hazards are quantified and integrated, and a structural inventory of nearly 195,000 buildings is compiled. Numerous maps and tables of inventory data and results are included to help prove the effectiveness of the GIS for

conducting a large regional earthquake hazard and risk analysis. The final loss estimates appear to be reasonable when compared to recent large earthquakes in metropolitan areas.



## ACKNOWLEDGMENTS

---

This report is based on the doctoral dissertation of Stephanie King. The research work was supported by the National Science Foundation Grant No. EID - 9024032 and the John A. Blume Earthquake Engineering Center. The data for the application was provided by the Applied Technology Council of Redwood City, California. Environmental Systems Research Institute, Redlands, California generously donated their Arc/Info™ software for use at the John A. Blume Earthquake Engineering Center which was a key component in the development of this report. The authors express their appreciation for the support provided by these organizations.

Several individuals gave valuable advice throughout the development of this research. Drs. Roger Borchardt and Carl Wentworth of the United States Geological Survey, Menlo Park, California introduced the authors to the utility of geographic information systems. Professor David Maidment of the University of Texas, Austin provided a broad prospective on the potential applications of geographic information systems technology and was responsible for bringing the first license of Arc/Info™ to the John A. Blume Earthquake Engineering Center. Discussions with Dr. Steve Winterstein and Professor Ronaldo Borja were very helpful and instructive. Christopher Rojahn, Roger Scholl, and Lawrence Reaveley's practical insight and advice throughout the development of this research was extremely valuable. The authors express their deep gratitude and thanks for the help and contributions of all of these individuals.





---

## TABLE OF CONTENTS

---

Chapter	Page
List of Tables .....	ix
List of Figures .....	xi
<b>1 Introduction .....</b>	<b>1</b>
1.1 Background .....	1
1.2 Objective .....	4
1.3 Scope .....	4
1.4 Organization of the Dissertation .....	6
<b>2 Geographic Information Systems and Regional Seismic Hazard and Risk Analysis .....</b>	<b>9</b>
2.1 Geographic Information System Technology .....	9
2.1.1 Data Types and Database Management .....	9
2.1.2 Analysis and Modeling Capabilities .....	13
2.1.3 GIS Software and Computer Hardware .....	14
2.2 Regional Seismic Hazard and Risk Analysis .....	15
2.2.1 Identification of Seismic Sources .....	16
2.2.2 Modeling of Earthquake Occurrences .....	16
2.2.3 Determination of Regional Bedrock Motion .....	19
2.2.4 Modeling Local Site Effects .....	20
2.2.5 Estimating Regional Damage Distributions .....	21
2.2.6 Estimating Regional Loss Distributions .....	22

2.3	Application of GIS Technology to Regional Seismic Hazard and Risk Analysis .....	22
2.3.1	Overview .....	23
2.3.2	Seismic Event Characterization .....	23
2.3.3	Regional Seismic Hazard Estimation .....	23
2.3.4	Regional Damage Distribution .....	25
2.3.5	Monetary and Non-Monetary Loss Estimation .....	25
3	Consideration of Local Site Effects .....	27
3.1	Overview .....	27
3.2	Soil Amplification .....	28
3.2.1	Empirical Multiplication Factors .....	28
3.2.2	Theoretical Transfer Function Models .....	30
3.2.3	Treatment of Soil Parameter Uncertainty .....	34
3.2.4	Dynamic Non-Linear Models .....	43
3.2.5	GIS-Based Regional Estimation of Surface Ground Motion .....	43
3.3	Secondary Seismic Effects .....	47
3.3.1	Liquefaction .....	47
3.3.2	Landslide .....	51
3.3.3	Surface Fault Rupture .....	53
3.4	Hazard Integration in the GIS Environment .....	54
3.4.1	Integration Methodology .....	54
3.4.2	Example Application .....	56
3.5	Summary .....	65
4	Earthquake Damage and Loss Estimation .....	67
4.1	Structural Inventories .....	67
4.1.1	Required Inventory Information .....	68
4.1.2	Sources of Inventory Data .....	69
4.1.3	Classification and Inference Schemes .....	71

4.1.4	Inventory Compilation Methodology .....	72
4.2	Damage Distributions .....	75
4.2.1	Definitions of Damage .....	75
4.2.2	Motion-Damage Relationships .....	76
4.2.3	Application of GIS Technology to Regional Damage Forecasting .....	80
4.3	Loss Distributions .....	81
4.3.1	Monetary Losses .....	82
4.3.2	Non-Monetary Losses .....	85
4.3.3	Application of GIS Technology to Regional Loss Forecasting .....	86
5	Case Study .....	89
5.1	Background and Scope .....	89
5.2	Seismic Hazard Analysis .....	91
5.2.1	Surface Ground Shaking .....	92
5.2.2	Local Site Effects .....	97
5.2.3	Hazard Integration .....	104
5.3	Earthquake Damage and Loss Estimation .....	104
5.3.1	Structural Inventory Development .....	106
5.3.2	Damage Estimation .....	116
5.3.3	Loss Estimation .....	130
5.4	Summary .....	139
6	Summary, Conclusions, and Future Work.....	151
6.1	Summary .....	151
6.2	Conclusions .....	153
6.3	Future Work .....	156
6.3.1	Site Effects, Hazard Integration, and Uncertatinty .....	156

6.3.2 Earthquake Damage and Loss .....	157
6.3.3 Utility of Regional Analysis .....	158
References .....	160

## LIST OF TABLES

---

Table	Page
3.1 Uncertainty analysis cases .....	36
3.2 Shear wave velocity parameters for surface geology units .....	42
3.3 Estimated liquefaction susceptibility of geologic sediments during strong ground shaking (after Youd & Perkins, 1978) .....	49
3.4 Example of hazard integration for a hypothetical region .....	57
3.5 Example heuristic rules for seismic hazard integration .....	64
4.1 Time to restore functionality after an earthquake for use class = retail store (from Applied Technology Council, ATC-13 Report, 1985) .....	84
4.2 Earthquake casualty estimates (from Applied Technology Council, ATC-13, 1985) .....	86
5.1 Social function classification for Salt Lake County, Utah (from Applied Technology Council, ATC-36, in progress) .....	109
5.2 Earthquake engineering classification for Salt Lake County, Utah (from Applied Technology Council, ATC-36, in progress) .....	111
5.3 Sources of inventory data for Salt Lake County, Utah (from Applied Technology Council, ATC-36, in progress) .....	113
5.4 Summary of current status of inventory data for Salt Lake County, Utah (from Applied Technology Council, ATC-36, in progress) .....	115
5.5 Expected values and standard deviation of damage factor (%) as a function of MMI for earthquake engineering classes in Salt Lake County, Utah (from Applied Technology Council, ATC-36, in progress) .....	123
5.6 Occupancy rates for social function classes in Salt Lake County, Utah (from Applied Technology Council, ATC-36, in progress) .....	131

5.7	Replacement costs for social function classes in Salt Lake County, Utah (from Applied Technology Council, ATC-36, in progress) .....	133
5.8	Loss-of-function parameters for social function classes in Salt Lake County, Utah for damage states 2, 3, and 4 (from Applied Technology Council, ATC-36, in progress) .....	135
5.9	Loss-of-function parameters for social function classes in Salt Lake County, Utah for damage states 5, 6, and 7 (from Applied Technology Council, ATC-36, in progress) .....	137
5.10	Casualty rates for damage states in Salt Lake County, Utah (from Applied Technology Council, ATC-36, in progress) .....	139
5.11	Summary of final results for all buildings in Salt Lake County, Utah .	147
5.12	Summary of final results for buildings in Salt Lake County, Utah by construction type .....	148
5.13	Summary of final results for all highway bridges in Salt Lake County, Utah .....	149
5.14	Summary of final results for highway bridges in Salt Lake County, Utah by structural type and function .....	150



## LIST OF FIGURES

---

Figure	Page
1.1 The role of geographic information systems in regional seismic hazard and risk analysis .....	3
1.2 The mapping process for regional multi-hazard seismic risk analysis through GIS .....	5
2.1 The information systems composing a fully-integrated geographic information system (after Frost, et al., 1992) .....	10
2.2 Illustration of data linkage in the GIS environment .....	12
2.3 The basic steps in a regional seismic hazard and risk analysis .....	17
2.4 Flowchart showing the basic procedure for a GIS-based regional multi-hazard seismic risk analysis .....	24
3.1 Illustration of the Ohsaki (1982) model for soil amplification .....	32
3.2 Post-strain site period as a function of the number of soil layers .....	37
3.3 Maximum spectral amplification as a function of the number of soil layers .....	38
3.4 Surface PGA values as a function of the number of soil layers .....	38
3.5 Period of maximum spectral amplification as a function of the number of soil layers .....	39
3.6 Map showing approximate predominant site periods in San Francisco, California .....	40
3.7 Map showing contours of bedrock elevation in San Francisco, California .....	41
3.8 Map showing contours of surface elevation in San Francisco, California .....	41
3.9 Map showing surface geologic units in San Francisco, California .....	42

3.10	Map showing buffer zones of estimated bedrock PGA values in San Francisco, California .....	46
3.11	Map showing final estimates of final surface PGA values in San Francisco, California based on the Kiremidjian, et al. (1991) model ..	46
3.12	GIS-based seismic hazard integration .....	55
4.1	Example inter-related database tables in a structural inventory (from Applied Technology Council, ATC-36, in progress) .....	74
4.2	Example damage-loss curves for different building construction classes (from Algermissen and Steinbrugge, 1984) .....	78
4.3	Example fragility curves (from Kircher and McCann, 1983) .....	78
4.4	Damage probability matrix for low-rise wood-frame buildings (from Applied Technology Council, ATC-13, 1985) .....	79
4.5	Expected damage factor with standard deviation as a function of MMI for low-rise wood-frame buildings (from Applied Technology Council, ATC-36, in progress) .....	79
4.6	Percentage of functionality as a function of time following an earthquake for use class = retail store (from Applied Technology Council, ATC-36, in progress) .....	85
5.1	Map showing locations of faults in Salt Lake County, Utah .....	90
5.2	Map showing buffer zones of ground shaking in Salt Lake County, Utah .....	93
5.3	Map showing regional distribution of general soil types in Salt Lake County, Utah .....	94
5.4	Map showing regional distribution of peak ground acceleration values in Salt Lake County, Utah .....	95
5.5	Map showing regional distribution of ground shaking hazard ( $MMI_{GS}$ ) in Salt Lake County, Utah .....	96
5.6	Map showing liquefaction potential in Salt Lake County, Utah .....	98
5.7	Map showing landslide potential in Salt Lake County, Utah .....	99
5.8	Map showing fault rupture zones in Salt Lake County, Utah .....	100
5.9	Map showing regional distribution of liquefaction hazard ( $MMI_{LIQ}$ ) in Salt Lake County, Utah .....	101
5.10	Map showing regional distribution of landslide hazard ( $MMI_{LAN}$ ) in Salt Lake County, Utah .....	102

5.11	Map showing regional distribution of fault rupture hazard ( $MMI_{FR}$ ) in Salt Lake County, Utah .....	103
5.12	Map showing regional distribution of combined seismic hazard ( $MMI_F$ ) in Salt Lake County, Utah .....	105
5.13	Interrelated database tables at inventory development stage (from Applied Technology Council, ATC-36, in progress) .....	107
5.14	Use of County Tax Assessor datafile in structural inventory development .....	108
5.15	Map showing commercial building inventory in Salt Lake County, Utah .....	117
5.16	Map showing highway bridge inventory in Salt Lake County, Utah ...	118
5.17	Map showing percentage of unreinforced masonry buildings in each Census tract in Salt Lake County, Utah .....	119
5.18	Map showing average design date of buildings in each Census tract in Salt Lake County, Utah .....	120
5.19	Map showing intermediate results for commercial buildings on top of combined seismic hazard ( $MMI_F$ ) in Salt Lake County, Utah .....	121
5.20	Map showing intermediate results for highway bridges on top of ground shaking hazard ( $MMI_{GS}$ ) in Salt Lake County, Utah .....	122
5.21	Map showing average expected damage factor (%) due to ground shaking hazard ( $MMI_{GS}$ ) in each Census tract in Salt Lake County, Utah .....	127
5.22	Map showing average expected damage factor (%) due to combined seismic hazard ( $MMI_F$ ) in each Census tract in Salt Lake County, Utah .....	128
5.23	Map showing percentage of buildings with expected damage factor greater than 60% due to combined seismic hazard ( $MMI_F$ ) in Salt Lake County, Utah .....	129
5.24	Interrelated database tables at final stage of analysis (from Applied Technology Council, ATC-36, in progress) .....	140
5.25	Map showing final results for commercial buildings in Salt Lake County, Utah .....	141
5.26	Map showing final results for highway bridges in Salt Lake County, Utah .....	142

5.27	Map showing total expected loss due to combined seismic hazard (MMI <sub>F</sub> ) in each Census tract in Salt Lake County, Utah .....	143
5.28	Map showing average number of days to restore buildings to 100% functionality due to combined seismic hazard (MMI <sub>F</sub> ) in each Census tract in Salt Lake County, Utah .....	144
5.29	Map showing total number of deaths due to combined seismic hazard (MMI <sub>F</sub> ) in each Census tract in Salt Lake County, Utah .....	145

### 1.1 Background

Every damaging earthquake reaffirms the importance of seismic hazard and risk analysis for estimating the consequences of an earthquake. Although some progress in the area of seismic prediction has been made, earthquakes cannot be accurately predicted in time, magnitude, or location. Even if an accurate prediction were possible, the earthquake occurrence and consequent damage potential could not be prevented. Seismic hazard and risk cannot be eliminated, but it can be effectively analyzed and possibly reduced by combining the available regional geologic and geographic information with recent technological developments.

A comprehensive regional seismic hazard and risk analysis is a fairly standard procedure that requires combining the effects of many factors. Each of these factors usually involves the modeling and analysis of both spatial and tabular data. The amount of requisite information can often be overwhelming, even for a small region. Recent advances in geographic information system (GIS) technology have created new opportunities for managing the large amount of data, for interfacing with external analysis programs, and for presenting the results in a manner that can be useful for disaster planning, hazard and risk mitigation, and rehabilitation strategy comparison (King and Kiremidjian, 1993).

A geographic information system can be used to integrate the various steps in a regional seismic hazard and risk analysis in a modular framework that has the flexibility to be updated with new analytical models and database information as the technology advances. The system is independent of analysis scale and geographic location, allowing analysis at any level and in any area where the necessary information is available.

Figure 1.1 illustrates how the GIS works to combine the separate modules needed for a regional seismic hazard and risk analysis. Seismic hazard due to ground shaking results from seismic source modeling or from a scenario event assumption. Seismic hazard due to local site effects such as soil amplification, liquefaction, landslide, and fault rupture can be estimated by combining the available soil parameter data with the current hazard models or by making use of existing maps showing estimated levels of these collateral hazards. Regional structural inventories, often stored in external database management systems, are combined with the seismic hazards to produce damage and loss distributions for the analysis region. Each of the various components of the regional seismic hazard and risk analysis depicted in Figure 1.1 will be discussed in detail in the following chapters.

Most of the previous work in the application of geographic information system technology to regional seismic hazard and risk analysis has been limited to methods usually considering only one type of seismic hazard and often applied to a small region or to a specific type of facility. Rentzis, et al. (1992) used a GIS to estimate damage and loss distributions due to ground shaking alone in a 50-year exposure period for residential and commercial buildings in Palo Alto, California. Borchardt, et al. (1991) developed a GIS-based methodology for identifying special study zones for strong ground shaking in the San Francisco Bay region based on regional surface geology and an intensity attenuation relationship for a repeat of the 1906 San Francisco Earthquake. Kim, et al. (1992) developed a GIS-based regional risk analysis program to interactively study the vulnerability of bridges in a regional highway network. McLaren (1992) describes the use of a GIS by Pacific Gas and Electric to aid in the evaluation of the likely effects of high-probability, large magnitude future earthquakes in PG&E's service territory and to set priorities for the mitigation of seismic hazards.

Due to recent improvements in the availability and quality of GIS technology, tabular database software, as well as computer hardware, a significant amount of current research has been devoted to incorporating GIS technology in seismic hazard and risk analysis. Very few of these studies, however, have considered combining the effects of the various seismic hazards such as ground shaking, soil amplification, liquefaction, landslide, and fault rupture. Additionally, most studies are conducted for a specific site or for a specific facility type. Currently, there is no existing methodology for integrating all of the separate modules necessary for a comprehensive regional seismic hazard and risk

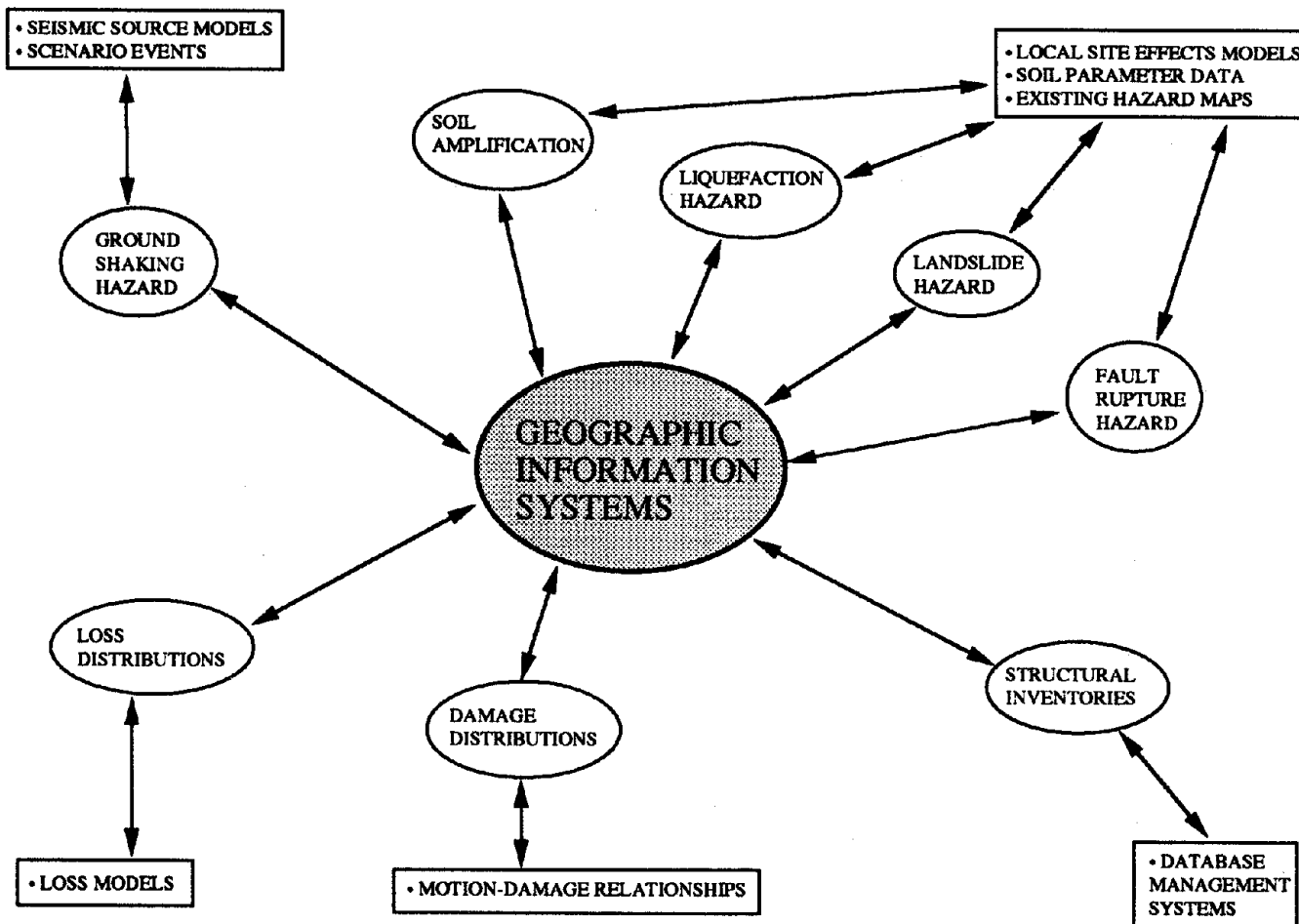


Figure 1.1. The role of geographic information systems in regional seismic hazard and risk analysis.

analysis in a manner that is flexible in geographic location, analysis scale, database information, and analytical modeling capabilities.

## 1.2 Objective

The objective of this research is the development of a methodology for using geographic information system technology to conduct a regional multi-hazard seismic risk analysis. Figure 1.2 illustrates the mapping process for combining the separate components of a regional seismic hazard and risk analysis in the GIS environment. Maps representing regional geologic and geographic information are overlaid and their attributes are combined to produce intermediate maps of regional seismic hazards. These hazard maps are then overlaid and combined with structural inventory maps to produce maps predicting regional damage distributions. Combining the map of damage distributions with a map of population distributions for the area results in final regional estimates of direct loss, indirect loss, and casualties. The modular design of the GIS-based analysis scheme allows new database information to be added and various analytical models to be included and compared for predictive accuracy.

A regional seismic hazard and risk analysis is used not only for estimating potential damage and loss to existing facilities, but also for planning locations and construction of future facilities and for analyzing and comparing the regional effects of various retrofit schemes. The GIS-based analysis is useful to engineers, planners, emergency personnel, government officials, and anyone else who may be concerned with the potential consequences of seismic activity in a given region. The results of a regional seismic hazard and risk analysis are usually presented in the form of microzone maps that serve as an effective means of transferring information from the scientific community to the professional community of decision makers involved in hazard and risk mitigation.

## 1.3 Scope

This research focuses on the development of a methodology for using geographic information system technology to integrate the various components necessary for a regional multi-hazard seismic risk analysis. In this dissertation, the seismic risk analysis includes consideration of primary hazards due to ground shaking and to local site effects



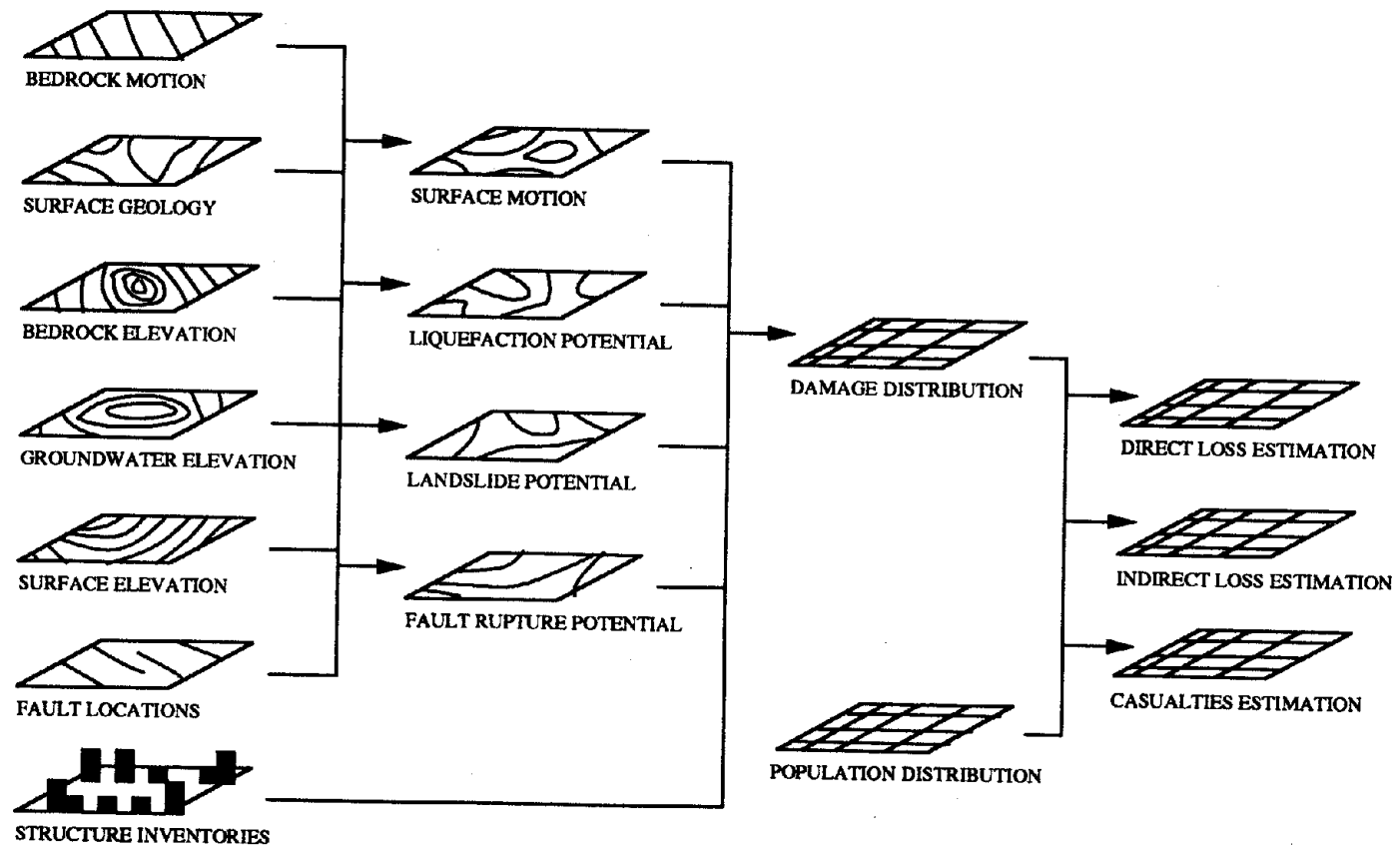


Figure 1.2. The mapping process for regional multi-hazard seismic risk analysis through GIS.

such as soil amplification, liquefaction, landslide, and surface fault rupture. Secondary hazards such as tsunami, conflagration, and inundation are not considered. The analysis incorporates structural inventories, motion-damage relationships, and loss modeling for estimating regional damage and loss distributions. Only those damages and losses associated with the primary hazards listed above are considered in the analysis methodology.

The integrated GIS-based analysis methodology presented in this dissertation is designed for seismic hazard and risk analysis on the regional, not site-specific level. The analysis results are intended to give general estimates of damage and loss distributions and to indicate areas that require further detailed investigation. These results are not intended to predict the expected damage and loss at a specific site or for a specific facility. For this reason, the models chosen to be included in the GIS-based analysis are fairly simplified and suitable for use with regional spatially-distributed data, which can often be incomplete in the amount and type of available information. The flexible framework of this GIS-based methodology will allow the analysis system to be updated and expanded with new models and database information.

In addition to the development of a methodology for a GIS-based regional seismic hazard and risk analysis, this work provides a unified approach for combining the regional damage and loss due to the primary hazards of direct ground shaking and the local site effects, namely soil amplification, landslide, liquefaction, and surface fault rupture. A simple hazard model for each of the hazards listed above is developed and implemented in the GIS environment. The effects of the various hazards are combined in a weighted-average approach. Local soil conditions play a major role in the modeling of the various seismic hazards, therefore a treatment of soil parameter uncertainty is included to account for the large variation in the amount and type of spatial geologic data that are available for a region.

## 1.4 Organization of the Dissertation

This dissertation presents a methodology for using geographic information system technology to conduct a regional multi-hazard seismic risk analysis. Chapter 2 gives a detailed description of a geographic information system (GIS). Spatial data structures and the functional elements of an integrated GIS are discussed. Within the GIS, points, lines,

and polygons with associated location and feature attributes are used to represent the characteristics of a region, such as the built environment and the distribution of geologic materials. The role of relational database management systems and external modeling and analysis programs in the GIS-based regional analysis methodology is also discussed here. Additionally, Chapter 2 gives a broad overview of seismic hazard and risk analysis. The primary seismic hazard of direct ground shaking is discussed in detail, but the seismic hazards due to local site effect are only briefly discussed as they are more thoroughly treated in the subsequent chapters. The methodology for integrating the modular components of the GIS-based regional multi-hazard seismic risk analysis, as indicated in Figures 1.1 and 1.2, is discussed here, with a more thorough treatment of each of the components given in the following chapters.

Chapter 3 addresses the seismic hazards due to local site effects. Soil amplification, liquefaction, landslide, and surface fault rupture are the local site effects considered in this research, although most of the work focuses on soil amplification. GIS-based hazard models are discussed for each of these effects and a methodology for combining them through a weighted-average approach is presented. Soil parameter data are also discussed in this chapter, including sources of the data and possible errors in the often incomplete spatially varying data. The uncertainty in the soil parameters and the effects of analysis model simplification for regional studies are also investigated in this chapter.

The estimation of regional distributions of damages and losses is described in Chapter 4. Structural inventories, including types of inventories, sources of and problems with inventory data, and an integration and compilation methodology are discussed. A background and overview of damage forecasting is given here, including descriptions of the various types of damage and the available motion-damage relationships. The estimation of loss distributions for both monetary and non-monetary loss is also discussed in this chapter. Monetary loss can include loss due to physical damage to structures and contents, loss of business revenue, and financing of repairs. Non-monetary loss can include fatalities, injuries, unemployment and homelessness. The application of GIS technology in the damage and loss estimation process is described in detail with a discussion of the use of microzone mapping for seismic hazard and risk mitigation purposes.

Chapter 5 presents a case study. A regional multi-hazard seismic risk analysis is performed for Salt Lake County, Utah, located in the Wasatch Fault Zone. A detailed description of the GIS-based analysis methodology is presented. A discussion of the sources of regional geologic, geographic, and structural inventory information, as well as the problems associated with incomplete information is also given. The procedure for synthesizing the massive amount of data and the assumptions and simplifications made in the regional study are described. Results and microzone maps for various stages of the analysis process are presented for illustration of the methodology.

Lastly, conclusions and recommendations for future work are given in Chapter 6.

## CHAPTER 2

# GEOGRAPHIC INFORMATION SYSTEMS AND REGIONAL SEISMIC HAZARD AND RISK ANALYSIS

---

### 2.1 Geographic Information System Technology

There are many definitions for a geographic information system (GIS) and there seems to be confusion as to what are the necessary components and capabilities of a true GIS. The most universal definition in the literature for a GIS is given by The Federal Interagency Coordinating Committee (1988) as "A system of computer hardware, software, and procedures designed to support the capture, management, manipulation, analysis, modeling and display of spatially referenced data for solving complex planning and management problems." Figure 2.1 is adapted from Frost, et al. (1992) and shows how different information systems work together to function as a fully-integrated GIS. Modern geographic information system technology has evolved from thematic cartography due to the combination of increased computational capabilities, refined analytical techniques, and a renewed interest in environmental/social responsibility. Throughout this evolution the primary goal has been to take raw data and transform it, through overlays and other analytical operations, into new information that can support the decision making process (Parent & Church, 1987). The remainder of this section gives a detailed overview of geographic information system technology, including the various components and their utility in a GIS-based regional multi-hazard seismic risk analysis.

#### 2.1.1 Data Types and Database Management

Data associated with a geographic information system can be divided into two general categories: graphic data and non-graphic data (Antenucci, et al., 1991). Graphic data are digital representation of map features, usually depicted as point, line, area, and annotation features. The graphic features can be stored in either vector or raster format.

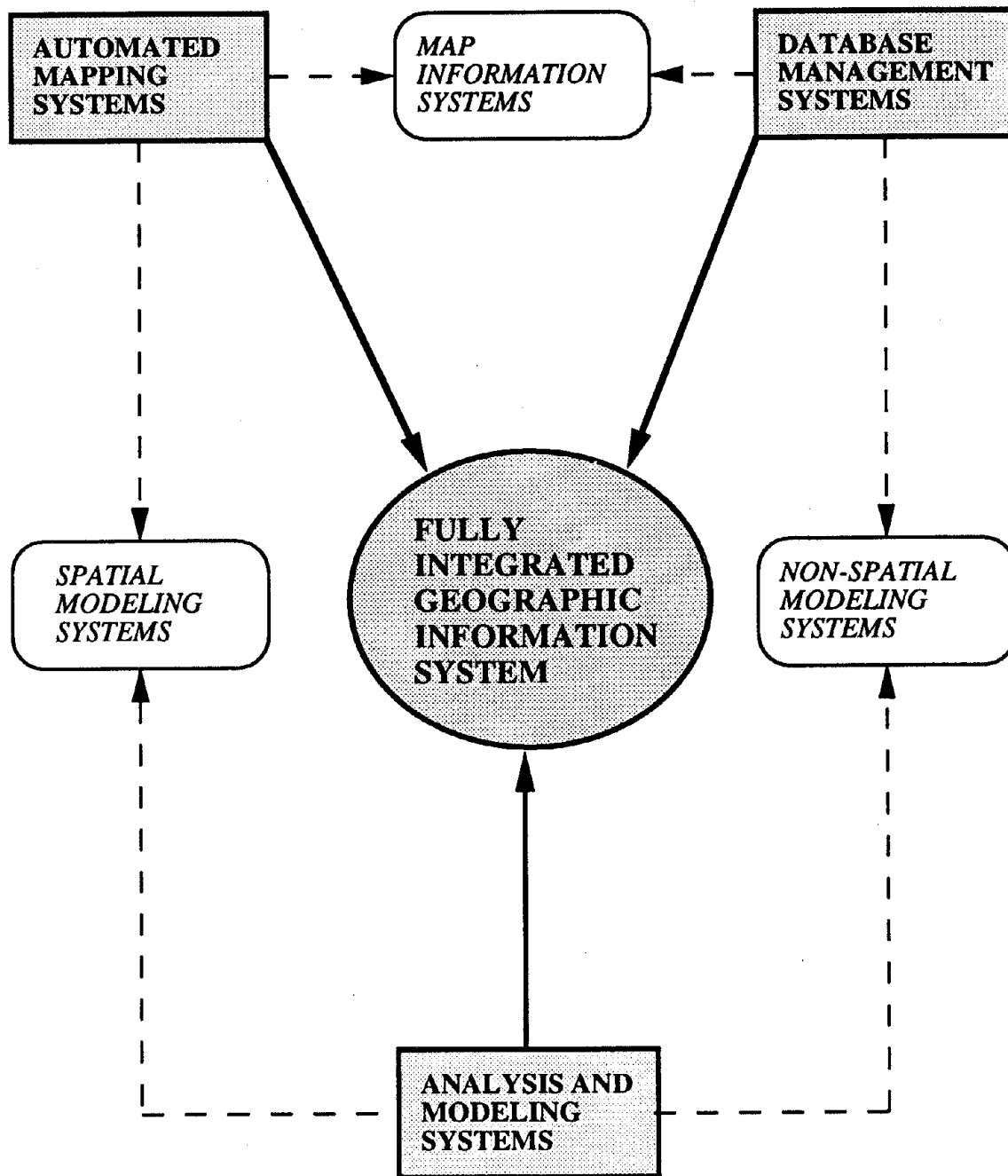


**Figure 2.1.** The information systems composing a fully-integrated geographic information system (after Frost, et al., 1992).

Vector data are represented by coordinates of point and line locations with rules for computing new coordinate locations and connecting the points as line or area features. Raster data are depicted by a uniform grid of cells or pixels. Most modern geographic information systems can handle both vector and raster representations of graphic data, but the vector format is generally preferred due to its efficiency in data storage and manipulation and its more attractive graphical display.

Non-graphic data are the attributes associated with the graphic data. They are stored in alphanumeric format and are representations of the characteristics, qualities, and relationships of map features and geographic locations. Figure 2.2 illustrates the relationship in a GIS between graphic and non-graphic data. Non-graphic or tabular data can be stored in the given database within a GIS, although these databases are often limited in their ability to store very large amounts of data and in their functional capabilities. As shown in Figure 2.2, most modern GIS programs have the ability to link both graphic and non-graphic data to tables of attribute information in an external high-level database management program.

The available coordinate systems in a GIS for storing, analyzing, and displaying graphic data are the Cartesian system and the geographic longitude/latitude system (Antenucci, et al., 1991). Coordinates are usually expressed in one of the numerous possible map projections that transform positions on the curved surface of the earth onto a flat map surface. A few of the commonly used projections are the State Plane Coordinate System, the Universal Transverse Mercator, the Albers Equal-Area Conic, and the Lambert Conformal Conic (ESRI, 1992). Most GIS programs have the ability to easily convert data from one projection to another without significant loss of accuracy.

The acquisition and input of data is typically the most costly and time-consuming part of implementing a GIS-based analysis (Ripple, 1989). Graphic data can be entered into a GIS through digitizing or photo-quality scanning an existing map. These two methods are the most time-consuming but they allow the user to have the most control and understanding of the accuracy and quality of the spatial data. Depending on the sophistication of the GIS, graphic data can also be entered in one of several digital file formats. A digital exchange file output from a computer-aided drafting system or a different geographic information system can be converted to a GIS map, although information such as line connectivity is often lost in the exchange due to the difference in system data structures. Standardized digital files such as the USGS Digital Line Graph

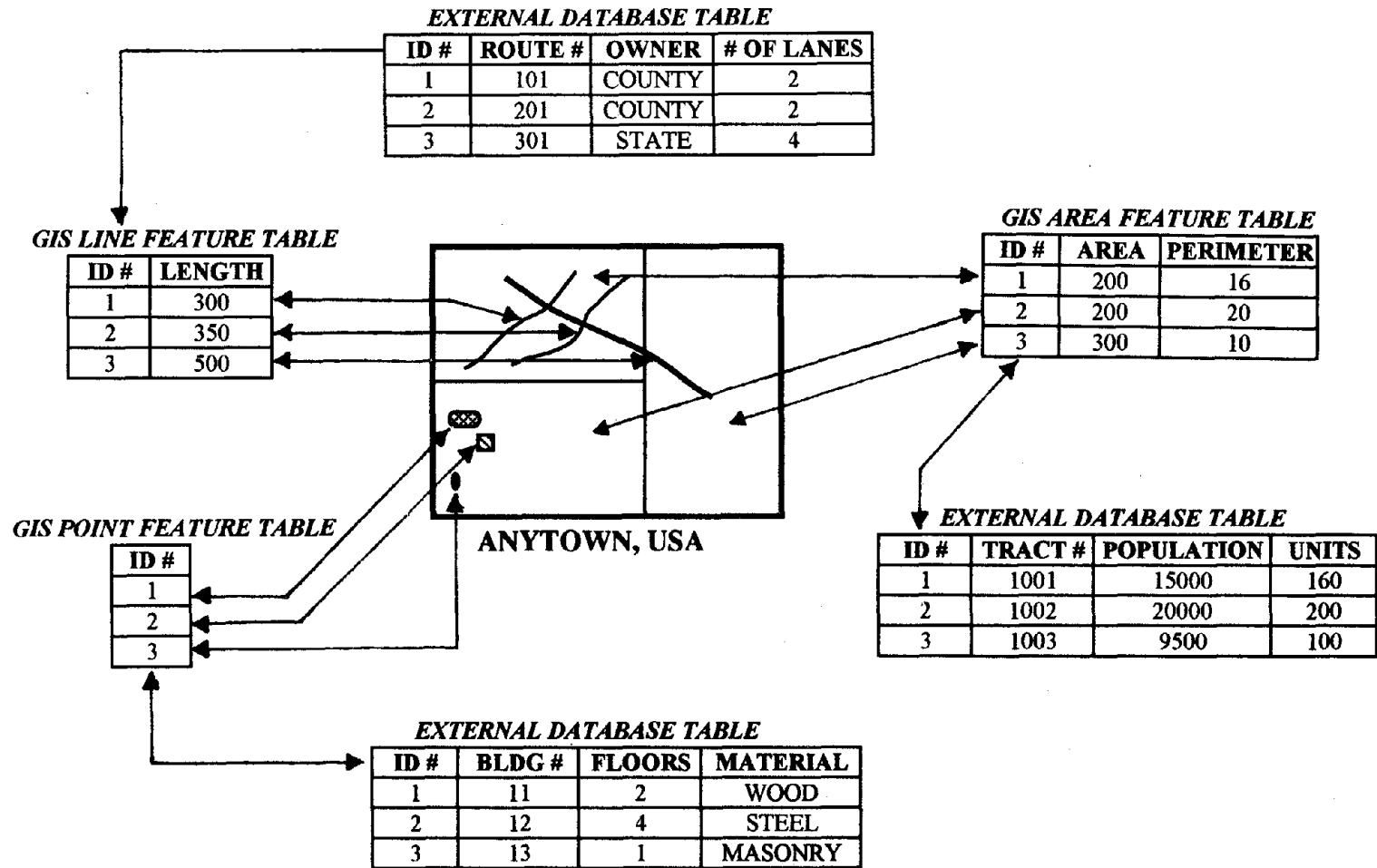


Figure 2.2. Illustration of data linkage in the GIS environment.



(DLG) files and the U.S. Census Bureau TIGER/Line files can be converted to maps in most GIS programs. Although these conversions are often "black-box" functions, the quality of the files is generally high, producing very accurate maps.

Non-graphic data associated with digitized or scanned graphic data must usually be entered by hand, requiring the attribute data to be assigned to each individual feature. This is generally a very time-intensive procedure, but again it allows the user to have control and understanding of the accuracy and make-up of the feature attribute tables. The several possible digital file formats for conversion to a GIS map usually contain the relevant attribute information for the graphic data. Depending on the quality and source of the digital file, the non-graphic data may lose information in the conversion process or require extensive database manipulations to be useful. As explained above, attribute data can also be stored in external database management systems and linked to the graphic data, requiring no exchange or conversion of information. If necessary, tabular data can be added to the GIS database by defining the table structure and then entering the data.

### 2.1.2 Analysis and Modeling Capabilities

One of the most important features of a geographic information system is the manipulation and analysis of both spatial (graphic) and tabular (non-graphic) data (Smith, et al., 1987). The procedures for data analysis typically found in most GIS programs include:

- (a) Map overlay procedures, including arithmetic, weighted average, comparison, and correlation functions.
- (b) Spatial connectivity procedures, including proximity functions, optimum route selection, and network analysis.
- (c) Spatial neighborhood statistics, such as slope, aspect ratio, profile, and clustering.
- (d) Measurements of line and arc lengths, of point-to-point distances, of polygon perimeters, areas, and volumes.
- (e) Statistical analysis, including histograms or frequency counts, regressions, correlations, and cross-tabulation.
- (f) Report generation, including maps, charts, graphs, tables, and other user-defined information.

Depending on the level of sophistication of a GIS, numerous application-specific analysis functions may exist. These include procedures such as kriging of geotechnical

data, air pollution dispersion, ground water flow, and highway traffic routing. Most systems include some sort of built-in programming capability usually in the form of a software-specific macro language. This allows the user to develop a set of functions or analysis procedures that can be stored in a user-defined library. Often, the GIS macro language is very simplified and is not able to handle very high level computational features such as recursion, numerous simulations, subscripted variables, and subroutines. For this reason, most GIS programs have the ability to communicate with external analysis and modeling programs. A system can typically output data in various formats to be used in various external programs such as spreadsheets, word processing, graphics, and other user-specified executable programs. The results of an external analysis can then be used by the GIS as both graphic and non-graphic data for further manipulation and analysis, or for final report and map generation.

Recently, the idea of using knowledge-based engineering techniques in a GIS environment has emerged. This requires the coupling of GIS software with an expert system, a computer program that performs an analysis of a given situation and determines an answer or predicted outcome based on known information and rules. Applications such as site selection of critical facilities, resource allocation studies, and retrofit of bridges and other structures have been shown to operate very effectively in the GIS-expert system analysis environment. Boyle and Dong (1991) describe the use of a GIS, an expert system, and a database management system in the commercial product IRAS (Insurance/Investment Risk Assessment System) to estimate the seismic hazard of particular locations. Jensen and Christensen (1986) use a knowledge-based GIS technique to select solid and hazardous waste disposal sites and Usery, et al. (1988) use a similar knowledge-based GIS procedure to perform engineering geologic mapping. Several other studies in this area are currently in progress, including many applications in the social sciences.

### 2.1.3 GIS Software and Computer Hardware

There are hundreds of commercially available GIS software packages. They vary greatly in characteristics such as analysis capabilities, transportability of data, user-friendliness, storage capacity, graphic display, communication with other software, computer hardware requirements, speed, and price. GIS technology is a rapidly changing field. New and improved software is continuously being developed to meet the increasing

popularity and use of geographic information systems in public agencies, private companies, educational programs, and several other areas. Kurt, et al. (1992) compare several commercially available GIS software packages developed for the microcomputer. They analyze thematic mapping and data queries, speed, compatibility with existing database information, conversion of maps between software, and the performance of a case study in each GIS.

Often the selection of a GIS package depends on the available computer hardware. Most of the currently available GIS software is designed for the microcomputer, as this type of computer has been the most popular in recent years. These packages are typically very user-friendly and relatively inexpensive, but are often lacking in computational speed, storage capacity, and communication with external programs. The microcomputer technology is rapidly improving in terms of speed, storage, and data exchange via the Windows™ environment, therefore these drawbacks should become irrelevant in the near future. The high performance workstation environment has recently become popular due to large cost reductions and the interest in file sharing among multiple users. A few of the more common GIS software packages are designed for the workstation environment. They typically require more time to learn and can be quite expensive, but are usually superior in analysis capabilities, data storage, speed, interfacing with external software, and macro language programming.

The GIS software package selected for this research is Arc/Info™ developed by the Environmental Systems Research Institute (ESRI) in Redlands, California. It is designed for the workstation environment and is the most commonly used commercially available GIS software. Although this software is used in the case study presented in Chapter 5, the information and methodologies presented in this dissertation are general and can be implemented in any geographic information system with the necessary data manipulation and analysis capabilities.

## 2.2 Regional Seismic Hazard and Risk Analysis

The goal of a regional seismic hazard and risk analysis is to quantify the potential damages and losses in a region due to future earthquakes. This analysis requires the synthesis of several types of information, as depicted in Figures 1.1 and 1.2. This section gives a broad overview of the classic approach to regional seismic hazard and risk analysis

and Section 2.3 describes how the analysis is conducted in the geographic information system environment.

The basic steps in a regional seismic hazard and risk analysis procedure typically include:

- (a) Identification of earthquake sources.
- (b) Modeling the occurrences of earthquakes on these sources.
- (c) Estimating the attenuation of earthquake motions between the sources and the region.
- (d) Evaluating the local site effects of soil amplification, liquefaction, landslide, and surface fault rupture.
- (e) Estimating the damages to the regional inventories.
- (f) Estimating the expected losses in the region.

The above steps are based on Lutz and Kiremidjian (1993) and are illustrated in Figure 2.3. A brief overview of these steps is given below with a more detailed description of steps (d), (e), and (f) given in later chapters of this dissertation.

## 2.2.1 Identification of Seismic Sources

The first step in a regional seismic hazard and risk analysis is the identification of the potential seismic sources that can affect the region. Seismic sources are geographical features with homogenous seismicity (Vasudevan, et al., 1992). They can be modeled as point, line, and area sources (Lutz and Kiremidjian, 1993). Point sources repeatedly generate earthquakes from exactly the same point and are quite rare. Line sources are used to represent earthquake faults that generate earthquakes with epicenters following a linear trend. Regions with high seismicity that is not attributable to a well-defined source are typically modeled as area sources.

## 2.2.2 Modeling of Earthquake Occurrences

The modeling of earthquake occurrences on each seismic source is the second step in the analysis. There are several occurrence models that have been proposed and a

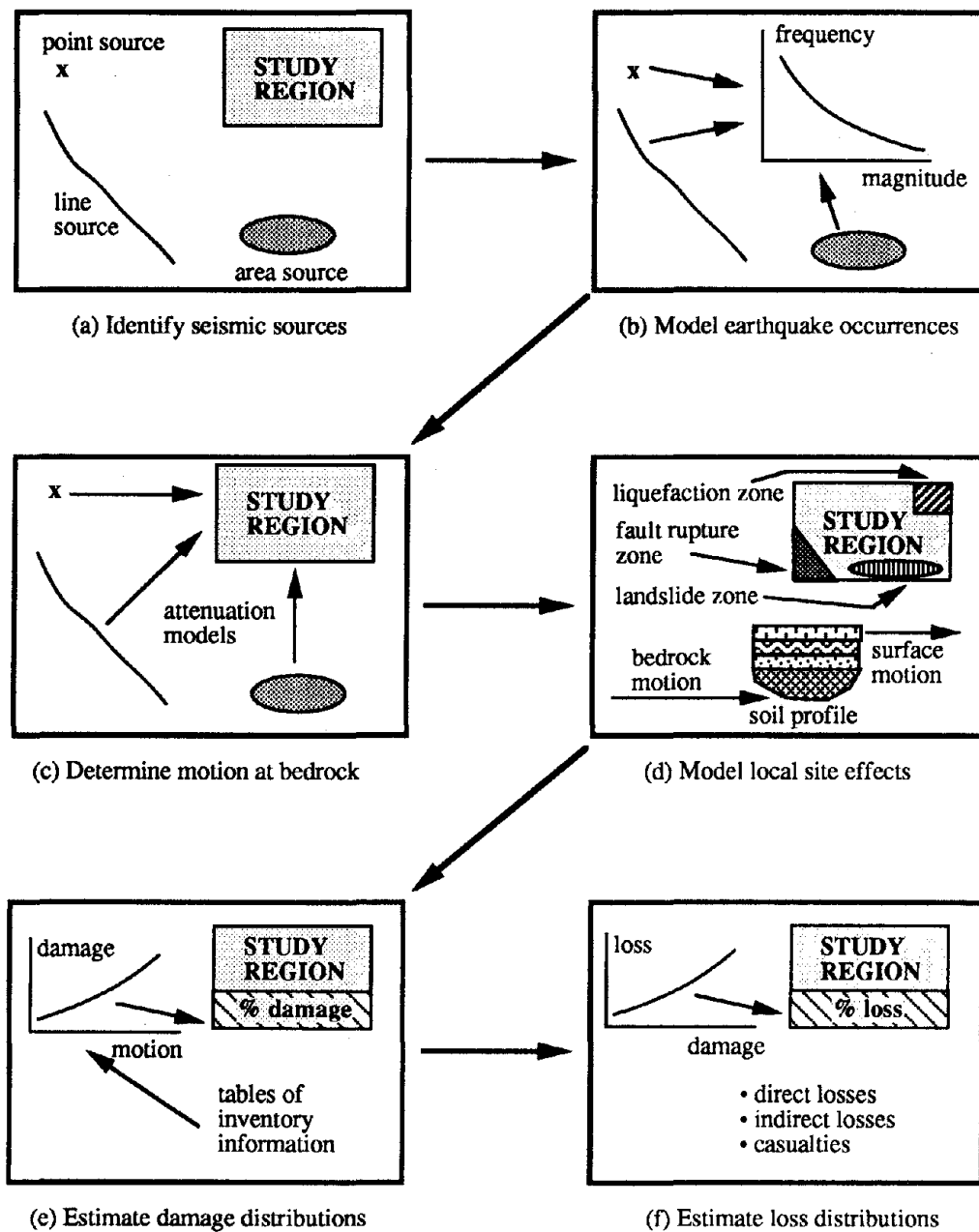


**Figure 2.3.** The basic steps in a regional seismic hazard and risk analysis.

complete review is provided by Anagnos and Kiremidjian (1988). The major classes of models include the Poisson models, the time-predictable models, and the slip-predictable models. These three major classes of models, as well as the deterministic scenario analysis method, are briefly discussed below. Other recently developed models include the random slip rate model (Suzuki and Kiremidjian, 1988) and the spatially and temporally dependent model (Lutz and Kiremidjian, 1993).

Poisson models are the simplest class of earthquake occurrence models and assume that earthquakes occur randomly in time, space, and magnitude. The rate of earthquake occurrences is assumed to be uniform and is estimated from empirical data using the Gutenberg-Richter magnitude-frequency equation. These models are memory-less and give a constant probability of an earthquake in the time period  $(t, t+\Delta t)$  given that there was no earthquake in the time period  $(0,t)$ . Poisson models are typically applied to regions with frequent, small magnitude earthquakes without spatial or temporal dependence.

Time-predictable models assume that earthquakes have a one-step temporal dependence (Anagnos and Kiremidjian, 1984). These models estimate the time of occurrence of the next earthquake given the size (seismic displacement) of the previous earthquake. A maximum stress release threshold and a constant stress accumulation rate are assumed. Knowing the amount of stress released by a given earthquake, the rate at which the stress will accumulate, and the maximum amount of stress the seismic source can accommodate, the time, but not size, of the next earthquake can be predicted. These models have been applied primarily to regions along plate boundaries.

Slip-predictable models also assume that earthquakes have a one-step temporal dependence (Kiremidjian and Anagnos, 1984). These models estimate the size of the next earthquake occurrence given the elapsed time since the previous earthquake. A minimum stress release threshold and a constant stress accumulation rate (as in the time-predictable model) are assumed. It is also assumed that when an earthquake occurs, all of the accumulated energy is released down to the minimum level. Knowing the time since the previous earthquake occurrence, the rate at which the stress will accumulate, and the minimum amount of stress to remain on the seismic source, the size, but not the time, of the next earthquake can be predicted. These models have been applied to the Middle American Trench in Mexico.

Two other recently developed models include the random slip rate model and the time and space dependent model. The random slip rate model (Suzuki and Kiremidjian, 1988) assumes a non-uniform stress accumulation rate and inhomogeneous properties for the fault. The slip rate for each earthquake on the fault is assumed to be random with the rate between events assumed to be constant. The time and space dependent model (Lutz and Kiremidjian, 1993) utilizes a generalized semi-Markov process for simulating fault behavior through time. The fault is discretized into short cells and the amount of slip accumulated on each cell and the amount of slip release on each cell due to earthquake occurrences is traced through time. The model can simulate the sizes and locations of earthquakes occurring along the fault for the time period of interest.

A deterministic scenario analysis can also be used in this step to model the occurrence of an earthquake. In this method the location, size, and time of occurrence of a future earthquake is assumed. The earthquake scenario can be a repeat of a previous seismic event in the area, but most often it is the maximum earthquake that the given seismic source is capable of generating, according to experts in the field. This method is often used by the insurance industry to make probable maximum loss (PML) estimates for their insured properties.

With the exception of the time and space dependent model, the earthquake occurrence models discussed in this section are simplified representations of the actual behavior of large, rare earthquakes. The Poisson model is typically applied to regions with small magnitude earthquakes without time and space dependence. The time-predictable, slip-predictable, and random slip rate models are adequate for seismic sources exhibiting temporal, but not spatial, dependence. The emphasis of the work presented in this dissertation is on regional seismic hazard and risk analysis for predicting damages and losses over a large area. For this reason, the deterministic scenario event occurrence model will be used to illustrate the GIS-based analysis methodology. This is the simplest model, as it requires little computation and is not region-specific, but as previously discussed, the analysis methodology is intended to be general, allowing more sophisticated models to be included instead.

### 2.2.3 Determination of Regional Bedrock Motion

After selecting one of the probabilistic occurrence models discussed above or assuming a deterministic seismic event scenario, the next step in the regional seismic

hazard and risk analysis is to determine the bedrock motion in the region. The most common method involves the use of an empirical attenuation relationship. These relationships express a given ground motion parameter in a region as a function of the size and location of an earthquake event. Numerous relationships have been developed in the past, typically by applying statistical regression analyses to recorded data. Campbell (1985) provides an excellent summary of attenuation relationship development. Often these relationships are developed with different functional forms and with different definitions of ground motion, magnitude, distance, and site conditions. These biases coupled with the scarcity of data for large magnitude events at short distances have recently led to investigations into more theoretical methods for predicting bedrock motion. Geophysical models based on seismic source mechanisms and wave-propagation theory have been proposed, but these models often require extensive source and site geology data and are more computationally intensive.

#### 2.2.4 Modeling Local Site Effects

Local geologic deposits are well known for their capabilities to modify the characteristics of seismic motions and influence the amount of damage to man-made facilities (Borcherdt, 1990). The local site effects are defined as soil amplification, liquefaction, landslide, and surface fault rupture. Soil amplification is the most common local site effect considered in a regional seismic hazard and risk analysis. There are several soil amplification models that estimate earthquake motion at the ground surface level given an input bedrock motion and a characterization of the local soil conditions. These models vary from simple multiplication factors that modify peak ground motion values based on recorded data to highly complex procedures that modify an entire earthquake time history based on non-linear dynamic soil response. Aki (1988) provides a good overview of the different types of soil amplification models.

The secondary local site effects of liquefaction, landslide, and surface fault rupture are typically more difficult to quantify and model than soil amplification. These effects are often summarized in the form of microzone maps that give a hazard potential in the form of a "yes" or "no" prediction of occurrence based on numerous assumptions. Kiremidjian (1992) describes the currently available hazard models for estimating the effects of soil amplification, surface fault rupture and earthquake-induced liquefaction and landslide, and



the need for a methodology that can accurately combine the seismic hazards due to these local site effects in a region.

The development of a methodology for combining the regional seismic hazards due to soil amplification, liquefaction, landslide, and surface fault rupture is one of the major components of the work presented in this dissertation. Chapter 3 gives a thorough discussion of this development in the GIS environment, as well as a more detailed description of the effects of local soil conditions on earthquake ground motion and the hazard associated with fault rupture and earthquake-induced liquefaction and landslide. Local soil parameter data have a critical role in the modeling of seismic hazard due to local site effects, therefore the treatment of soil parameter uncertainty is also discussed in Chapter 3.

### 2.2.5 Estimating Regional Damage Distributions

Once the seismic hazard due to ground shaking and local site effects has been adequately characterized, the next step in a regional seismic hazard and risk analysis is the estimation of damages to structural facilities. Damage forecasting requires a detailed inventory of the facilities in a region and well-defined relationships between earthquake motion (including local site effects) and both structural and non-structural facility damage. The development of an accurate and complete structural inventory for a region is often the most time-consuming, expensive, and important step in regional damage estimation. Most of the previous work in this area has focused on developing regional inventories for a specific type of facility, such as buildings (Vaseduvan, et al., 1992) and lifelines (Applied Technology Council, ATC-25, 1991).

One of the major components of the work presented in this dissertation is the development of a methodology for integrating and compiling an accurate and complete inventory of all structural facilities in a region. This methodology and its implementation in the GIS-based analysis process is thoroughly discussed in Chapter 4. A detailed overview of the various descriptions of damage and of the currently available relationships between earthquake motion and facility damage is also presented in Chapter 4.

## 2.2.6 Estimating Regional Loss Distributions

The final step in a regional seismic hazard and risk analysis is the estimation of regional losses based on the damage distributions predicted in the previous step. Several types of loss can be identified, typically divided into monetary and non-monetary loss. Monetary loss for a facility depends on the physical characteristics and use of the facility. This loss is often identified as resulting from (a) structural damage; (b) non-structural damage to contents and architectural components; (c) loss of business revenue; (d) relocation of occupants, contents, or function; (e) clean-up and security; and (f) financing of repairs (Kiremidjian, 1992). Non-monetary loss due to seismic activity typically depends on the characteristics of the regional population and can include effects such as fatalities, injuries, unemployment, and homelessness.

The description given above does not include the secondary losses associated with fire-following earthquake, tsunami, and inundation due to dam failure. These losses can often surpass the primary monetary and non-monetary losses, but are considered to be beyond the scope of this dissertation. The typical regional seismic hazard and risk analysis is limited to monetary loss due only to structural damage and to non-monetary loss due only to casualties. Geographic information system technology provides an excellent environment for analyzing and combining the various regional loss estimates due to a given seismic occurrence. Methods for estimating the loss types discussed in the previous paragraph in the GIS-based regional seismic hazard and risk analysis will be described in Chapter 4.

## 2.3 Application of GIS Technology to Regional Seismic Hazard and Risk Analysis

Section 2.1 of this chapter gave a detailed description of geographic information system technology and Section 2.2 presented a broad overview of regional seismic hazard and risk analysis. This section explains how these two topics fit together, that is the use of GIS technology for conducting a regional seismic hazard and risk analysis. The development of a GIS-based analysis methodology is the main focus of the research presented in this dissertation.

### 2.3.1 Overview

Figure 2.4 presents a detailed flowchart of the steps involved in a GIS-based regional seismic hazard and risk analysis. The circles represent methodology steps, the squares represent database information, and the triangles represent intermediate and final results. The general procedure illustrated in Figure 2.4 will be described below. A more detailed discussion for the areas of new development will be presented later in Chapters 3 and 4. As discussed in Chapter 1, the regional analysis presented here is somewhat simplified, but capable of being modified and updated in the future. A few important features such as conflagration loss and building-lifeline interaction analysis are omitted in order to focus on the development of the overall GIS-based analysis methodology and the new improvements in areas such as local site effect hazard and structural inventory compilation. Chapter 5 presents a case study that illustrates the application of this methodology to a study region in Salt Lake County, Utah.

### 2.3.2 Seismic Event Characterization

As shown in Figure 2.4, the first intermediate result in the regional analysis is the characterization of a seismic event. This typically requires a map of the region that identifies the potential seismic sources. A source is selected and an occurrence model is applied either by implementing the model within the GIS or by linking it as an external executable program. An alternate method for determining the characteristics of a seismic event is to assume a scenario earthquake occurring on a given source. Database tables of seismic activity in the region are often used to aid in the occurrence modeling procedure and in the assumption of a historical scenario earthquake.

### 2.3.3 Regional Seismic Hazard Estimation

The second intermediate result shown in Figure 2.4 is the estimation of seismic hazard in the region. This procedure typically requires several geologic and geographic maps of the region. The bedrock motion in the region resulting from the seismic event must first be determined. This is often done by applying one of the attenuation functions within the GIS or again by linking the function as an external executable program. The GIS-based procedure for estimating regional bedrock motion is straight-forward and will not be discussed further, except with respect to the case study presented in Chapter 5.

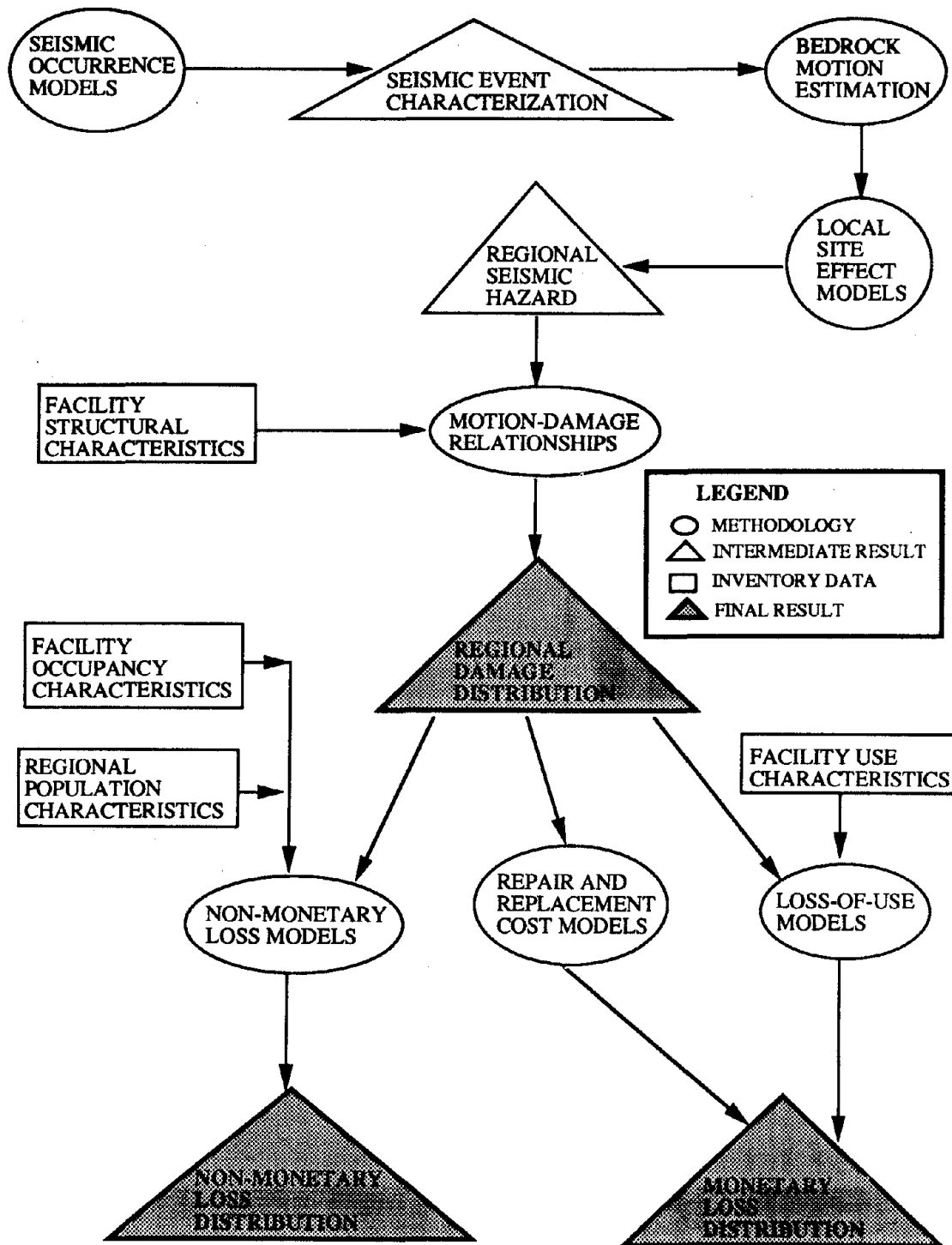


**Figure 2.4.** Flowchart showing the basic procedure for a GIS-based regional multi-hazard seismic risk analysis

Quantifying and combining the seismic hazard due to local site effects (soil amplification, liquefaction, landslide, and fault rupture) is one of the main areas of new development presented in this dissertation. The procedure involves developing models for each of the effects, assembling the necessary geologic and geographic maps and databases, applying the models either within the GIS or as linked external programs, and then overlaying and combining the resulting hazard maps. The development of this hazard analysis methodology is more thoroughly discussed in Chapter 3.

### 2.3.4 Regional Damage Distribution

The first final result obtained in the analysis procedure illustrated in Figure 2.4 is a regional damage distribution for the study area. Damage forecasting typically requires a detailed and accurate structural inventory for the region, a quantification of the regional seismic hazard, and equations relating damage to hazard for each facility type. The spatial database structure of a GIS environment is ideal for this procedure. Structural inventory information can be stored in tables within the GIS database or in tables in an externally linked database management program. Relationships to estimate facility damage are typically applied within the GIS, but can also be used through external program links. The general procedure involves combining maps of seismic hazard with maps of facility locations according to set motion-damage relationships producing maps of regional damage distribution. The resulting maps are useful for purposes such as resource allocation and rehabilitation prioritization. The development of a methodology for compiling an accurate and complete structural inventory is one of the major components of this research, therefore damage forecasting in a GIS-based environment will be described in detail in Chapter 4.

### 2.3.5 Monetary and Non-Monetary Loss Estimation

Recent seismic events have demonstrated that the monetary loss resulting from earthquake damage to major metropolitan areas can run into the billions of dollars (Kiremidjian, 1992). World-wide statistics of annual fatalities due to earthquakes can be just as alarming. As shown in Figure 2.4, the final and most important result of a regional seismic hazard and risk analysis is the estimation of monetary and non-monetary loss distributions. As with damage forecasting, the GIS environment is ideal for estimating loss distributions. The procedure typically involves combining maps of damage

distributions with maps and database tables of regional facility and population inventories according to relationships defining loss as a function of damage. The resulting microzone maps of regional loss distribution help to illustrate areas requiring further study for possible earthquake loss mitigation strategies. New improvements to loss estimation and a detailed description of the GIS-based analysis methodology are discussed further in Chapter 4.

## CHAPTER 3

# CONSIDERATION OF LOCAL SITE EFFECTS

---

### 3.1 Overview

It is well understood that earthquake damage to life and property results primarily from strong-ground shaking and indirect shaking-induced hazards such as liquefaction, landslide, and surface fault rupture. Severe earthquakes of the last decade in Mexico, Armenia, and the United States have reemphasized the importance of local geologic site conditions in estimating the regional damage and consequent losses due to future major earthquakes (King, et al. 1993). Evidence obtained from the 1989 Loma Prieta Earthquake indicated a strong geotechnical influence on the observed damage and casualties. The majority of the deaths and damage that resulted were related to geotechnical factors, denoted by the large number of failures that occurred due to liquefaction, soil amplification, and landslide (Clough, et al, 1993).

Seismic zonation maps for strong-ground shaking, liquefaction, landslide, and surface fault rupture can play a significant role in mitigating the effects of earthquakes in urbanized regions. As discussed in the previous chapter, a geographic information system provides an ideal environment for compiling and integrating regional databases of spatial geologic and geotechnical information for purposes of seismic zonation. One of the main goals of this research is the development and illustration of a methodology for implementing and combining the seismic hazard models for each of the local site effects as part of a GIS-based multi-hazard regional seismic risk analysis. This chapter discusses in detail the different hazard models and their integration in the GIS environment. The various models for soil amplification are described in Section 3.2. A treatment of soil parameter uncertainty for one of these models is also presented in this section. Section 3.3 gives an overview of the quantitative models that are currently available for estimating the secondary seismic effects of liquefaction, landslide, and surface fault rupture. The

GIS-based methodology for integrating the seismic hazards associated with these secondary effects is presented in Section 3.4.

## 3.2 Soil Amplification

Soil amplification of earthquake motion is one of the most difficult site effects to model. The difficulties result from (a) the lack of sufficient data on local soil parameters; (b) the lack of sufficient strong ground motion data at locations with different surface soil types; (c) the lack of sufficient strong ground motion data from vertical array measurements; (d) the inability to accurately quantify the non-linear characteristics of soil; and (e) the use of approximate models to represent the true non-linear behavior of soils when subjected to dynamic forces (Kiremidjian, et al., 1991).

The effect of local geology on the characteristics of earthquake ground motion has been a much researched subject, dating back to observations made after the 1906 San Francisco Earthquake. Numerous methodologies have been proposed for estimating the surface ground motion from the motion at the bedrock level and the geologic characteristics of the local soil conditions. Current methods for estimating ground motion site amplification can generally be divided into three types: (a) empirical multiplication factors; (b) theoretical transfer function models; and (c) dynamic non-linear models. The remainder of Section 3.2 contains a detailed description of these three types of soil amplification methods, including a treatment of soil parameter uncertainty for one of the theoretical transfer function models. Also included in this section is a discussion of the GIS-based approach to estimating regional ground surface motion as well as an example GIS implementation of one of the empirical multiplication factor models.

### 3.2.1 Empirical Multiplication Factors

Often the most simple method of quantifying the effect of local soil conditions on the amplification of earthquake ground motion is the use of empirical multiplication factors. This method involves multiplying a selected ground motion parameter such as peak ground acceleration (PGA) or peak ground velocity (PGV) at the bedrock level by an empirically-derived factor to estimate the ground motion parameter at the surface. These factors are often functions of the severity of shaking at the bedrock level and the properties of local soil conditions such as shear wave velocity and thickness of soil



deposits. Aki (1988) conducted an in-depth review of local site effects on strong ground motion and concluded, "The most realistic approach to the microzonation is then to determine empirical site-amplification factors for as many sites as possible by the regression analysis of earthquake data, and correlate them with various geotechnical parameters of the site which are relatively easier to measure."

Several multiplication factors have been developed for various regions based on statistical analysis of observed strong ground motion data. Kiremidjian, et al. (1991) developed simple site-dependent PGA and PGV amplification factors for the San Francisco Bay Area based on an analysis of 52 rock and soil site recordings from the 1989 Loma Prieta Earthquake. These factors are a function of the input PGA or PGV, and the depth to bedrock and average shear wave velocity of the soil deposit. Section 3.2.5 illustrates the implementation of this model in a GIS environment. Borchardt (1992), Idriss (1990), Seed, et al. (1976) and Trifunac (1976) are a few of the many researchers who have analyzed strong ground motion data to develop ratios of peak ground motion values for different soil conditions.

Modifying only the peak ground motion values such as PGA and PGV is often not a suitable means of representing the soil amplification effects of local site conditions because the frequency contents of both the input bedrock motion and the soil deposit are not considered in the analysis. PGA values are usually amplified by high frequency motions, PGV values tend to be amplified by medium frequency motions, and low frequency motions usually amplify PGD values. For this reason a great deal of past research has focused on the effect of local soil conditions on amplification of ground motion spectra such as spectral acceleration ( $S_a$ ), spectral velocity ( $S_v$ ), and spectral displacement ( $S_d$ ). Spectral amplification is often measured for peak values, values at certain frequencies or periods, average values, and the entire spectra.

Mohraz (1976) studied the earthquake response spectra on different geologic conditions recorded from several earthquakes. Borchardt (1990) thoroughly analyzed earthquake response spectra from the 1989 Loma Prieta Earthquake recorded at various geologic conditions in the San Francisco Bay area. These studies and others such as Trifunac (1976), Phillips and Aki (1986), and Seed, et al. (1976) have shown that soil amplification is frequency-dependent with a cross-over period at approximately 0.2 seconds. Above this period the ground motion is amplified by the local site conditions and below it the ground motion is attenuated by the local site conditions. Observations such

as these have led to a review of the methods of site characterization currently used in several structural design codes for new buildings. It is the accepted practice to classify soil sites as one of three or four broad types and then use a corresponding site-factor in the calculation of the applied lateral force to the structure. It is anticipated that the next generation of structural design codes will employ a more frequency-dependent site classification with some consideration of the fundamental site period (Whitman, 1992).

### 3.2.2 Theoretical Transfer Function Models

Earthquake motions at the surface of horizontally stratified soil can be treated as a result of the filtering of horizontal shear waves going through successive reflections and refractions in the soil deposit (Newmark and Rosenblueth, 1971). Linear wave propagation theory has become one of the most widely used techniques for assessing the effects of local soil conditions on the amplitude and frequency contents of seismic motions in soil deposits (Kausel and Roësset, 1984). This method involves idealizing the soil deposit as horizontally layered strata overlying rock with incident vertically propagating horizontal shear waves. The dynamic equations of motion are solved in the frequency domain with the soil deposit acting as a linear filter having a transfer function that depends on the viscoelastic material properties of the soil. Non-linearities in the soil material are typically modeled by iterative use of the linear solution, adjusting the material properties at each step to be compatible with the computed level of strain.

The linear transfer function model for soil amplification has been the subject of earthquake engineering research since the early 1950's when the work of Thomson (1950) and Kanai (1957) first suggested the methodology. Numerous linear transfer functions with varying degrees of complexity and required soil properties have been proposed for modifying different spectral ordinates. The general form of the equation for a spectrum at the ground surface level is typically given as:

$$S_s(\omega) = H(\omega)S_r(\omega) \quad (3.1)$$

where:

$S_s(\omega)$  = the spectral amplitude at the ground surface level

$S_r(\omega)$  = the spectral amplitude at the bedrock level

$H(\omega)$  = the linear transfer function

$\omega$  = the circular frequency in rad/sec

Most of these transfer functions have been theoretically derived and then verified with empirical data from either strong ground motion or microtremor recordings, although there has been much disagreement about the applicability of microtremor results because the material properties of the soil often remain in the linear range at these low levels of strain. A brief overview of the most commonly used linear transfer functions is given below. The various iterative methods for including the effects of non-linear soil material properties will not be discussed in this section, but Section 3.2.4 will include a brief treatment of non-linear soil behavior.

One of the first transfer functions developed for modeling spectral ratios is the Haskell-Thomson (Thomson, 1950) propagation matrix for a vertically traveling shear wave. This matrix relates the shear stress and displacement at the top of a soil layer to the stress and displacement at the bottom of the layer using parameters such as the frequency of the incoming shear wave, the soil layer thickness, and the shear wave velocity and damping in the layer (Seale and Archuleta, 1989). Newmark and Rosenblueth (1971) developed a linear transfer function for the ratio of pseudovelocity spectra between two layers based on the work of Kanai (1957). Their ratio is a function of the density of the material in each layer, the shear wave velocity in each layer, the predominant period of the soil site, and the predominant period of the incoming seismic waves.

Ohsaki (1982) also formalized a linear transfer function that uses the average shear wave velocity, depth, and damping coefficient in each layer to represent the spectral amplification of ground motion in a soil deposit. Tsai and Housner (1970) and Faccioli (1976) developed frequency-based soil amplification methodologies that use similar soil parameters but consider a more rigorous modal-superposition analysis.

The most commonly used transfer function model is included in the computer program SHAKE developed by Schnabel, et al. (1972). SHAKE discretizes the soil profile into several layers and uses an iterative technique to represent the non-linear behavior of the soil by adjusting the material properties at each iteration step. The required input information includes shear modulus vs. shear strain and damping coefficient vs. shear strain curves, the depth, shear wave velocity, and unit weight of each soil layer, the location of the water table, and the time history input at the base of the soil profile.

The SHAKE program is used in Section 3.2.3 to investigate soil parameter uncertainty and the effect of soil profile simplification.

Although the transfer function method of soil amplification is an improvement over the peak value multiplication factor method in its representation of the frequency contents of the earthquake motion and soil profile, there are a few criticisms of this technique (Ho, et al. 1991). The assumption of horizontal stratigraphy and vertically incident seismic waves may not adequately represent the true conditions. Equivalent linear models that employ iterative techniques can often over-simplify the actual non-linear behavior of the soil material. The simple transfer function models often capture the soil amplification effects only at the predominant period of the soil profile as illustrated for the Ohsaki (1982) model in Figure 3.1, and can often over-estimate the effects of resonance. Despite these drawbacks, transfer function methods are typically utilized in a regional multi-hazard seismic risk because they are able to give an adequate representation of soil amplification over a large region with a reasonable level of input and analysis effort.

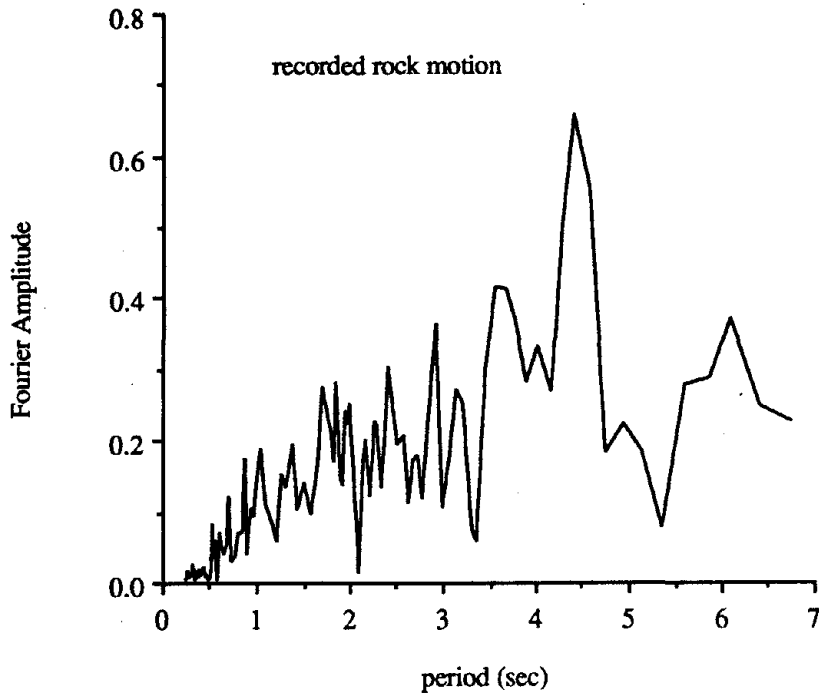
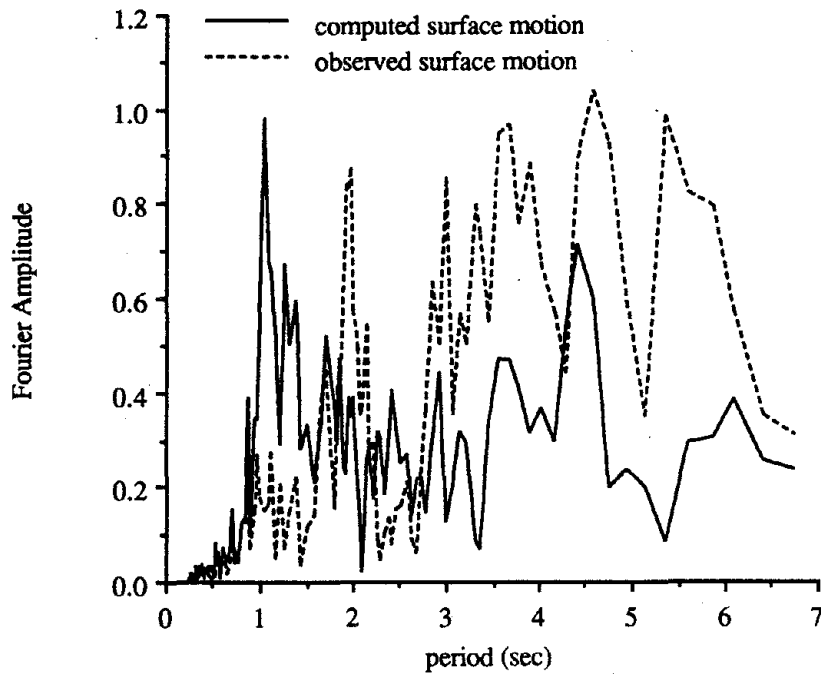
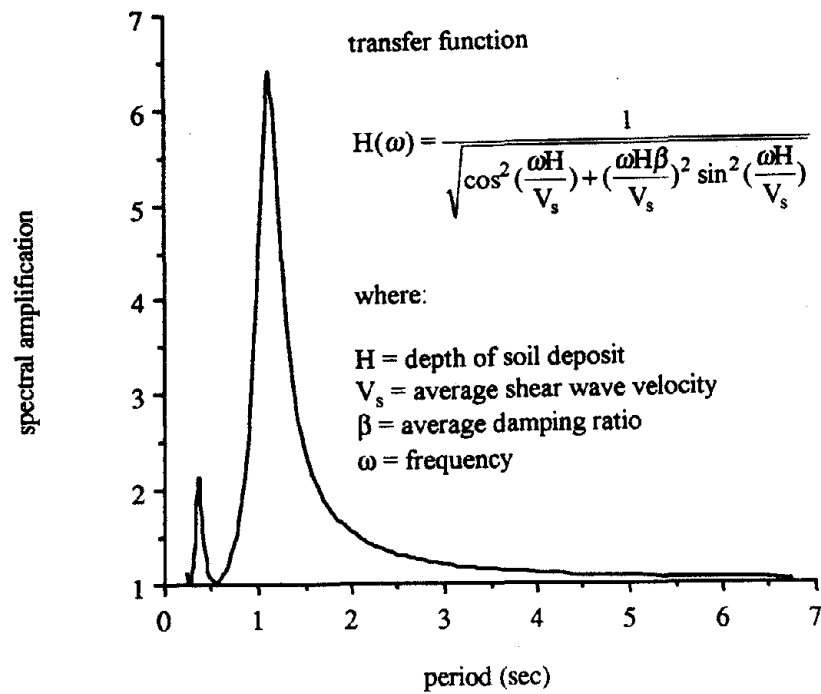


Figure 3.1. Illustration of the Ohsaki (1982) model for soil amplification.



**Figure 3.1.** Illustration of the Ohsaki (1982) model for soil amplification, continued.

### 3.2.3 Treatment of Soil Parameter Uncertainty

Soil parameter data play an important role in the seismic hazard modeling of local site effects, therefore this chapter would be incomplete without a discussion of the uncertainty associated with regional geologic and geotechnical data. Several analytical techniques for modeling spatial variability in soil parameter data, such as the method of kriging, have been proposed (Journel and Huijbregts, 1978, Journel, 1989, Vanmarcke, 1977, and Fenton and Vanmarcke, 1991). Other techniques involving a random vibration approach to certain hazard models have been suggested (Hong and Rosenblueth, 1987, Faccioli, 1972, Faccioli, 1976, and Christian, 1980). These are computationally too intensive for application over a wide region, therefore they are not considered in this dissertation.

The purpose of this section is to present the results of a simplified analysis for treating uncertainties in the dynamic response of soils. The analysis involves the use of the soil amplification computer program SHAKE (Schnabel, et al., 1972), previously discussed in Section 3.2.2, to study the effects of various soil property distributions on the ground motion response parameters. The error introduced by soil profile simplification is also treated in the analysis. A brief overview of the uncertainties associated with spatially-distributed geologic and geotechnical data as well as an example that applies some of the results of the uncertainty analysis in a GIS-based soil site characterization model are also presented in this section.

#### **Soil Parameter Data**

Difficulties in predicting the effects of local site conditions on seismic ground motions are typically due to (a) the lack of accurate information about the local soil properties; and (b) the lack of understanding about the true dynamic behavior of the geologic deposits (King and Kiremidjian, 1993). Uncertainty associated with soil dynamic behavior has been previously discussed in this chapter as regional modeling error and is typically considered an important research topic in the field of geotechnical engineering. Uncertainty associated with the often inaccurate and incomplete regional soil parameter data is the focus of this section. A thorough discussion of the problems and errors associated with compiling soil parameter data, particularly soil properties varying with depth for a regional study, is provided in Kiremidjian, et al. (1991).

The simplified uncertainty analysis presented in this section is based on the SHAKE computer program, therefore the uncertain soil parameters and the studied response values correspond to those used in this soil dynamics model for site amplification. Although this model provides a site-specific analysis, it is understood that the methodology could also be repeated over a grid or mesh of points for regional applications. This uncertainty analysis methodology can be extended to other local site effect hazard models, provided that the required input soil parameters can be explicitly defined and assigned probability distributions.

### **Uncertainty Analysis**

In order to study the effect of uncertainties in soil parameter data on ground motion response values and the error introduced by soil profile simplification, the SHAKE (Schnabel, et al, 1972) computer program for modeling site amplification through bi-linear soil dynamic behavior is used. The following soil properties are assumed to be uncertain in each layer:

- (1) Layer thickness,  $h_i$
- (2) Shear wave velocity,  $v_i$
- (3) Damping,  $\gamma_i$
- (4) Unit weight,  $w_i$

and the following surface ground motion response parameters are analyzed:

- (1) Post-strain site period
- (2) Peak ground acceleration
- (3) Maximum spectral amplification
- (4) Period at which the maximum spectral amplification occurs

The distributions on the soil properties are assumed to be either uniform, normal, or lognormal, with coefficients of variation of 25% and 35%. The mean values are assumed to be the measured data from bore-hole investigations at the site.

A case study is performed for a soil profile at Treasure Island with the recorded motion at Yerba Buena Island for the 1989 Loma Prieta Earthquake as the input rock motion. This well known soil-rock recording station pair is located in the San Francisco Bay. It is utilized here because several studies have shown the agreement between the

recorded surface motion at Treasure Island and the surface motion computed by using the SHAKE program with the Yerba Buena record as the input motion (Hryciw, et al, 1991, Idriss, 1991, and Seed, et al, 1990). The uncertainty analysis is conducted for four different discretizations of the soil profile. The resulting ground response values from 8,5,3, and 2 layer profiles are compared. In each case the total depth of the deposit is held constant, but adjacent layer soil parameters are combined to study the error introduced by assuming a simplified soil profile. Table 3.1 presents a summary description of the 36 uncertainty analysis cases performed for this study.

**Table 3.1.** Uncertainty analysis cases

CASE	DEPTH		SHEAR WAVE VELOCITY		DAMPING		UNIT WEIGHT	
	dist.	COV	dist.	COV	dist.	COV	dist.	COV
1	U	20%	U	20%	U	20%	U	20%
2	N	20%	N	20%	N	20%	N	20%
3	LN	20%	LN	20%	LN	20%	LN	20%
4	N	15%	N	20%	LN	20%	LN	15%
5	N	15%	N	30%	LN	30%	LN	15%
6	N	20%	N	25%	LN	25%	LN	20%
7	U	35%	U	35%	U	35%	U	35%
8	N	35%	N	35%	N	35%	N	35%
9	LN	35%	LN	35%	LN	35%	LN	35%

notes: U = uniform distribution  
N = normal distribution  
LN = lognormal distribution  
4 different layer discretizations were analyzed (2, 3, 5, and 8 layers)



Figure 3.2 shows the variation of the post-strain site period as a function of the number of layers in the soil profile for various distribution cases. The site period values increase from the 2-layer to the 3-layer case and then remain fairly constant. The uniform distribution produces an under-estimation of the site period, but the other distributions seem to have little effect. Figure 3.3 shows the resulting peak ground acceleration values plotted as a function of the number of layers for the different distribution cases. The acceleration values increase as the number of layers increase and appear to be insensitive to the various distribution types. Figure 3.4 shows the variation of maximum spectral amplification also as a function of the number of layers in the profile for various distribution cases. The results for spectral amplification are almost identical to those for peak ground acceleration in that the values increase with the increasing number of layers and they seem to be insensitive to distribution type. The final ground motion response value studied is the period at which the maximum spectral amplification occurs, shown in Figure 3.5 as a function of the number of layers for the different distribution types. As expected, these results parallel those for the post-strain site period shown in Figure 3.2. The period values decrease slightly but are generally insensitive to the number of layers, and the uniform distribution case produces an under-estimated value for the period.

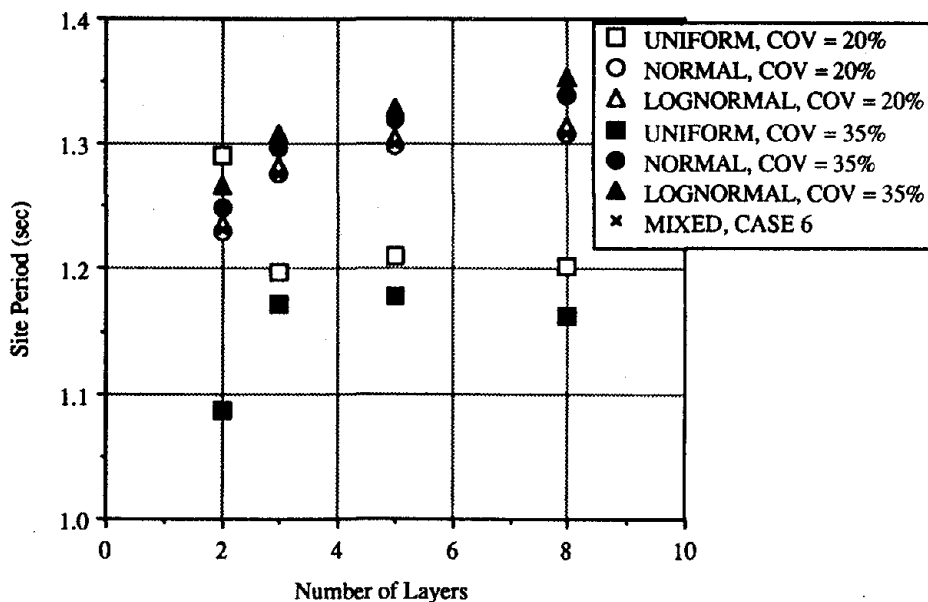


Figure 3.2. Post-strain site period as a function of the number of soil layers.

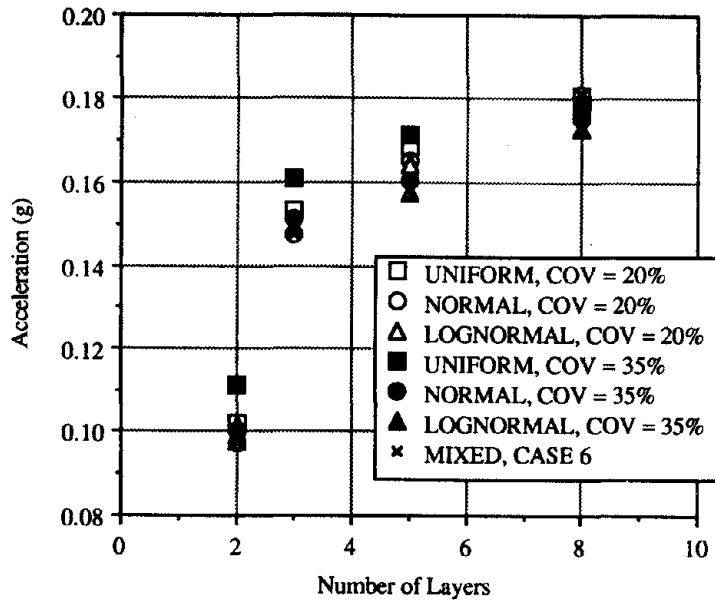


Figure 3.3. Surface PGA values as a function of the number of soil layers.

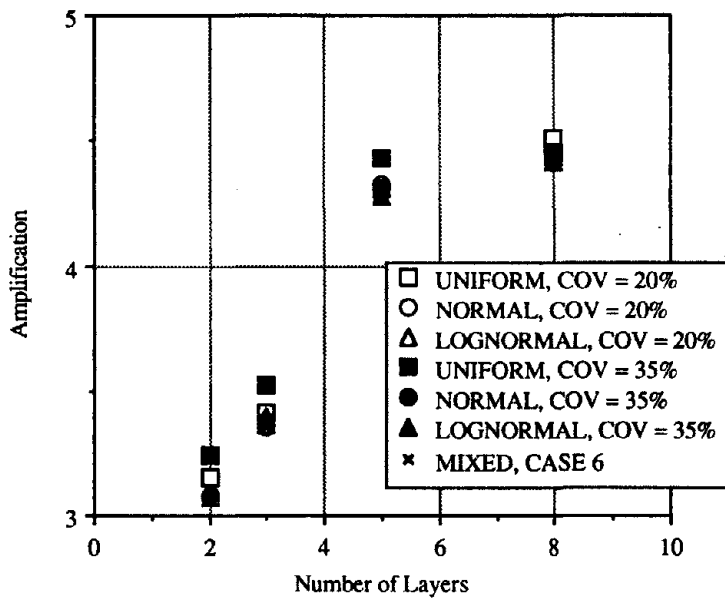
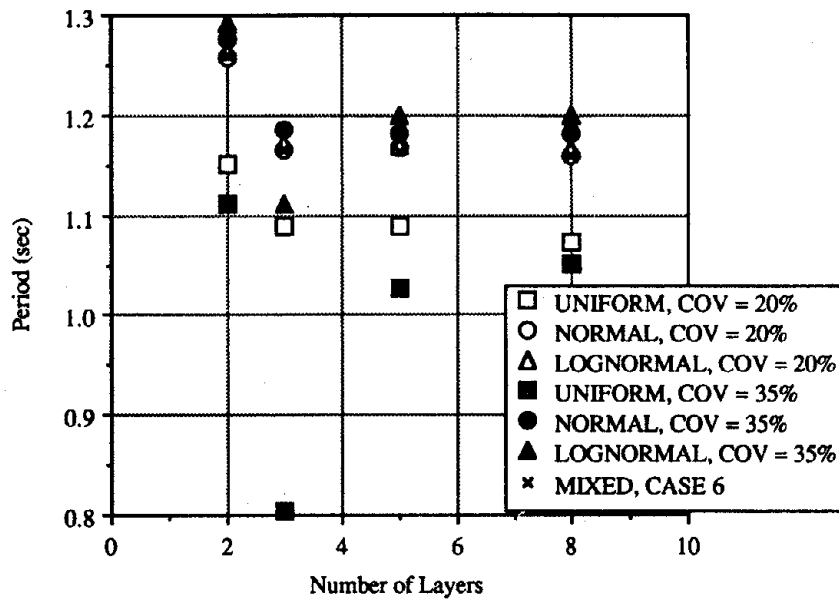


Figure 3.4. Maximum spectral amplification as a function of the number of soil layers.



**Figure 3.5.** Period of maximum spectral amplification as a function of the number of soil layers.

The results of this simple case study indicate that surface peak ground acceleration and maximum spectral amplification values are sensitive to the number of layers, but not to the type of distribution on the soil parameters. For post-strain site period and the period at which the maximum spectral amplification occurs, the results indicate that both response values are insensitive to the number of layers, but can be underestimated when the soil properties are assumed to be uniformly distributed. These results suggest that for regional evaluation of predominant site period, a simplified soil profile may be assumed, but for soil amplification estimation, a detailed soil profile is required.

### Observation of Sensitivity Study

The results of the case study presented here indicate that the modeling assumption of a simplified soil profile may be justified for regional estimates of predominant site period. This section illustrates an example GIS-based characterization of site period, assuming a simplified soil profile model. In this application the approximate predominant period,  $T$ , of a soil deposit is given as (Dobry, et al., 1976):

$$T = \frac{4H}{V_s} \quad (3.2)$$

where:

H = the thickness of the soil deposit

$V_s$  = the average shear wave velocity in the deposit

Figure 3.6 shows a map of the San Francisco Peninsula with regional predominant site periods estimated by equation 3.2. This microzone map is produced in the GIS by first combining the maps of surface and bedrock elevations shown in Figures 3.7 and 3.8 to give regional estimates for the depth of soil deposits. The surface geology map shown in Figure 3.9 and its related database, Table 3.2, giving estimates of average shear wave velocity for various geologic units, are then combined with the computed depth values according to equation 3.2. This simple example illustrates the proficiency of GIS technology for performing a regional analysis and displaying the results in an effective manner.

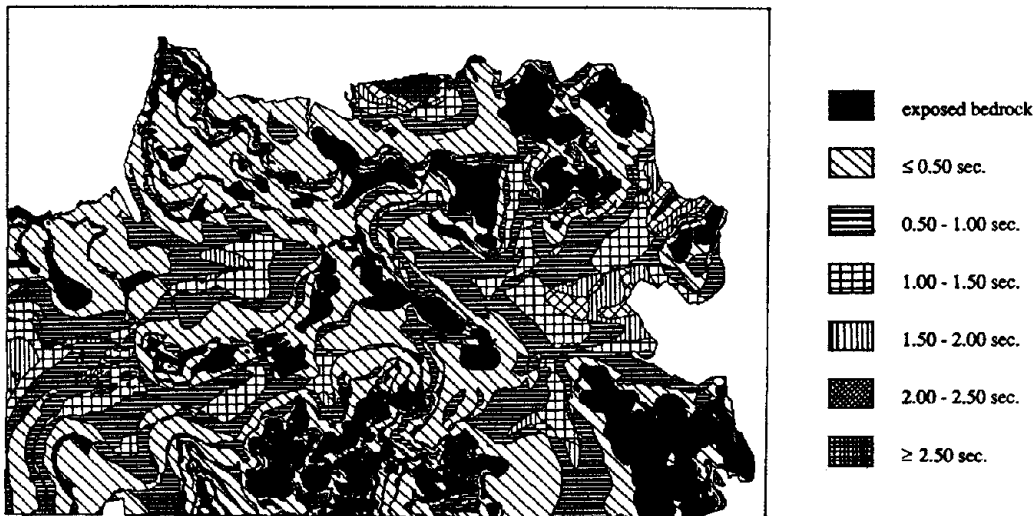


**Figure 3.6.** Map showing approximate predominant site periods in San Francisco, California.

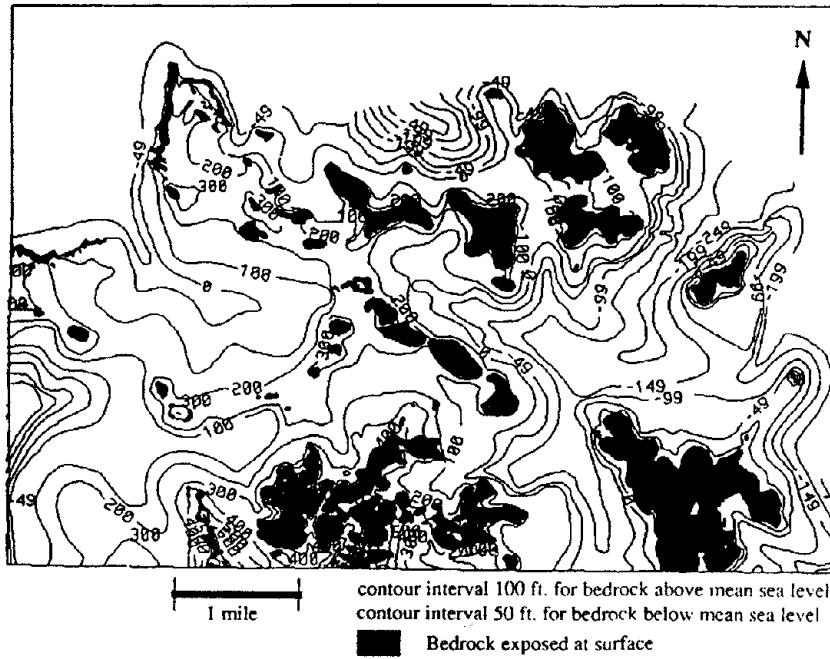


**Figure 3.7.** Map showing contours of bedrock elevation in San Francisco, California.

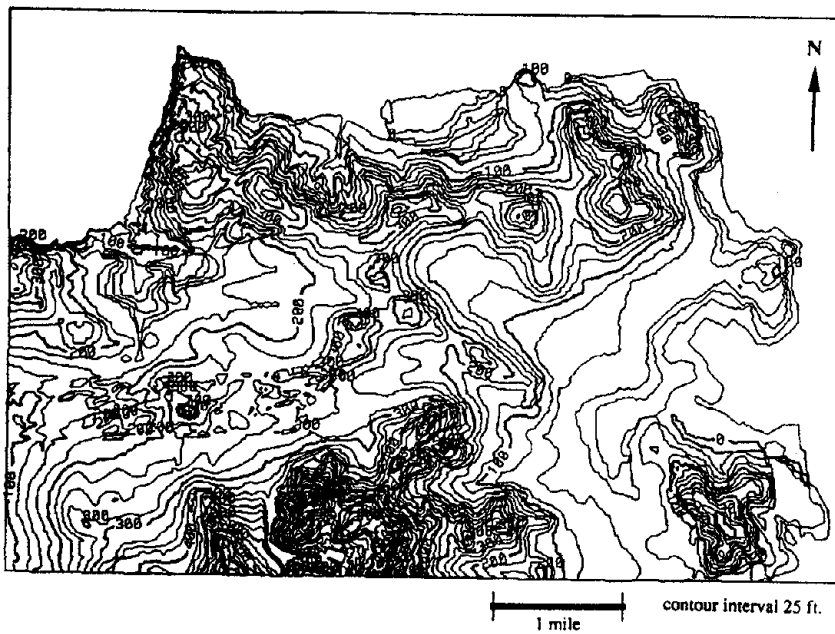


**Figure 3.8.** Map showing contours of surface elevation in San Francisco, California.

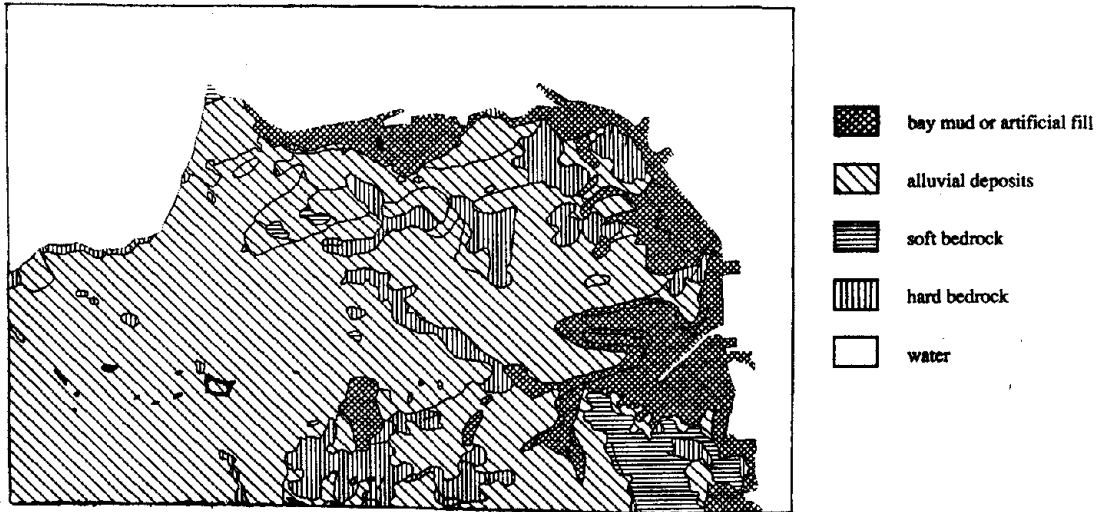


**Figure 3.9.** Map showing surface geologic units in San Francisco, California.

**Table 3.2.** Shear wave velocity parameters for surface geology units.

<b>GEOLOGIC UNIT</b>	<b>SHEAR WAVE VELOCITY (m/sec<sup>2</sup>)</b>	<b>S<sub>t</sub> PARAMETER</b>
bay mud / artificial fill	130	.6769
alluvial deposits	310	.2839
soft bedrock	445	.1978
hard bedrock	670	.1313

### 3.2.4 Dynamic Non-Linear Models

The third type of method for estimating soil amplification involves the use of dynamic non-linear models. These models are similar to the two previously discussed methods in that they idealize the soil profile as a system of horizontal layers with a vertically incident seismic motion at the base. However, the non-linear models are typically much more computationally intensive because they solve the dynamic equations of motion with time-step integration. The non-linear behavior of the soil material is usually modeled by hysteretic stress vs. strain and damping vs. strain relationships, and soil properties are updated at each time step to be compatible with the calculated level of strain. Although these models give the most accurate representation of the non-linear effects of soil on seismic motion, they typically require excessive computer time and very detailed site specific soil parameter information, often rendering them impractical for soil amplification analysis on regional basis. A brief overview of a few of the more commonly used dynamic non-linear models is included below for completeness.

Several dynamic non-linear models for characterizing the seismic response of a soil profile have been proposed in recent years, typically varying in the time-step integration technique and the hysteretic models used for representing non-linear soil material properties. Martin and Seed (1978) developed the computer program MASH that uses the cubic inertia time-step integration method for faster convergence and the Davidenkov stress-strain model for non-linear soil behavior. Joyner and Chen (1975) use a spring and friction element model for non-linear soil behavior and compare the results of their model using three different iteration techniques with the observed surface motion. Pyke (1979) compares several relationships for modeling the non-linear stress-strain behavior of soil including the Davidenkov model that gives shear stress in terms of shear strain, and the Ramberg-Osgood model that gives shear strain in terms of shear stress. Singh, et al. (1981) compare surface motions computed with the Ramberg-Osgood non-linear soil model and the SHAKE equivalent-linear analysis program with recorded ground motions at several study sites. They conclude that the non-linear model more accurately represents the true dynamic behavior of the soil profiles.

### 3.2.5 GIS-Based Regional Estimation of Surface Ground Motion

The spatial database structure of a geographic information system is ideal for estimating the effects of soil amplification of earthquake ground motion over a large

region. Three different types of soil amplification models were previously discussed in this section. The non-linear time-step integration methods are considered impractical for regional application and will not be further discussed in this dissertation. The linear transfer function models are typically the most widely used and give an adequate level of accuracy on a regional basis. The peak value multiplication factors are often the simplest and most efficient soil amplification models to apply over a large region, but they typically fail to capture non-linear soil behavior and the frequency contents of the ground motion and the soil profile.

A map showing the regional distribution of seismic motion at the bedrock level is estimated by applying an attenuation model with an assumed occurrence model or scenario event. The seismic motion can be in the form of a peak value for use in the multiplication factor models or in a spectral form for use in the transfer function models. Regional maps of the soil parameter data required for input to the assumed soil amplification model are then overlaid on the bedrock motion map to estimate the surface ground shaking in the region. An example application of GIS technology to regional soil amplification, utilizing the peak value multiplication factors developed by Kiremidjian, et al. (1991), is presented in this section.

The simplified example illustrates a GIS-based analysis for estimating surface peak ground acceleration (PGA) values for a region in San Francisco, California. Regional bedrock PGA values are estimated using the Joyner and Boore (1988) attenuation function with an assumed 7.0 magnitude event occurring on the northern section of the San Andreas Fault. Regional soil amplification factors are calculated using an empirical function developed by Kiremidjian, et al. (1991) based on 52 recorded motions from the 1989 Loma Prieta Earthquake. The PGA amplification is assumed to be a function of the depth to bedrock at the site, the average shear wave velocity of the soil in the top 30 meters, and the input PGA at the bedrock level. The regional surface PGA values are estimated according to the following equation:

$$A_s = \beta_a A_r \quad (3.3)$$

where:

$A_r$  = the PGA at the bedrock level

$A_s$  = the PGA at the surface level

$\beta_a$  = the soil amplification factor determined by the following equations:



$$\log\beta_a = [a_0 - a_1 \log A_T]^m - 1.5 \quad (3.4)$$

where:

$$a_0 = c_0 + c_1 S_t + c_2 \log d_p \quad (3.5a)$$

$$m = d_0 + d_1 S_t + d_2 \log d_p \quad (3.5b)$$

$$a_1 = e_0 + e_1 S_t + e_2 \log d_p \quad (3.5c)$$

$S_t$  = 88 / the shear wave velocity in the top 30 meters of soil

$d_p$  = the depth to bedrock at the soil site

$c_0, c_1, c_2, d_0, d_1, d_2, e_0, e_1, e_2$  = the regression constants

The regional depth to bedrock values ( $d_p$ ) in equation 3.5 are computed by overlaying the two maps of regional bedrock and surface elevation contours shown in Figures 3.7 and 3.8. The shear wave velocity factors ( $S_t$ ) in equation 3.5 are calculated from the regional surface geology map shown in Figure 3.9 and the related database table shown in Table 3.2. A map of buffer zones of regional bedrock PGA values ( $A_T$ ) was developed by applying the Joyner and Boore (1988) attenuation function to a map of the San Andreas Fault. The Joyner and Boore (1988) attenuation function is given by:

$$\log A_T = 0.43 + 0.23(M - 6) - \log(r_0^2 + h^2)^{1/2} - 0.0027(r_0^2 + h^2)^{1/2} \quad (3.6)$$

where:

$M$  = the magnitude of the assumed earthquake (7.0 in this example)

$r_0$  = the parallel distance from the buffer zone to the fault

The resulting map of buffer zones of regional bedrock PGA values ( $A_T$ ) is shown in Figure 3.10. Figure 3.11 shows the final map giving regional estimates of surface PGA values ( $A_s$ ) produced by combining the spatial soil parameter data contained in Figures 3.7 through 3.10 and Table 3.2 according to equations 3.3 to 3.5 given above.

The example described in this section is included in this dissertation only for purposes of illustrating the use of GIS technology in a regional soil amplification study. It shows the application of an amplification function over a large area, with regions of mapped values representing the variables in the equation. Rather than predicting site specific surface ground motions, the results are intended to give relative levels of surface PGA values for broad regions and to indicate areas requiring further detailed investigation.

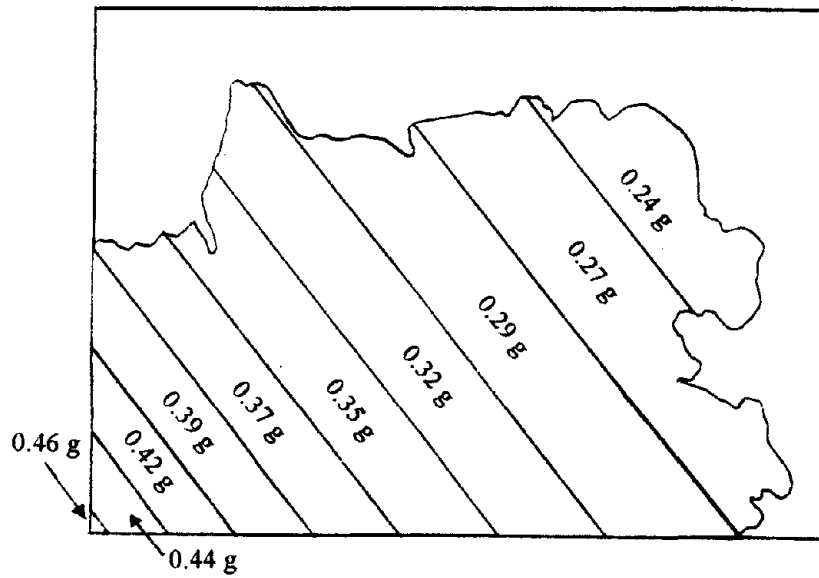


**Figure 3.10.** Map showing buffer zones of estimated bedrock PGA values in San Francisco, California.

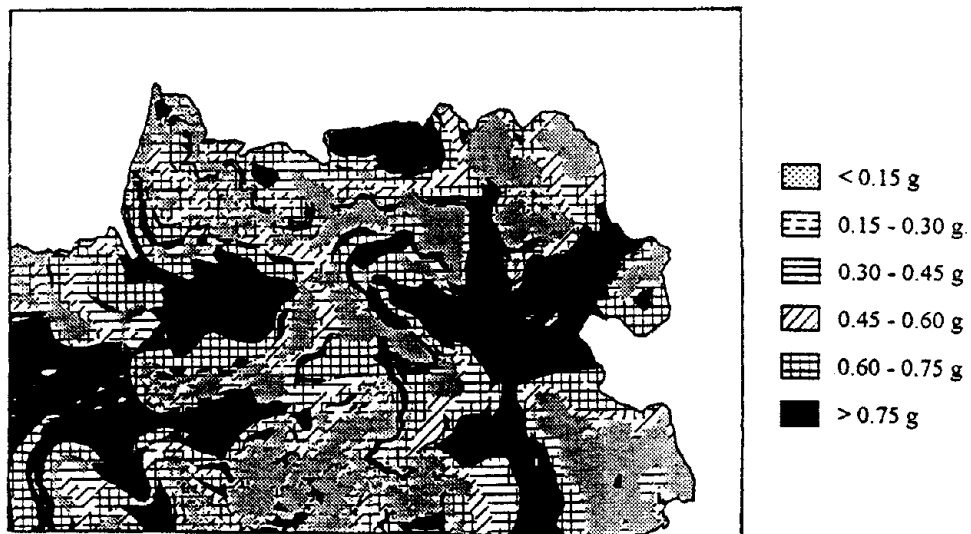


**Figure 3.11.** Map showing final estimates of final surface PGA values in San Francisco, California based on the Kiremidjian, et al. (1991) model.

### 3.3 Secondary Seismic Effects

Unlike the local site effect of soil amplification described above, the secondary seismic effects of liquefaction, landslide, and surface fault rupture have very few quantitative models associated with them. Microzone maps of hazard potential have been developed for these three effects for several regions. The hazard potential maps typically either give a "yes" or "no" estimation of occurrence for an assumed scenario earthquake, or they give a "high", "moderate", "low", or "very low" estimation of occurrence based on a given set of probability thresholds. The probabilities are typically associated only with the occurrence of ground shaking levels and do not include the occurrence of the site effects.

Very few probabilistic models for liquefaction, landslide, and surface fault rupture have been developed (Kiremidjian, 1992). For this reason, one of the most common methods for estimating these site effects in a regional multi-hazard seismic risk analysis is to just increase the level of estimated surface ground motion in areas where these effects are likely to occur. The definition of "likely to occur" is often very subjective and varies from study to study. Damage from the three effects, and in some cases ground shaking as well, is typically summed in a conservative manner. The remainder of Section 3.3 is devoted to an overview of the quantitative models that are available for estimating the secondary seismic effects of liquefaction, landslide, and surface fault rupture. A less conservative methodology for integrating these effects in the GIS environment is presented in Section 3.4, along with an illustrative example of the methodology.

#### 3.3.1 Liquefaction

Soil liquefaction is often described as the loss of shear strength in soil due to elevated pore water pressure (Chang, et al., 1991). Earthquake shaking induces shear stresses in the soil that cause the saturated cohesionless granular soil particles to rearrange and excess pore water pressures to build up. The damaging effects of soil liquefaction have been well recognized since the Niigata and Alaska Earthquakes of the early 1960s. The types of failures associated with liquefaction include: (a) sinking or overturning of structures; (b) excessive differential settlement of structures; (c) sand boils; and (d) surface lateral spreading. There are several factors that influence liquefaction such as the geologic history of the deposit, the depth of the ground water table, the grain size distribution, the density of the soil, and the ground slope, often requiring expert evaluation (Juang and

Elton, 1991). This detailed investigation is necessary for a site-specific soil liquefaction assessment, but more simplified models are required for quantitative analysis on a regional basis.

Regional liquefaction hazard mapping is typically done using either a geologic or a geotechnical technique (Juang and Elton, 1991). Table 3.3 shows one of the most well known geologic techniques developed by Youd and Perkins (1978). It gives a qualitative estimate ranging from "very high" to "very low" to indicate the likelihood of liquefaction in various soil deposits under seismic loading. During the past 25 years, several geotechnical techniques for analyzing soil liquefaction have been proposed, resulting from the need for a more quantitative estimate of regional liquefaction hazard. Most of these techniques involve the comparison of the cyclic stress ratio generated by an earthquake with the cyclic stress ratio which would be required to liquefy the soil (Youd, 1991).

The most commonly applied technique is that developed by Seed and Idriss (1971). They compute the cyclic stress ratio generated by the earthquake (CSRE) at a particular depth below the ground surface as:

$$\text{CSRE} = 0.65(a_{\text{max}} / g)(\sigma_0 / \sigma_0')r_d \quad (3.7)$$

where:

- $a_{\text{max}}$  = the PGA at the ground surface (in % of  $g$ )
- $g$  = the acceleration of gravity (in  $g$ )
- $\sigma_0$  = the total overburden stress in the soil at the depth in question
- $\sigma_0'$  = the effective overburden stress in the soil at the depth in question
- $r_d$  = the depth-dependent stress reduction factor

The cyclic stress ratio required to induce liquefaction of the soil (CSRL) is determined from empirical charts relating CSRL to corrected penetration resistance,  $(N_1)_{60}$ , calculated from standard penetration test (SPT) values as:

$$(N_1)_{60} = C_n(ER_m / 60)N_m \quad (3.8)$$

where:

- $C_n$  = the  $\sigma_0'$ -dependent correction factor
- $ER_m$  = the SPT measured potential energy value

**Table 3.3.** Estimated liquefaction susceptibility of geologic sediments during strong ground shaking (after Youd & Perkins, 1978).

TYPE OF DEPOSIT	GENERAL DISTRIBUTION OF COHESIONLESS SEDIMENTS IN DEPOSITS	LIKELIHOOD THAT COHESIONLESS SEDIMENTS, WHEN SATURATED, WOULD BE SUSCEPTIBLE TO LIQUEFACTION (BY AGE OF DEPOSIT)			
		<500 YR	HOLOCENE	PLEIS-TOCENE	PRE-PLEIS-TOCENE
(a) CONTINENTAL DEPOSITS					
River channel	Locally variable	Very high	High	Low	Very Low
Flood plain	Locally variable	High	Moderate	Low	Very Low
Alluvial fan and plain	Widespread	Moderate	Low	Low	Very Low
Marine terraces and plains	Widespread	---	Low	Very Low	Very Low
Delta and fan-delta	Widespread	High	Moderate	Low	Very Low
Lacustrine and playa	Variable	High	Moderate	Low	Very Low
Colluvium	Variable	High	Moderate	Low	Very Low
Talus	Widespread	Low	Low	Very Low	Very Low
Dunes	Widespread	High	Moderate	Low	Very Low
Loess	Variable	High	High	High	Unknown
Glacial till	Variable	Low	Low	Very Low	Very Low
Tuff	Rare	Low	Low	Very Low	Very Low
Tephra	Widespread	High	High	Unknown	Unknown
Residual soils	Rare	Low	Low	Very Low	Very Low
Sebka	Locally variable	High	Moderate	Low	Very Low
(b) COASTAL ZONE					
Delta	Widespread	Very high	High	Low	Very Low
Esturine	Locally variable	High	Moderate	Low	Very Low
Beach - High Wave	Widespread	Moderate	Low	Very Low	Very Low
Beach - Low Wave	Widespread	High	Moderate	Low	Very Low
Lagoonal	Locally variable	High	Moderate	Low	Very Low
Fore shore	Locally variable	High	Moderate	Low	Very Low
(c) ARTIFICIAL					
Uncompacted Fill	Variable	Very high	---	---	---
Compacted Fill	Variable	Low	---	---	---

$N_m$  = the measured SPT resistance value

The empirical charts estimate the CSRL needed to induce soil liquefaction for a given magnitude event and  $(N_1)_{60}$  value. The CSRE at the soil site due to the given magnitude earthquake is calculated by equation 3.7. If the computed CSRE is equal to or greater than the CSRL then liquefaction is assumed to occur at the site for the given earthquake event.

A more recently developed geotechnical method for evaluating soil liquefaction was proposed by Iwasaki, et al. (1982). This method is similar to the Seed and Idriss (1971) method described above in that it also involves the calculation of a stress ratio giving a "yes" or "no" answer for the occurrence of liquefaction, but the Iwasaki, et al. (1982) method goes one step further by attempting to quantify the severity of the liquefaction. The stress ratio or liquefaction resistance factor,  $F_L$ , is defined as:

$$F_L = R / L \quad (3.9)$$

where:

R = the soil liquefaction capacity factor

L = the dynamic load induced in the soil by the seismic motion

R is assumed to be a function of the SPT value and the effective overburden pressure in the soil and is calculated from equations for different ranges of mean grain size,  $D_{50}$ . The equation for calculating L is almost identical to that given for CSRE in equation 3.7. The severity of liquefaction is quantified with a liquefaction potential index,  $I_L$ , defined as:

$$I_L = \int_0^{20} Fw(z) dz \quad (3.10)$$

where:

z = the depth below the ground surface (in meters)

$F = (1 - F_L)$  for  $F_L \leq 1.0$  and  $F = F_L$  for  $F_L > 1.0$

$w(z) = (10 - 0.5z)$  for  $z \leq 20$  m. and  $w(z) = 0$  for  $z > 20$  m.

The computed values of  $I_L$  range from 0 for a non-liquefiable soil to 100 for a 20 meter thick layer of highly liquefiable soil. Based on observations at numerous Japanese soil

sites, Iwasaki, et al. (1982) concluded that sites with  $I_L$  greater than about 15 suffered severe liquefaction and sites with  $I_L$  less than about 5 were not likely to liquefy.

Because of the detailed site-specific data needed for the more quantitative geotechnical methods of analyzing soil liquefaction, the qualitative geologic methods have often been preferred for regional hazard estimation. However, with the recent improvements in geographic information systems for storage and analysis of spatial geotechnical data, the quantitative methods are quickly becoming more common in regional hazard analysis. Luna (1993) describes the implementation of the Iwasaki, et al. (1982) liquefaction potential index method in the GIS environment. Section 3.4 of this chapter discusses a methodology for combining the effects of liquefaction with those of the other local site conditions in a regional multi-hazard seismic risk analysis.

### 3.3.2 Landslide

The effects of earthquake-induced landslide have received much less research attention than the seismic effects of soil amplification and liquefaction discussed in the previous sections. Landslide hazard is typically very difficult to quantify because landslides come in many forms and are caused by a variety of processes. The local site factors that affect landslides generally include slope stability, geology, slope angle, hydrological conditions, vegetation, land use, and severity of the earthquake. Most of these factors are necessary for the investigation of an individual slope, but for seismically-induced landslide analysis on a broad regional basis, the factors are typically limited to slope angle, geology, location of previous landslides, magnitude of the seismic event, and distance from the seismic source (Hansen and Franks, 1991).

As with liquefaction, regional landslide hazard has traditionally been analyzed in a qualitative manner utilizing expert opinion, although recently more quantitative geotechnical methods have been proposed. The qualitative methods typically produce microzone maps indicating the relative susceptibility of various regions to landslides with no investigation into the possible triggering mechanisms for the land movement. The maps often result from an expert analysis of regional factors such as previous landslide locations, geologic deposits, and topography.

The complicated nature of the landslide process has made regional estimates of this local site effect very difficult to define quantitatively. Most of the recent research in this field has focused on determining the critical level of a given ground motion parameter that will trigger landslides in various geologic deposits. Wieczorek, et al. (1985) model a landslide as a translational failure on an infinite slope with a depth of 3 meters. They define three classes of geological units, assign shear strength parameters for each class, and then perform stability analyses using dry and saturated conditions to obtain the static factor of safety (FS) for each class. Based on the static FS, the critical acceleration to begin the process of slope failure,  $a_c$ , is computed as:

$$a_c = (FS - 1)g \sin\theta \quad (3.11)$$

where:

$\theta$  = the slope angle

FS = the factor of safety determined from a static slope stability analysis

$g$  = the acceleration of gravity

Several recorded strong ground motions were analyzed to develop average curves of induced landslide displacement versus  $a_c$ . The critical levels of displacement to produce structural damage are identified, such as 100 mm for cohesive slides and 20 mm for tensile rock slides (Wilson and Keefer, 1985). The  $a_c$  values that correspond to these assumed critical displacement values are determined from the displacement vs. acceleration curves. These  $a_c$  values are compared to the regional estimates of surface peak ground acceleration to give a prediction for the occurrence of damaging earthquake-induced landslides in the area.

There have been very few implementations of quantitative landslide hazard models in the GIS environment, therefore this method of analysis will not be discussed further in this dissertation. Instead, a qualitative approach utilizing regional maps showing relative susceptibility of landslides in various geologic deposits will be used to describe earthquake-induced landslide hazard. The GIS-based integration of this description of landslide hazard with the hazards associated with the other local site effects is described in Section 3.4 of this dissertation.



### 3.3.3 Surface Fault Rupture

The final local site effect to be considered is differential ground displacement due to surface fault rupture. Several empirical relationships have been developed for various faulting mechanisms that relate earthquake magnitude to length of fault rupture and length of fault rupture to horizontal ground displacement, but very few methods for estimating differential ground displacement hazard have been proposed. Kiremidjian (1984) formalized a methodology for determining probabilities of horizontal ground displacement at specific locations on a fault of finite length. This method is applied in the San Francisco Bay Area and includes a procedure for estimating stresses and strains induced in a pipe crossing the fault. The Applied Technology Council (ATC-13, 1985) defines two different zone widths around an active fault. For various magnitude earthquakes, differential fault displacements are estimated with corresponding expected damage factors for both subsurface and surface structures.

For a probabilistic seismic hazard and risk analysis in an area with well understood faulting mechanisms, the differential ground displacement model proposed by Kiremidjian (1984) is ideal for estimating fault rupture hazard. However, for a deterministic seismic hazard and risk analysis on a regional basis, the simplified procedure of defining specific buffer zones around an active fault and then estimating the corresponding differential displacement for the given faulting mechanism and various earthquake magnitudes (Applied Technology Council, ATC-13, 1985) is often adequate. This methodology may be too conservative in that the buffer zone is typically defined for the entire length of the active fault when in reality only a portion of the fault will rupture in an earthquake. For a scenario earthquake of given size and location, this methodology and the corresponding estimated damage factors for subsurface and surface structures provide an effective means of quantifying the local site effects of fault rupturing.

The seismic hazard associated with surface fault rupture is typically limited to a narrowly banded region, therefore this local site effect has received much less attention than liquefaction or landslide in earthquake engineering research. Public ordinances, such as the Alquist-Priolo Special Studies Zone Act of 1972 that restricts new construction within 50 feet of an active geologic fault in California, have reduced the regional risk associated with surface faulting. Most of the research in fault rupture hazard has been concerned with the risk to extended lifeline structures, such as highways, buried pipelines, bridges, tunnels, and canals, that unfortunately must sometimes cross active fault zones.

Studies applying GIS technology to differential displacement hazard have only recently been considered. The next section in this chapter presents a GIS-based methodology for estimating this hazard in conjunction with the other local site effects.

## 3.4 Hazard Integration in the GIS Environment

One of the major objectives of the work presented in this dissertation is the development and illustration of a GIS-based methodology for integrating the seismic hazards associated with the local site effects of soil amplification, liquefaction, landslide, and surface fault rupture. The local site effects and the various models for representing the hazard associated with each effect have been discussed in the previous sections of this chapter. When observing earthquake damage it is almost impossible to determine how much of the damage can be separately attributed to each local site effect, therefore the final regional seismic hazard distribution is based on a weighted average combination of the hazards associated with each effect. The basic steps in the hazard integration methodology are presented below followed by an example that illustrates the methodology for a hypothetical region. This section covers only the estimation of seismic hazard levels; the mapping from hazards to regional estimates of damage and losses is the subject of Chapter 4.

### 3.4.1 Integration Methodology

The regional seismic hazard integration methodology presented here is intended to be general enough so as to allow the application of more or less sophisticated models depending on the availability of information in the desired analysis region. Every analysis region is different, therefore the quantification of the secondary site effects and the weighting scheme for combining the various seismic hazards is heuristic, based on judgment and expert opinion about the influence of local site conditions in the region and the accuracy of the available geologic and geotechnical information. Section 3.4.2 illustrates a simplified example of seismic hazard integration for a hypothetical region. The basic steps in the methodology are listed below and illustrated in Figure 3.12.

- (1) A map showing the distribution of the bedrock-level ground shaking in the region is developed. The shaking can be described in terms of peak ground motion values, spectral values, or intensities. Sections 2.2.2 and 2.2.3

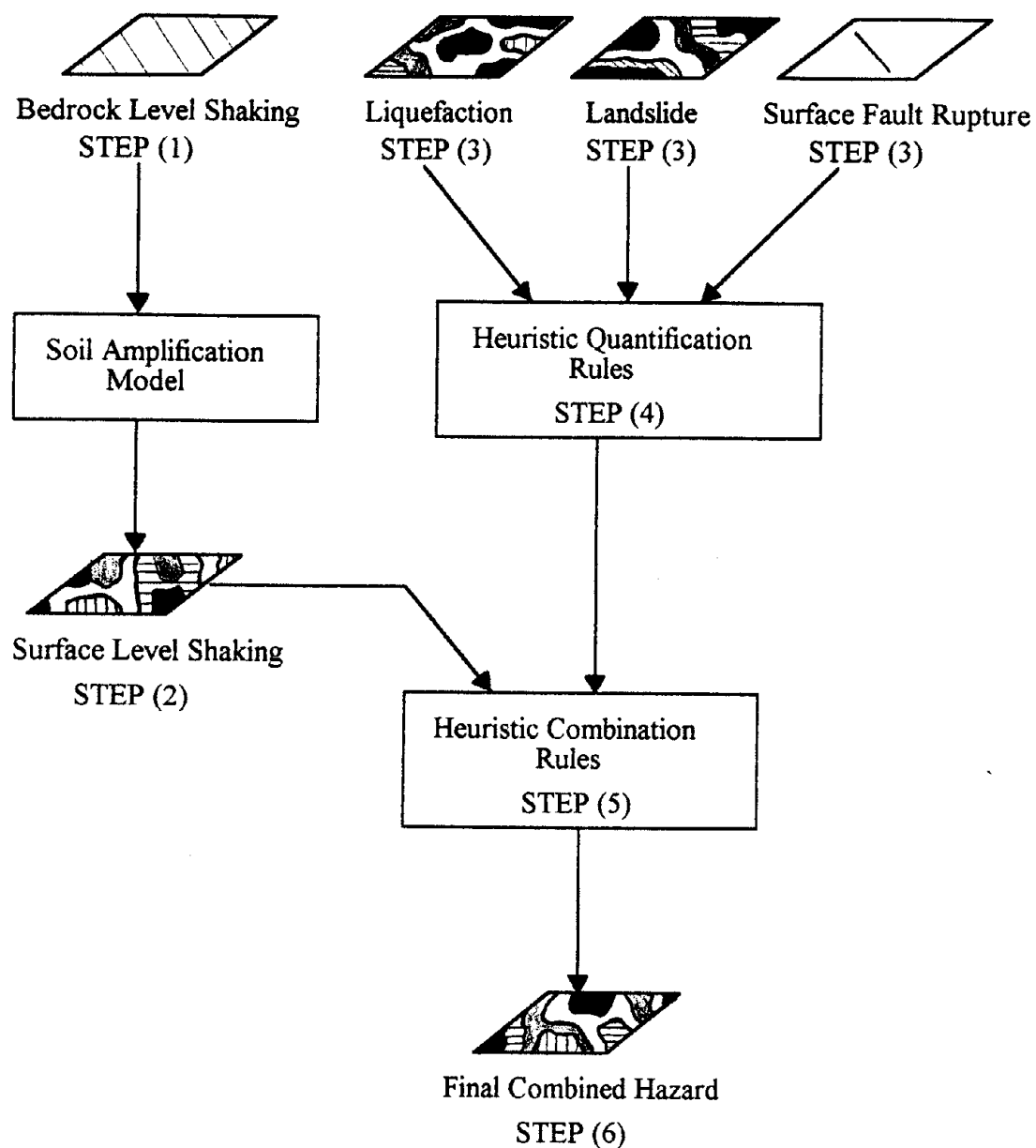


**Figure 3.12.** GIS-based seismic hazard integration.

discussed the modeling of earthquake occurrences and bedrock-level shaking.

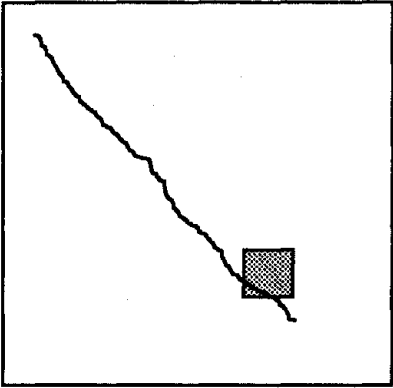
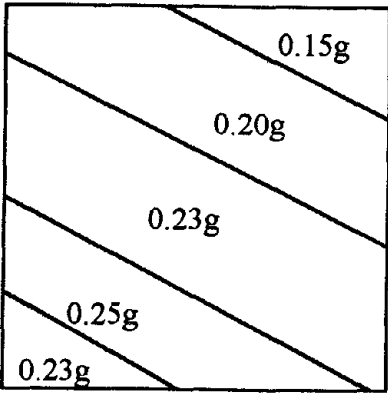
- (2) A map showing the distribution of the surface-level ground shaking in the region is developed. This shaking is described in the same manner as the bedrock-level ground shaking in Step (1). The various methods for soil amplification were discussed in Section 3.2.
- (3) Maps showing the distribution of hazards due to secondary site effects in the region are developed. Various models for these effects (surface fault rupture, liquefaction, and landslide) were described in Section 3.3.
- (4) Rules are defined to quantify the regional hazard distributions developed in Step (3). These rules are based on expert opinion about the local geology and the history of the severity of secondary seismic effects in the region. The rules should quantify the hazards in a consistent manner that allows them to be combined as described in Step (5).
- (5) Rules are defined to combine the seismic hazards of surface ground shaking and the local site effects of surface fault rupture, liquefaction, and landslide. The hazard combination rules are in the form of weighted averages with the weights determined by local expert opinion. The weights depend on knowledge about the behavior of the local geology and the relative accuracy associated with each hazard. The increased hazard due to two or more effects occurring simultaneously is also considered in these rules.
- (6) A final map showing the distribution of combined hazard in the region is developed by over-laying the maps developed in Steps (2) and (3) according to the heuristic rules defined in Steps (4) and (5).

### 3.4.2 Example Application

The hypothetical example presented in this section contains many simplifications to help illustrate the GIS-based seismic hazard integration methodology described in the previous section. The simplifications and assumptions correspond to the actual geologic and geotechnical information that is typically available for a comprehensive seismic hazard analysis conducted for a region such as a city or county. The case study presented in Chapter 5 discusses the currently available regional hazard information and provides a

more realistic example of the integration methodology. The simplified example of hazard combination for a hypothetical region is outlined in Table 3.4. The example maps and corresponding descriptions of the integration process are presented together for clarity.

**Table 3.4.** Example of hazard integration for a hypothetical region.

<b>DESCRIPTION OF SIMPLIFIED EXAMPLE OF HAZARD INTEGRATION</b>	
	<p>Figure (a) shows the assumed fault map of the area. The analysis region is indicated by the small square.</p>
	<p>Figure (b) shows the regional distribution of bedrock-level shaking. For simplicity, the ground shaking parameter is assumed to be PGA. The values are computed by assuming a scenario event on the fault shown in Figure (a) and then applying an attenuation relationship to the region.</p>

**Table 3.4.** Example of hazard integration for a hypothetical region, continued.

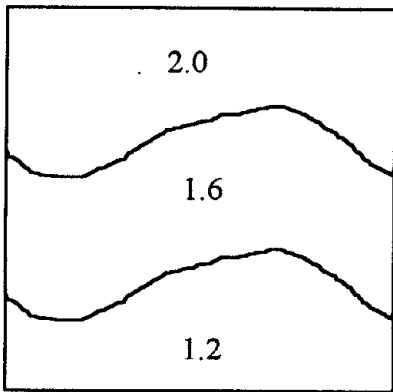


Figure (c)

Figure (c) shows the regional distribution of assumed PGA amplification factors based on the local geologic conditions in the area.

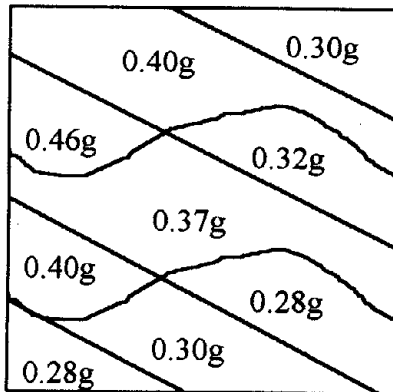


Figure (d)

Figure (d) shows the regional distribution of surface-level PGA values. This map is produced by over-laying the PGA amplification factor map shown in Figure (c) on the map of bedrock-level PGA values shown in Figure (b).

**Table 3.4.** Example of hazard integration for a hypothetical region, continued.

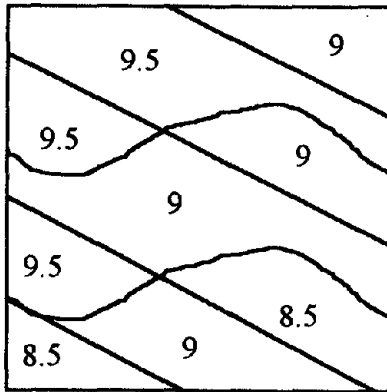


Figure (e)

It is assumed that the final combined seismic hazard will be quantified in terms of Modified Mercalli Intensity (MMI). This assumption allows for the use of previously derived relationships between MMI and structural damage for computing regional damages and losses as discussed in Chapter 4. There are several relationships for converting PGA to MMI. The equation used here was developed by Trifunac and Brady (1975) and is given as:

$$\log(\text{PGA}) = 0.014 + 0.3(\text{MMI}) \quad (1)$$

Figure (e) shows the regional distribution of ground shaking hazard ( $\text{MMI}_{\text{GS}}$ ). This map is developed by applying equation (1) to the map of surface-level PGA values shown in Figure (d). As discussed in Chapter 4, the MMI scale is subjective and assigned as integer values, therefore the  $\text{MMI}_{\text{GS}}$  values in Figure (e) are rounded to the nearest 0.5.

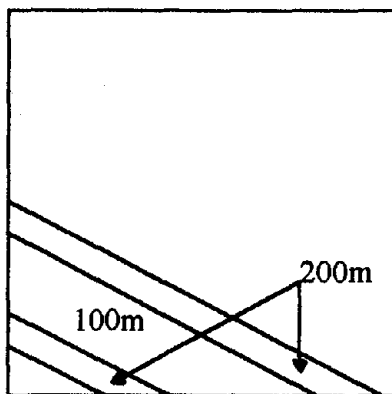


Figure (f)

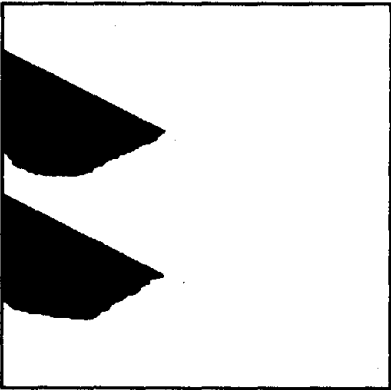
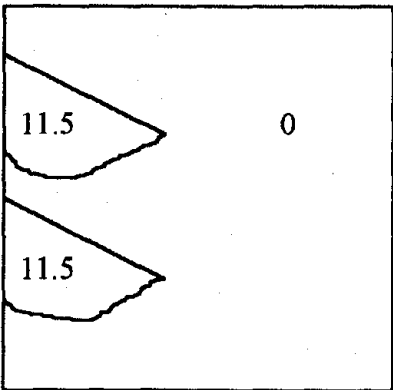
Figure (f) shows the buffer zones of 100 and 200 meters around the assumed fault rupture for the scenario event. The definition of these buffer zones is an example of the heuristic rules necessary to determine areas of surface fault rupture hazard.

**Table 3.4.** Example of hazard integration for a hypothetical region, continued.

	<p>To quantify the seismic hazard due to surface fault rupture hazard, the following heuristic rules are assumed for this example:</p>
<p>Figure (g)</p>	<p>For regions in the 100 meter buffer zone:</p> $MMI_{FR} = MMI_{GS} + 2 \quad (2a)$
	<p>For regions in the 200 meter buffer zone:</p> $MMI_{FR} = MMI_{GS} + 1 \quad (2b)$
	<p>Otherwise:</p> $MMI_{FR} = 0 \quad (2c)$
<p>Figure (g) shows the regional distribution of surface fault rupture hazard (<math>MMI_{FR}</math>). This map is developed by over-laying Figure (f) on the map of ground shaking hazard (<math>MMI_{GS}</math>) shown in Figure (e) according to equations 2a through 2c.</p>	
	<p>Figure (h) shows the assumed regional distribution of critical surface PGA values (<math>A_{crit}</math>) required to induce liquefaction based on geotechnical investigations.</p>
<p>Figure (h)</p>	



**Table 3.4.** Example of hazard integration for a hypothetical region, continued.

	<p>Figure (i) shows the regional distribution of liquefiable soils. This map is produced by over-laying Figure (h) on the map of surface-level PGA values shown in Figure (d). Areas with liquefiable soils (<math>A_{crit} \leq</math> the surface-level PGA value) are shown here in black.</p>
<p>Figure (i)</p>	<p>The following example heuristic rules are used to quantify the seismic hazard due to liquefaction:</p>
	<p>For regions with liquefiable soils:</p>
<p>Figure (j)</p>	$MMI_{LIQ} = MMI_{GS} + 2 \quad (3a)$
<p>developed by over-laying Figure (i) on the map of ground shaking hazard (<math>MMI_{GS}</math>) shown in Figure (e) according to equations 3a and 3b.</p>	<p>Otherwise:</p>
	$MMI_{LIQ} = 0 \quad (3b)$

**Table 3.4.** Example of hazard integration for a hypothetical region, continued.

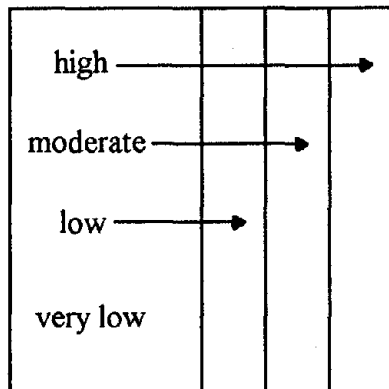


Figure (k)

Figure (k) shows the assumed qualitative description of landslide hazard in the region. Areas are designated as having "high", "moderate", "low", or "very low" landslide potential.

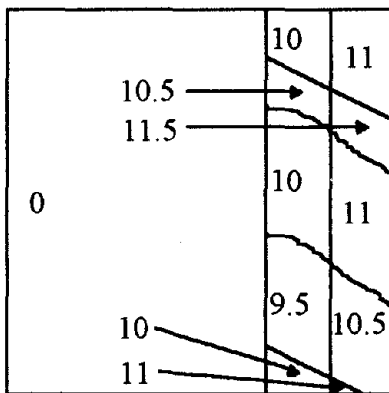


Figure (l)

To quantify the seismic hazard due to landslide ( $MMI_{LAN}$ ), the following heuristic rules are assumed for this example:

For regions designated as "high":

$$MMI_{LAN} = MMI_{GS} + 2 \quad (4a)$$

For regions designated as "moderate":

$$MMI_{LAN} = MMI_{GS} + 1 \quad (4b)$$

Otherwise:

$$MMI_{LAN} = 0 \quad (4c)$$

Figure (l) shows the regional distribution of landslide hazard ( $MMI_{LAN}$ ). This map is developed by over-laying Figure (k) on the map of ground shaking hazard ( $MMI_{GS}$ ) shown in Figure (e) according to equations 4a through 4c.

**Table 3.4.** Example of hazard integration for a hypothetical region, continued.

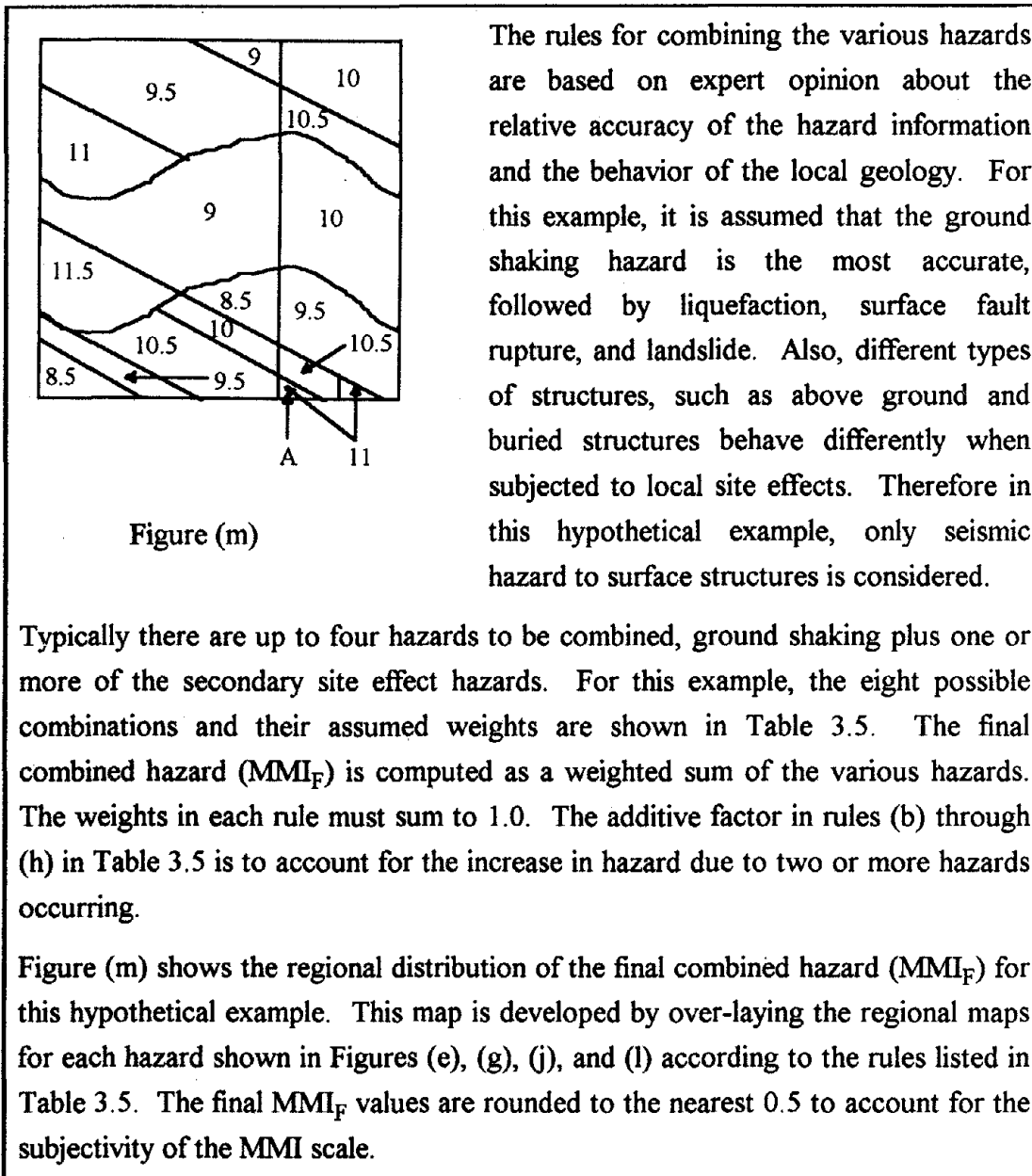


Table 3.5. Example heuristic rules for seismic hazard integration.

RULE	POSSIBLE HAZARDS	WEIGHTING SCHEME FOR FINAL COMBINED HAZARD (MMI <sub>F</sub> )
(a)	ground shaking	$MMI_F = MMI_{GS}$
(b)	ground shaking + liquefaction	$MMI_F = .55MMI_{GS} + .45MMI_{LIQ} + 0.5$
(c)	ground shaking + fault rupture	$MMI_F = .60MMI_{GS} + .40MMI_{FR} + 0.5$
(d)	ground shaking + landslide	$MMI_F = .65MMI_{GS} + .35MMI_{LAN} + 0.5$
(e)	ground shaking + liquefaction + fault rupture	$MMI_F = .40MMI_{GS} + .30MMI_{LIQ} + .30MMI_{FR} + 1.0$
(f)	ground shaking + liquefaction + landslide	$MMI_F = .40MMI_{GS} + .35MMI_{LIQ} + .25MMI_{LAN} + 1.0$
(g)	ground shaking + fault rupture + landslide	$MMI_F = .45MMI_{GS} + .30MMI_{FR} + .25MMI_{LAN} + 1.0$
(h)	ground shaking + liquefaction + fault rupture + landslide	$MMI_F = .30MMI_{GS} + .25MMI_{LIQ} + .25MMI_{FR} + .20MMI_{LAN} + 1.5$

notes:

1.  $MMI_F$  must be less than or equal to 12.
2.  $MMI_{GS}$  = ground shaking hazard from Table 3.4, Figure (e).
3.  $MMI_{FR}$  = surface fault rupture hazard from Table 3.4, Figure (g).
4.  $MMI_{LIQ}$  = liquefaction hazard from Table 3.4, Figure (j).
5.  $MMI_{LAN}$  = landslide hazard from Table 3.4, Figure (l).

The numerical computations carried out in the GIS during this hazard integration can be illustrated by considering the small area indicated by "A" on Figure (m) in Table 3.4. This area has a final combined seismic hazard of  $MMI_F = 11$ , computed as follows:

$$MMI_{GS} = 9 \quad (\text{Table 3.4, Figure (e)})$$

$$MMI_{FR} = 11 \quad (\text{Table 3.4, Figure (g)})$$

$$MMI_{LIQ} = 0 \quad (\text{Table 3.4, Figure (j)})$$

$$MMI_{LAN} = 10 \quad (\text{Table 3.4, Figure (l)})$$

Rule (g) from Table 3.5 applies for this area and is given as:

$$MMI_F = .45MMI_{GS} + .30MMI_{FR} + .25MMI_{LAN} + 1.0$$

which results in:

$$MMI_F = .45 \times 9 + .30 \times 11 + .25 \times 10 + 1.0 = 10.85 \approx 11$$

The example presented here is only hypothetical and cannot be compared to empirical data. The intent is to illustrate the general methodology for a GIS-based integration of the seismic hazards associated with local site effects. Several simplifying assumptions were made, but the integration process can easily be extended to include more analytical hazard models, different heuristic region-specific hazard combination rules, and empirical data verification.

## 3.5 Summary

This chapter covers several topics concerning local site conditions, therefore a summary section is included to highlight the main points.

Section 3.2 covered the various methods for soil amplification, including empirical multiplication factors, theoretical transfer functions, and dynamic non-linear models. An uncertainty analysis was carried out for one of the commonly used theoretical transfer function methods. The results indicated that a simplified soil profile may be adequate for regional estimates of site predominant period. This was illustrated in a GIS-based application for a region in the San Francisco Bay area. A second example of the use of

GIS technology for regional seismic hazard analysis was described in Section 3.2.5. Surface ground motion values were estimated for the same region in the San Francisco Bay area using one of the empirical multiplication factor methods.

Section 3.3 discussed the secondary seismic effects, namely liquefaction, landslide, and surface fault rupture. An overview of each secondary effect was given, including a description of the currently available techniques for modeling the associated hazards.

A GIS-based seismic hazard integration methodology was described in Section 3.4. The general steps for combining the hazard associated with ground shaking, liquefaction, landslide, and surface fault rupture in a heuristic weighted average approach were identified. A hypothetical example was included to illustrate the integration methodology. The extension from seismic hazard to damage and loss estimation, as well as a general overview of earthquake damages and losses, is the subject of Chapter 4.

## CHAPTER 4

# EARTHQUAKE DAMAGE AND LOSS ESTIMATION

---

### 4.1 Structural Inventories

The development of a complete and detailed inventory of structures is typically the most crucial, time consuming, and expensive component of a regional seismic risk analysis. The accuracy of the final regional estimates of damage and loss is highly dependent upon the accuracy of the underlying structural inventory developed for the area. Although the accumulation of inventory data on a structure-by-structure basis would produce the most accurate inventory, this method is neither practical nor feasible for a regional study. The most widely used methods typically involve a consolidation of the information contained in various existing structural inventory databases. Vasudevan, et al. (1992) developed a methodology for compiling an integrated inventory of buildings and Rentzis, et al. (1992) applied this methodology to the development of a building inventory based primarily on the Tax Assessor's database for the city of Palo Alto, California. French, et al. (1991) presents a thorough discussion of building inventory development, including an overview of existing data sources and schemes for classifying buildings. Emmi and Horton (1993) developed an inventory of residential and commercial buildings in Salt Lake County, Utah for use in an earthquake property damage and casualty risk analysis. The Applied Technology Council (ATC-25, 1991) compiled an inventory of all major lifelines in the United States from information contained in various government databases.

These and other regional earthquake damage and loss studies have typically involved structural inventory development for one specific type of facility, such as residential and commercial buildings, water systems, highway bridges, government buildings, and emergency facilities. One of the major components of the work presented

in this dissertation is a methodology for compiling a complete and detailed structural inventory for all facility types, particularly for a regional damage and loss assessment utilizing geographic information system technology. Structural inventory development typically involves four major parts: (a) identification of required inventory information or database attributes; (b) acquisition and review of available data sources; (c) development of engineering classification schemes; and (d) integration and compilation of the complete inventory. The remainder of Section 4.1 discusses these four issues and an example illustration of this methodology for regional structural inventory development is presented in Chapter 5.

### 4.1.1 Required Inventory Information

The information to be included in a structural inventory often depends upon the classes of facilities under consideration and the type of analysis being conducted. For the most general regional seismic hazard and risk analysis, information about the location, use, and structural properties of each facility is typically desired. Several studies have discussed characteristics of structural inventories in detail (Applied Technology Council, ATC-13, 1985, Rentzis, et al, 1992, Vasudevan, et al., 1992, and French, et al. 1991), therefore only a brief overview of the desired inventory information is given in this section. Even for a small region, the databases of structural inventory information can quickly become very large, resulting in excessive computer storage and inefficient analyses. For this reason, the number of included data attributes should be kept to a minimum through the use of several inter-related database tables in the inventory compilation methodology.

The data attributes most commonly required for a structural inventory include:

- (a) *Location Attributes.* Information such as street address, longitude and latitude, and U.S. Census Tract, used in determining the ground shaking and other local site effects to which the structure may be subjected.
- (b) *Use Attributes.* Information such as a use code or social function class (Applied Technology Council, ATC-13, 1985), used in determining losses (replacement or repair cost, loss of business use, casualties, and other socio-economic effects).



- (c) *Structural Property Attributes.* Information such as construction material, type of framing system, age, height, square footage, length, and present condition, used to determine the engineering classification (Applied Technology Council, ATC-13, 1985) or indicate the expected structural damage for a given ground shaking parameter.

The available databases for compiling an inventory of structures can often be incomplete, out-dated, inaccurate, or available only in paper format. The compilation of a complete and accurate structural inventory typically requires the integration of several existing databases of information from various public and private sources. Missing attributes are often inferred from known data by use of expert opinion or fuzzy logic. Recent advances in computer software technology, namely geographic information systems, relational database management systems, and expert systems have increased the efficiency and accuracy of structural inventory development. Section 4.1.2 describes the various available databases and Section 4.1.3 discusses the inference of missing attributes, primarily the assignment of earthquake engineering and social function classifications. Finally the integration and consolidation of information for a complete and accurate inventory of structures, including the use of geographic information system technology, is addressed in Section 4.1.4.

## 4.1.2 Sources of Inventory Data

There are numerous available databases for inventory development that vary greatly in completeness, accuracy, and type of included information. The use of these databases can result in large reductions in the time and cost associated with developing a complete inventory of structures for a region. The databases most commonly used as sources of inventory data include: (a) Federal Government Databases; (b) State Government Databases; (c) Local Government Databases; and (d) Private Sector Databases. Only a brief overview of these four sources of inventory data is given below, as several studies have provided detailed reviews of the various available databases, including their data attributes, area of coverage, accuracy, completeness, cost to obtain, media format, and frequency of update (see Applied Technology Council, ATC-13, 1985, French, et al. 1991, Vasudevan, et al. 1992, and Rentzis, et al. 1992).

- (a) *Federal Government Databases.* Two common sources of data are the Federal Emergency Management Agency (FEMA) and the U.S. Census Bureau. FEMA maintains numerous databases of information for various facilities and various business sectors on the national, state, and local levels. The U.S. Census Bureau has databases of population, housing, economics, and linear features for various geographical areas.
- (b) *State Government Databases.* Examples of these include the California State Architect's database of information on all state-owned buildings, the California Seismic Safety Commission's database of unreinforced masonry buildings, the various databases typically belonging to a state's Department of Transportation, and the databases maintained by state universities.
- (c) *Local Government Databases.* These are often the most commonly used and include such sources as the County Tax Assessor's files, the various databases maintained by school districts, the public utilities databases of lines and other equipment, the county and city building permit files, and other databases containing regional information about facilities such as police stations, hospitals, fire stations, and emergency broadcast stations.
- (d) *Private Sector Databases.* Several private companies and agencies have compiled databases of information on various facilities for specific purposes. Examples of these include the Insurance Services Office's files of large buildings for fire risk assessment, the Real Estate Multiple Listing of property currently for sale, the private utilities databases of lines and other equipment, the Dun and Bradstreet database of business establishments, the various databases maintained by religious districts, and several databases developed from satellite imagery processing.

### 4.1.3 Classification and Inference Schemes

Prior to the development of an inventory of structures, two classification systems are typically required. One system classifies each structure according to its structural response to earthquake excitation for purposes of regional damage estimation. The second system classifies each structure according to its use and provides for the regional estimation of monetary and non-monetary losses. Almost every study of regional damage and loss assessment has developed definitions for these two classification systems. The most widely used are the Earthquake Engineering Facility Classification and the Social Function Classification developed by the Applied Technology Council (ATC-13, 1985) for all facility types in California. Although these definitions are for a specific region, they are very comprehensive and can easily be modified for use in other regions as illustrated in the case study presented in Chapter 5.

The use of existing databases for inventory development typically requires the application of expert systems or fuzzy logic for inferring missing data attributes and for assigning the two classifications discussed above. These classification and inference rules are highly dependent upon the content and format of the inventory data sources and the expert knowledge about the history and current state of structural development in the study region. Rules for inferring missing data attributes and assigning classifications are often based either upon statistical relationships developed in nearby regions or upon the opinions of experts in the area. The use of secondary data sources with broad regional averages is another means of inferring database information. Occasionally there is not enough known information to make an exact data inference, therefore a rule may assign probabilities or weights to inferred data. Examples of three basic types of classification and inference rules are listed below. The case study presented in Chapter 5 illustrates the use of similar rules in the development of a regional inventory of structures.

(a) *Example rule for inferring missing data attributes:*

**IF** (census tract = 1001 and material = wood)

**THEN** (date built = 1970)

(b) *Example rule for assigning earthquake engineering classification:*

**IF** (use = residential and date built < 1950 and number of stories = 1)

**THEN** (engineering class = unreinforced masonry)

(c) *Example rule for assigning social function classification:*

**IF** (date built > 1980 and number of stories = 2 and material = light metal)

**THEN** (social function class = 50% light industrial and 50% heavy industrial)

#### 4.1.4 Inventory Compilation Methodology

The previous sections of this chapter have given a brief overview of the various aspects of regional inventory development including the required information, the sources of data, and the classification and inference schemes. This section describes a methodology for integrating and combining the various available data sources in order to develop a complete regional inventory of structures. Integration methodologies have been developed for building inventories by French, et al (1991), Vasudevan, et al. (1992), and Rentzis, et al. (1992), and for lifelines by the Applied Technology Council (ATC-25, 1991). Very few studies have considered the development of a complete and accurate inventory of all facilities for a regional earthquake damage and loss estimation (Applied Technology Council, ATC-13, 1985, Massachusetts Civil Defense Agency, 1991, and Applied Technology Council, ATC-36, in progress).

The methodology for compiling a regional inventory of all facilities depends upon the contents and format of the available sources of data. It is assumed that the inventory is for a large region in which several electronic databases of various structural information already exist, therefore the use of field survey techniques is considered only as a last resort for certain facility types. Several inter-related database tables of facility characteristics are used to describe the regional exposure to earthquake damage and losses. The use of inter-related tables helps to reduce the large amount of required data storage by eliminating repeated attributes through the use of relational identification numbers or indexed values.

Figure 4.1 shows a simplified example subset of database tables in a final inventory of structures. A more thorough example of the integration methodology as well as the use of the inventory in a regional earthquake loss estimation is illustrated in the case study presented in Chapter 5. The basic steps in compiling a regional structural inventory, such as that shown in Figure 4.1, include:

- (1) Determine the data attributes to be included in each table and the interaction among the various database tables in the final structural inventory.
- (2) Determine the use or social function classification to be used in the inventory.
- (3) Determine the structural or earthquake engineering classification to be used in the inventory.
- (4) For each major social function class defined in Step (2), identify and acquire the first and second level sources (based on completeness and accuracy) of available database information.
- (5) Analyze the available database information in each source and consult local experts to define heuristic rules for inferring minor social function classifications, earthquake engineering classifications, and missing data attributes.
- (6) Apply the rules defined in Step (5) for each first level source identified in Step (4) to fill in the final inventory tables defined in Step (1).
- (7) Apply the rules defined in Step (5) for each second level source identified in Step (4) to check the accuracy of the information contained in the final inventory tables for each major social function class. This check is typically done by one of the following three methods:
  - (a) *Geographic Location.* A geographic information system allows several sets of database information to be mapped and overlaid for identification of data discrepancies. A GIS can also be used for address matching and for the application of inference rules that may involve spatial instead of tabular data manipulations.
  - (b) *Regional Averages.* Existing databases of broad regional averages can be used to identify areas that appear to be missing or over-estimating data.
  - (c) *Expert Opinion.* Local experts familiar with the history and current state of structural development in the region can help to identify possible data errors.

- (8) Determine if the desired level of accuracy and completeness has been achieved for the final inventory of structures. If not, identify those major social function classes requiring further inventory development and either repeat steps (4) through (7) with alternative existing databases (third and fourth level sources), or utilize field survey techniques to compile the final inventory.

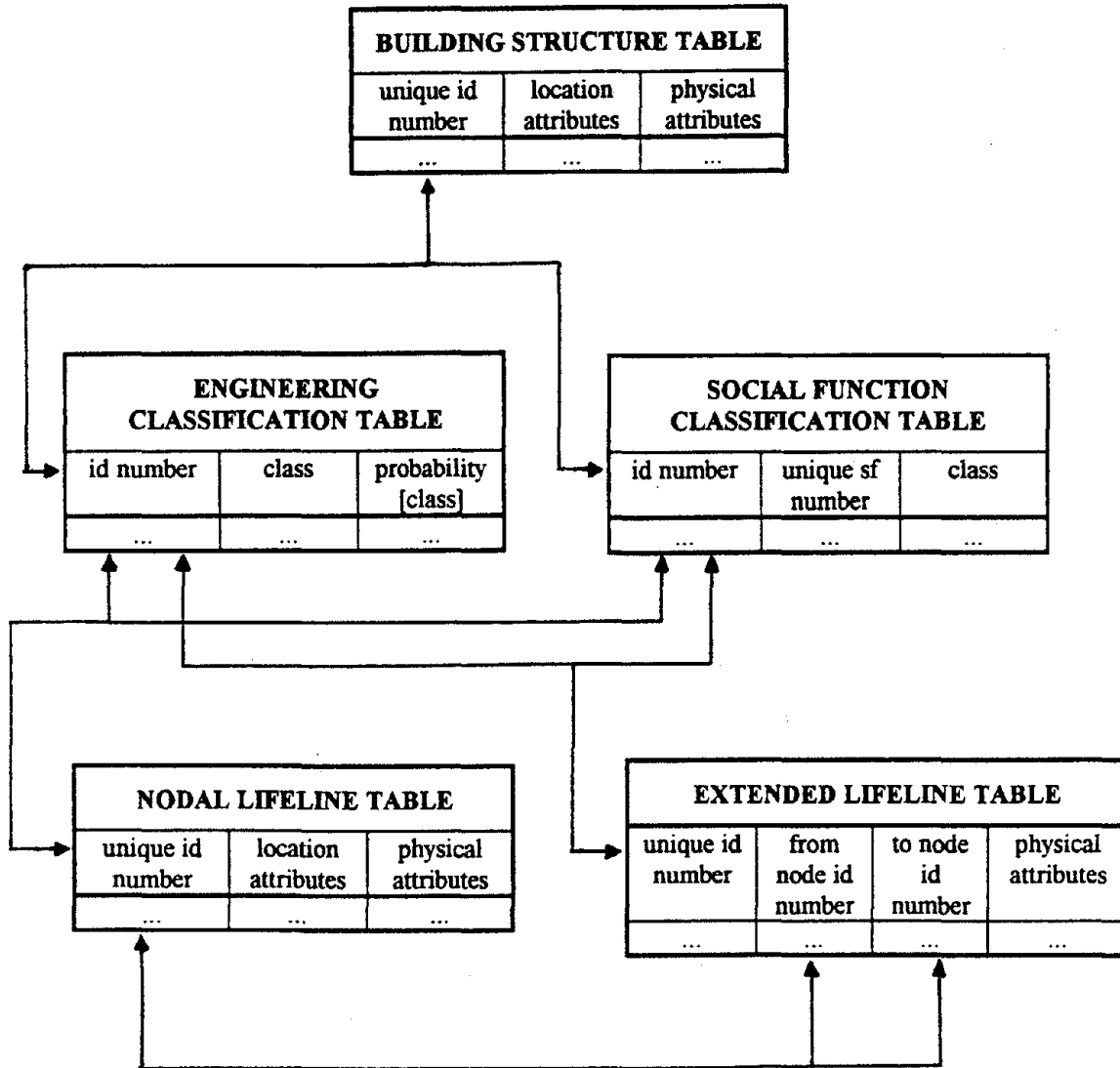


**Figure 4.1.** Example inter-related database tables in a structural inventory (from Applied Technology Council, ATC-36, in progress).

## 4.2 Damage Distributions

Methods for estimating regional distributions of earthquake damage to buildings, bridges, dams, utility systems, and other man-made structures have been the subject of extensive research over the past several decades (Rojahn, 1993). Reitherman (1985) provides a detailed review of over thirty earthquake damage estimation methods. Damage assessment for a region typically depends upon three factors: (1) the level of seismic hazard in the region, including the effects of local site conditions; (2) the distribution of facilities in the region, according to earthquake engineering class; and (3) the definition of functions that relate the expected levels of damage for the various earthquake engineering classes to the estimated levels of seismic hazard. The estimation of regional seismic hazard, including local site effects, was discussed in Chapter 3, and the previous section of this chapter covered earthquake engineering classification and the development of an inventory for describing the regional distribution of facilities. The purpose of Section 4.2 is to provide an overview of the procedure for estimating regional damage distributions in the GIS environment. There are several definitions for damage and also several relationships for estimating damage due to given levels of seismic hazard for various facility types, therefore a brief overview of these two topics is also included in this section.

### 4.2.1 Definitions of Damage

There are several parameters used to express earthquake damage and terms such as "damage ratio", "damage factor", and "damage index" have different meanings to different authors. Regional damage can be given, for example, in percent financial loss or percent of structures damaged to a certain degree. Damage to a given structure can be described in terms of damage to the individual elements, often based on dynamic response measures. The term "damage index" is typically taken to mean the characterization of individual element (local) or entire structure (global) damage based on response parameters such as ductility ratio, inter-story drift, and dissipated energy (see Park and Ang, 1985 and Chung, Meyer, and Shinozuka, 1987). These indices are generally too structure specific to be considered for regional damage description, therefore they will not be discussed in the remainder of this dissertation. The term "damage ratio" is typically defined as (Applied Technology Council, ATC-13, 1985):

$$\text{Damage Ratio (DR)} = \frac{\text{number of structures damaged}}{\text{total number of structures}} \quad (4.1)$$

The level of damage required for a building to be considered "damaged" is often ambiguous, and this type of ratio can typically be derived from other estimates of regional damage, therefore this damage measure will not be further discussed.

The most widely used measure of earthquake damage is an expression of damage in terms of percent financial loss that can be applied to all types of structures (Rojahn, 1993). This measure is typically given the name "damage factor" and is defined as (Applied Technology Council, ATC-13, 1985):

$$\text{Damage Factor (DF)} = \frac{\text{dollar loss}}{\text{replacement cost}} \quad (4.2)$$

This definition of damage will be used throughout this dissertation. The methodology for applying GIS technology to regional damage estimation, however, is intended to be general, allowing the use of any damage definition.

## 4.2.2 Motion-Damage Relationships

Motion-damage relationships are used to estimate earthquake damage for each facility type due to various levels of ground shaking. These relationships, also known as vulnerability functions, are typically expressed in terms of (Kiremidjian, 1992):

- (1) *Damage-Loss Curves.* These relationships, shown in Figure 4.2, were developed by Algermissen and Steinbrugge (1984) for use by the Insurance Services Office. They estimate mean damage ratios (number of damaged buildings divided by the total number of buildings in a region) as a function of ground shaking intensity for various building types.
- (2) *Fragility Curves.* These curves (Kircher and McCann, 1983) describe the probability that a specified damage level will be exceeded for a given intensity of ground motion. The curves are typically developed for all facility types in the general form:

$$P\{D \geq d|Y\} = 1 - F_{D|Y}(d|Y) \quad (4.3)$$



where:

D, d = damage level

Y = ground motion intensity

An example of these curves is shown in Figure 4.3.

- (3) *Damage Probability Matrices (DPM)*. These matrices, first introduced by Martel (1964) and later modified by Whitman (1973), describe the probability that a structure is in a specified damage state given the level of ground shaking intensity. In ATC-13 (Applied Technology Council, 1985), they are derived from the probability distribution of damage given ground shaking intensity,  $f_{D|Y}(d|Y)$ , where D, d, and Y are defined as in equation 4.3, illustrating the analytical relationship between DPMs and fragility curves. A Beta distribution is frequently used to describe the uncertainty in damage for a given ground shaking intensity. An example of one of the 78 DPMs developed by the Applied Technology Council (ATC-13, 1985) for facilities in California is shown in Figure 4.4.
- (4) *Expected Damage Factor Curves*. These curves are just another representation of the relationship between damage and ground shaking intensity that can be used to derive DPMs and fragility curves. There is no difference in the information that is conveyed or can be obtained through the use of fragility curves, DPMs, and expected damage curves. Provided that the parameters ( $\lambda$ ,  $\nu$ ) of the Beta distribution  $f_{D|Y}(d|Y)$  are known, the expected value and standard deviation of damage (in this case, damage factor or percent financial loss) for each level of ground shaking intensity can be computed as follows:

$$E[D|Y] = 100 \frac{\lambda}{\lambda + \nu} \quad \text{in \%} \quad (4.4)$$

$$\sigma_{D|Y} = 100 \frac{\sqrt{\lambda\nu}}{(\lambda + \nu)\sqrt{(\lambda + \nu + 1)}} \quad \text{in \%} \quad (4.5)$$

An example curve, corresponding to the DPM illustrated in Figure 4.4, is shown in Figure 4.5.

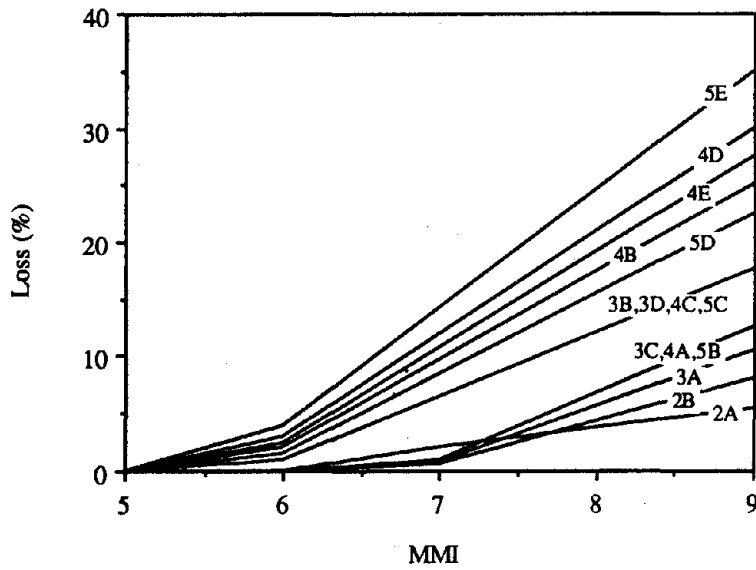


**Figure 4.2.** Example damage-loss curves for different building construction classes (from Algermissen and Steinbrugge, 1984).

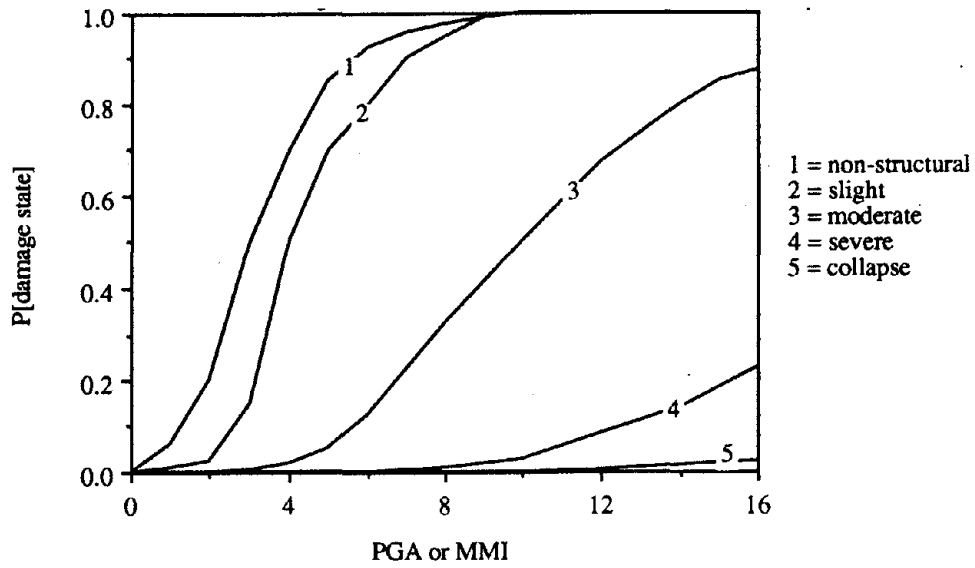


**Figure 4.3.** Example fragility curves (from Kircher and McCann, 1983).

DAMAGE STATE	DAMAGE FACTOR (%)	MMI VI	MMI VII	MMI VIII	MMI IX	MMI X	MMI XI	MMI XII
1	0	3.7	-	-	-	-	-	-
2	0-1	68.5	26.8	1.6	-	-	-	-
3	1-10	27.8	73.2	94.9	62.4	11.5	1.8	-
4	10-30	-	-	3.5	37.6	76.0	75.1	24.8
5	30-60	-	-	-	-	12.5	23.1	73.5
6	60-100	-	-	-	-	-	-	1.7
7	100	-	-	-	-	-	-	-

**Figure 4.4.** Damage probability matrix for low-rise wood-frame buildings (from Applied Technology Council, ATC-13, 1985).

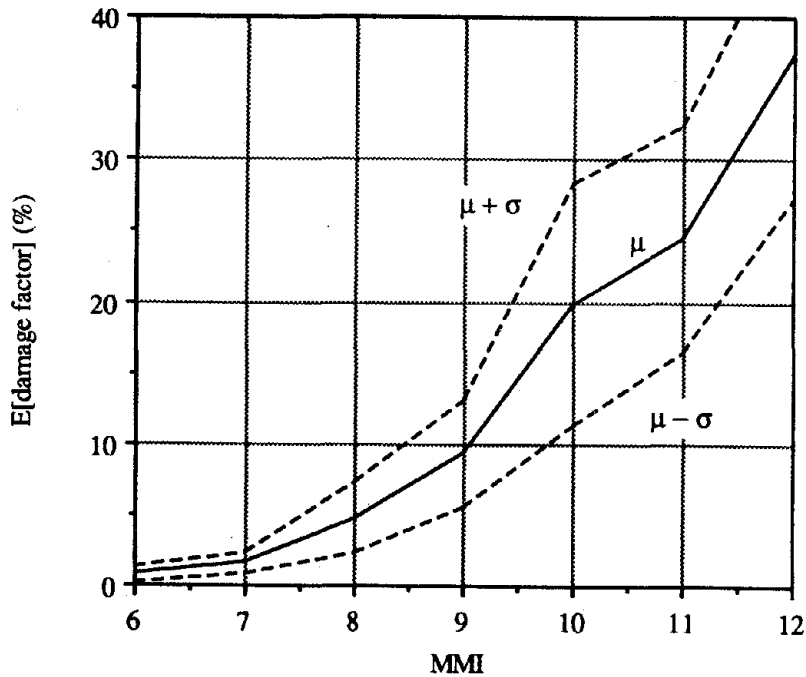


**Figure 4.5.** Expected damage factor with standard deviation as a function of MMI for low-rise wood-frame buildings (from Applied Technology Council, ATC-36, in progress).

For the illustration of regional damage estimation in the GIS environment, the motion-damage relationships will be described in terms of expected damage factor curves, the simplest of the four representations discussed above, although the methodology is intended to be general enough to allow extension to more complex motion-damage relationships. As briefly discussed in Chapter 3, the regional seismic hazard in this dissertation is quantified in terms of the Modified Mercalli Intensity (MMI) scale. Although this subjective scale has many drawbacks, it has traditionally been used in the motion-damage relationships of most major earthquake loss studies (Rojahn, 1993). Current research is focusing on the development of vulnerability functions based on other less subjective ground motion parameters.

### 4.2.3 Application of GIS Technology to Regional Damage Forecasting

The spatial data storage and analysis capabilities of a geographic information system make it an ideal environment for conducting a regional damage estimation. Section 3.4 of the previous chapter discussed the integration of various seismic hazards in the GIS environment, producing the final distribution of MMI values for the example region shown in Figure (m) of Table 3.4. For the illustration of a GIS-based analysis, the regional damage estimation described in this section will be simplified to include the following two steps, repeated for each facility in the inventory of structures:

- (1) Determine the level of seismic hazard for the facility by mapping it according to its geographic location, typically longitude and latitude coordinates, to the map of estimated regional MMI levels, such as that shown in Figure (m) of Table 3.4.
- (2) Determine the expected damage factor (percent financial loss) for the facility and the given MMI level based on the motion-damage relationship defined for the facility's earthquake engineering class, such as the curve shown in Figure 4.5. If a facility is assigned to more than one earthquake engineering classification in a probabilistic manner, then the expected damage for the facility is estimated by combining the expected damage

computed for each class in a weighted average approach based upon the given probabilities.

As an example, consider a structure classified as low-rise wood-frame building, located in the area designated as "A" in Figure (m) of Table 3.4. The final MMI level for this region was computed in Section 3.4.2 to be 11. Using the expected damage factor curve for low-rise wood-frame buildings given in Figure 4.5, the expected damage factor is estimated to be 24%. Modern GIS technology provides a means for the efficient repetition of this computation for all facilities in a region. As previously discussed, the results, such as the 24% expected damage factor computed above, are not to be used for site-specific analysis. The damage estimates are based on several simplifying assumptions and are intended to give regional distributions of expected damage for a given earthquake occurrence model. The microzone mapping capabilities of the GIS can be used to illustrate these distributions in a format that can be very useful for hazard mitigation and emergency planning purposes.

### 4.3 Loss Distributions

Direct monetary losses due to earthquake damage in major metropolitan areas can run into the billion of dollars (Kiremidjian, 1992). For example, the 1989 Loma Prieta Earthquake is estimated to have caused a direct monetary loss of 5.9 billion dollars, with another 15% to 25% of this total due to indirect losses (ABAG, 1991). Steinbrugge, et al. (1981) estimate \$62.2 billion (1980 dollars) in direct property losses for the Los Angeles, California metropolitan area due to a magnitude 7.5 earthquake on the Newport-Inglewood Fault. The figures for non-monetary losses, such as casualties and homelessness, can be just as devastating. Since the beginning of this century, major earthquakes in the seismic regions of world have caused more than 1.25 million fatalities (Agbabian and Chilingarian, 1991). For example, the 1988 Spitak, Armenia Earthquake caused more than 25,000 casualties and left over 500,000 people homeless.

Loss statistics such as these emphasize the importance of regional seismic hazard and risk analysis for estimating earthquake losses for purposes such as emergency planning and hazard mitigation. Research on the topic of earthquake loss estimation has typically

paralleled that of regional damage estimation, as losses are typically considered to be functions of damage. However, earthquake loss studies have often received more attention in the earthquake engineering community, typically because estimates of dollar loss and casualties are more easily understood than measures such as damage factors and damage ratios. Over the last century, the rate of fatalities per severe earthquake has not decreased despite our advances in technology (Shah, 1993), indicating the on-going need for research in the area of earthquake loss mitigation.

The estimation of regional damage distributions for an integrated inventory of structures was covered in the previous sections of this chapter. The purpose of Section 4.3 is to provide an overview of the procedures for using the estimated regional damage and corresponding structural inventory to predict both monetary and non-monetary loss distributions, particularly through the use of GIS technology. Chapter 5 presents a case study of a GIS-based regional earthquake loss analysis, illustrating the various methodologies that have been covered in this dissertation, from estimating the levels of seismic hazard to forecasting the final losses.

### 4.3.1 Monetary Losses

Monetary losses resulting from an earthquake are typically due to: (1) direct structural damage, such as failed beams, excessive deflections, and differential settlement to man-made facilities; and (2) indirect effects, such as damage to non-structural elements and contents, clean-up and financing of repairs, and loss of facility use (down time). The Applied Technology Council (ATC-13, 1985) provides a good overview of the different types of monetary losses, as well as the widely-used methodologies for estimating them, therefore only a brief discussion of the two types of monetary losses listed above will be presented here.

Although there are several methods for estimating losses due to direct structural damage, most are computed as a function of the replacement cost of the facility and the estimated damage to the facility. For purposes of illustrating the application of GIS technology to regional loss estimation, a simple formula for computing the direct losses to a facility will be used and is given as:

$$E[\text{Loss}] = E[\text{DF}] \times (\text{replacement cost}) \quad (4.4)$$

where:

$E[\text{DF}]$  = the expected damage factor estimated for the facility, defined in Section 4.2.1 as the ratio of the dollar loss to the replacement cost of the facility.

Replacement cost for a facility is typically computed as the product of the area or length of the facility and the replacement cost per unit area or length for the given facility type. Replacement costs are generally dependent upon the use or social function class of the facility and often vary for different study locations. Local experts in construction practices are often consulted to help develop tables of replacement costs for various facility classifications.

Indirect monetary losses are much more difficult to quantify than losses due to direct structural damage. Often the contents and non-structural components of a facility are assigned a monetary value that is a given percentage of the total value of the facility based on the social function class of the facility. The damage factor for the contents and components is either assumed to be the same as that of the facility, or it is calculated through the use of one of the previously discussed motion-damage relationships developed specifically for contents and components. Monetary loss is then computed as the product of the damage factor and the replacement cost. Although this is an important and often sizable loss, the estimation is considered to be beyond the scope of this dissertation and it will not be further discussed.

Other indirect monetary losses are typically due to clean-up, financing of repairs, and loss of business use. These socio-economic effects of earthquake damage are the subject of much current research in the economic community. Models for post-earthquake clean-up and financing have not been developed, but several methods for estimating loss of business use, or down time, have been suggested (Applied Technology Council, ATC-13, 1985 and ATC-25, 1991 and Massachusetts Civil Defense Agency, 1989). Loss of business use for a facility is typically a function of two factors: (a) the social function class of the facility and (b) the damage factor computed for the facility due to the given

earthquake event. Down time is then estimated based on opinions of experts in the field and expressed in one of the following two ways that can easily be derived from each other:

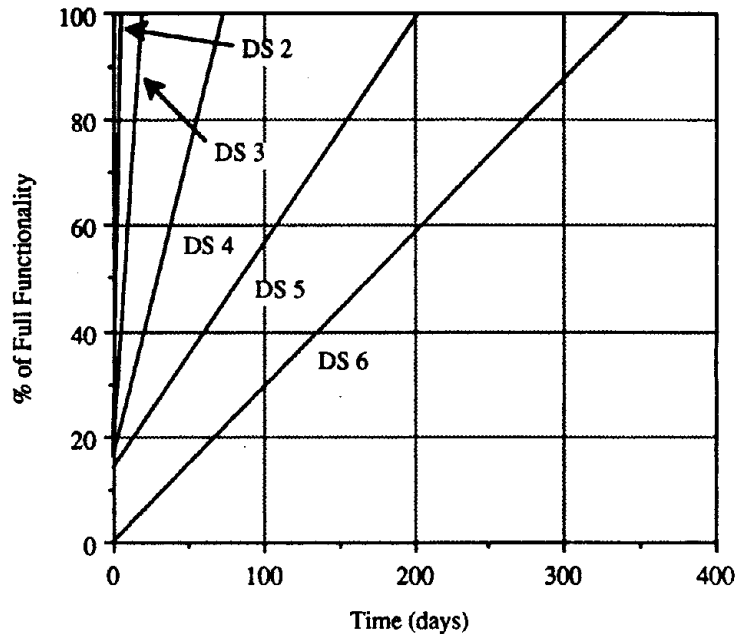
- (1) The required time (in days) after the earthquake to restore the facility to a given level of service, typically defined as a percentage of the full functionality of the facility.
- (2) The level of service (percentage of full functionality) of the facility at a given time after the earthquake.

Table 4.1 and Figure 4.6 illustrate the two representations of the down time discussed above for a facility use type defined by the Applied Technology Council (ATC-13, 1985). The extension from an estimation of down time to a monetary loss is a very complicated process that depends on numerous socio-economic factors currently under study. The interaction of various facilities in a region, such as the effects of the loss of lifeline use on the loss of business use in a building served by those lines, is also assumed to be too complicated to be included in this dissertation. For the purpose of illustrating regional earthquake loss estimation in the GIS environment, only those losses associated with direct structural damage and loss of business use will be considered. As previously discussed, GIS technology allows new models to be tested and compared and then added to the regional damage and loss analysis.

**Table 4.1.** Time to restore functionality after an earthquake for use class = retail store (from Applied Technology Council, ATC-13, 1985).

<b>DAMAGE STATE</b>	<b>DAMAGE FACTOR (%)</b>	<b>Days to restore to 30% of full functionality</b>	<b>Days to restore to 60% of full functionality</b>	<b>Days to restore to 100% of full functionality</b>
1	0	-	-	-
2	0-1	1.2	2.4	5.8
3	1-10	3.4	10.2	20
4	10-30	9.8	44.6	71
5	30-60	37	111.6	202.7
6	60-100	114.7	213.7	343.1
7	100	-	-	439.3





**Figure 4.6.** Percentage of functionality as a function of time following an earthquake for use class = retail store (from Applied Technology Council, ATC-36, in progress).

### 4.3.2 Non-Monetary Losses

Non-monetary earthquake losses typically include fatalities, injuries, unemployment and homelessness. Earthquake-induced casualties have traditionally been a common research topic in the earthquake engineering community, although very few general quantitative models have been proposed. Casualty statistics from earthquakes occurring in the United States are typically very limited, and those from foreign earthquakes are assumed to be inadequate due to large variations in construction and occupancy. Earthquake casualty models are often developed from expert opinion, such as the model suggested by the Applied Technology Council (ATC-13, 1985). Although this model was developed for the state of California and has been criticized for being overly simplified, it does provide a methodology for computing fatalities and injuries on a regional basis. Table 4.2 illustrates the model by providing estimates of deaths and injuries as a function of damage factor. This table is typically used in conjunction with a table of

day and night occupancy rates for facilities of various social function classes to predict earthquake-induced casualties.

**Table 4.2.** Earthquake casualty estimates (from Applied Technology Council, ATC-13, 1985).

DAMAGE STATE	DAMAGE FACTOR (%)	Fraction of Minor Injuries	Fraction of Major Injuries	Fraction Dead
1	0	0	0	0
2	0-1	3/100,000	1/250,000	1/1,000,000
3	1-10	3/10,000	1/25,000	1/100,000
4	10-30	3/1,000	1/2,500	1/10,000
5	30-60	3/100	1/250	1/1,000
6	60-100	3/10	1/25	1/100
7	100	2/5	2/5	1/5

Models for the other non-monetary earthquake losses, such as homelessness and unemployment, have not been fully developed as these effects depend on several factors that are typically difficult to quantify. Casualties will be the only non-monetary earthquake loss treated in this dissertation, but future inclusion of other socio-economic models in the GIS-based regional analysis is anticipated. The final section of Chapter 4 presents a brief illustration of the application of GIS technology for estimating regional earthquake losses due to direct structural damage, loss of business use, and casualties. The case study in Chapter 5 provides a detailed illustration of regional earthquake damage and loss evaluation in the GIS environment.

### 4.3.3 Application of GIS Technology to Regional Loss Forecasting

The spatial distribution of earthquake losses in a region is often used for purposes such as resource allocation, disaster planning, and various social and economic studies.

Geographic information systems provide a powerful tool for storing and manipulating the large amount of data typically required for a regional earthquake loss estimation. Several types of monetary and non-monetary losses were previously discussed in this chapter, but for illustration of the GIS-based earthquake loss evaluation methodology, only those losses due to direct structural damage, loss of business use, and casualties will be considered in this dissertation.

The computation of monetary losses due to direct structural damage is quite straight-forward as discussed in Section 4.3.1. Equation 4.4 is typically used in conjunction with a table of replacement costs for various facility use types to compute the loss for each facility. Regional losses can be estimated by calculating the loss for each individual facility and then aggregating the results on a given basis, such as by Census tract, city block, zip code, earthquake engineering class, or social function class. For example, in Section 4.2.3, a low-rise wood frame building located in the area designated as "A" in Figure (m) of Table 3.4 was estimated to have a damage factor of 24%. Assuming that this building is used as a single family dwelling with an estimated replacement cost (1993 dollars) of \$85/square foot, for a 3000 square foot building, the predicted monetary loss would be \$61,200.

As discussed in Section 4.3.1, loss of business use is typically computed for each facility as a function of the damage factor due to the earthquake event and the social function class of the facility. Unless a model for extending down time to monetary loss or a model for studying the effects of facility interaction is included in the GIS-based analysis, the only regional aggregation of results for loss of business use is typically the average of the values for the different facility use types to be used for comparative purposes. As an example, if the low-rise wood frame building discussed in the previous paragraph were a retail trade store instead of a single family dwelling, the loss of business use would be computed from Table 4.1 and Figure 4.6 and a damage factor of 24% as:

Time to restore to 30% functionality:	9.8 days
Time to restore to 60% functionality:	44.6 days
Time to restore to 100% functionality:	71 days
Functionality at 3-days:	20%

The final regional earthquake loss estimation to be illustrated is the death and injury loss. The prediction of casualties is typically computed in a two-step process for each facility in a region. First the day and night occupancy values are estimated for the facility based on the square footage and social function class of the facility. Next, the death and injury rates for a given damage factor (Table 4.2) are used with the occupancy values to predict the fraction of dead and injured persons in the facility.

Similar to monetary losses due to direct structural damage, regional casualties can also be aggregated on several levels, such as by area or facility type and use. For example, the daytime occupancy rate of a single family dwelling is assumed to be 1.2 persons per 1000 square feet. Therefore, the day occupancy of the example 3000 square foot low-rise wood-frame building of the previous paragraphs would be 3.6 persons. Table 4.2 estimates rates of 1 in 2,500 major injuries and 1 in 10,000 deaths for a facility with a damage factor of 24%. Using these values with the 3.6 person daytime occupancy results in 0.0144 major injuries and 0.00036 deaths in this building due to the assumed earthquake event. These casualty estimates are meaningless when reported for only one structure. Typically, these estimates are made for each structure in a region and then a summary value of deaths and injuries for the whole region is reported.

As indicated in Section 4.2.3, the resulting values such as \$61,200, 9.8 days, 24%, and 0.0144 major injuries are not intended to be used for a site-specific analysis of one facility. The models from which these values are computed are simplified in order to be applicable to regional damage and loss estimation on a broad scale. Values are computed for one facility to illustrate the effectiveness of GIS technology for storing, manipulating, and displaying the spatial data involved in a regional seismic hazard and risk analysis. This chapter has described structural inventory development and provided an overview of regional earthquake damage and loss estimation. The next chapter illustrates these concepts as well as those of the previous three chapters through a case study of a GIS-based multi-hazard regional seismic risk assessment in Salt Lake County, Utah.

## 5.1 Background and Scope

The case study presented here is part of an on-going seismic hazard and risk analysis sponsored by the Federal Emergency Management Agency (FEMA) for the seismically active areas in the state of Utah (see Applied Technology Council, ATC-36, in progress). The purpose of the project is to develop databases of structural inventories and collateral hazards, as well as the algorithms and methodologies for estimating earthquake damage and losses, for the counties of Salt Lake, Weber, Davis, Tooele, and Utah. The methodologies are general, allowing application in other seismically active regions of the United States. FEMA intends to use the results to: (1) plan pre-disaster mitigation and emergency management efforts; (2) quickly assess the emergency situation, its major impact, and the emergency response needs during the first hours after an emergency; and (3) plan and execute post-disaster efforts.

The five counties of Salt Lake, Weber, Davis, Tooele, and Utah are located in the Wasatch Fault Zone, one of the longest and most active extensional fault zones in the western United States. Significant historical earthquakes have been documented in this region, but no events have occurred since the middle 1800s when the area was first developed. The earthquake damage and loss estimation presented in this case study is for a scenario event, a magnitude 7.5 earthquake on the Salt Lake Segment of the Wasatch Fault. Salt Lake County, which is intersected by the Wasatch Fault as shown in Figure 5.1, has a high potential for earthquake damage and losses with a population of nearly 750,000 people and a large percentage of structures that have not been designed to resist earthquake forces. Therefore, a detailed seismic hazard and risk analysis is being conducted for Salt Lake County. The results will be extrapolated to the other four less populated counties.

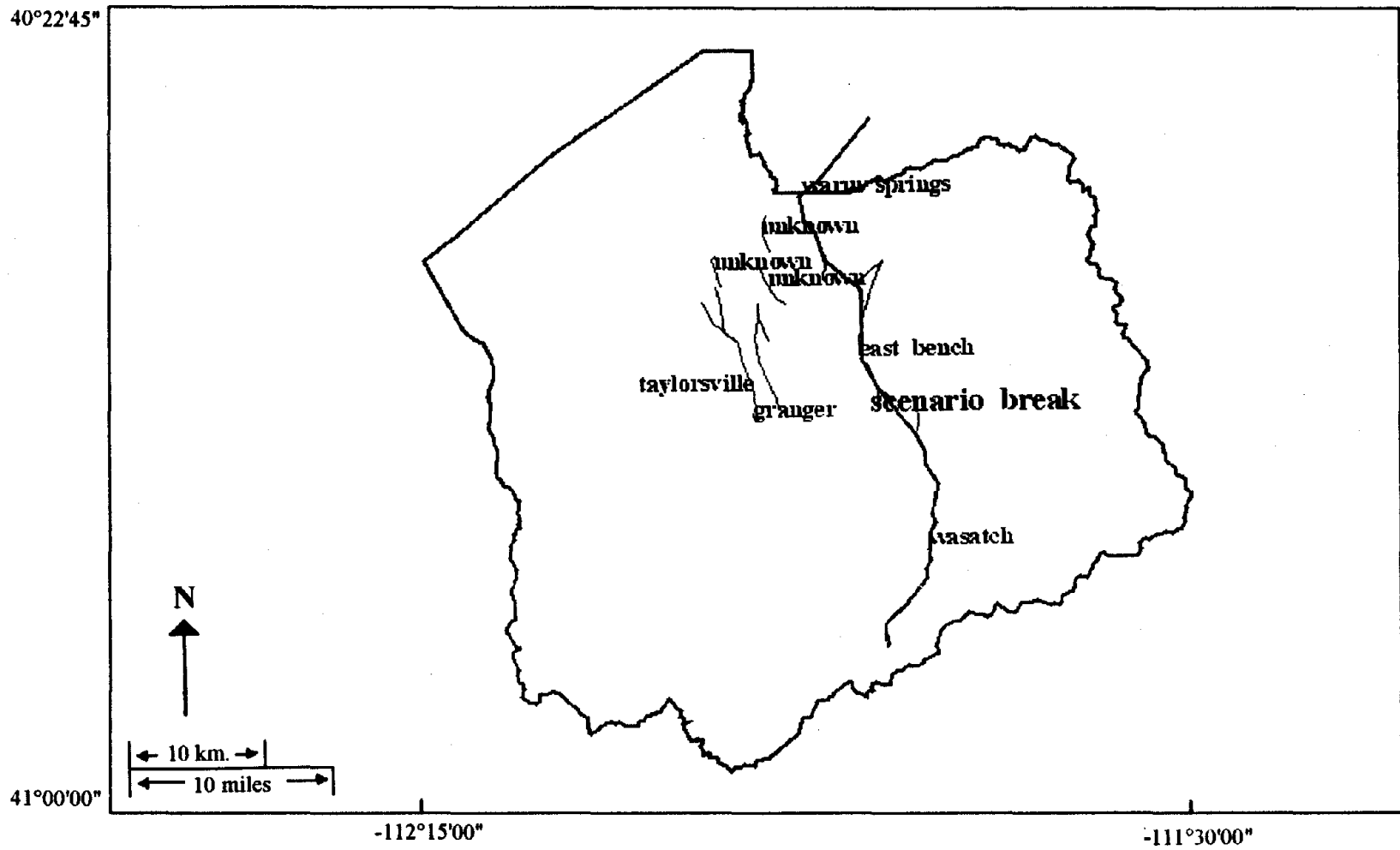


Figure 5.1. Map showing locations of faults in Salt Lake County, Utah.

The databases and methodologies for this project have been developed for analysis on a structure-by-structure basis, with summaries at the Census tract level. Salt Lake County contains over 150 Census tracts with more than 200,000 structures, therefore only a subset of the data with results presented as summaries at the Census tract level will be used in this chapter to illustrate the GIS-based regional seismic hazard and risk analysis. The databases and methodologies contain all of the information that is available to date, however, additional information is still being gathered under the Applied Technology Council project. The results and microzone maps presented here are preliminary and intended only for illustrative purposes. The final report for the Utah earthquake damage and loss estimation will be published in 1994 by the Applied Technology Council (ATC-36, in progress).

The case study presented in this chapter follows the GIS-based regional analysis methodology illustrated in Figure 2.4. Section 5.2 covers the GIS-based seismic hazard analysis for the region. Surface ground shaking and local site effects are treated, including an illustration of the hazard integration methodology presented in Chapter 3. Section 5.3 details the regional earthquake damage and loss estimation. The current development of the structural inventory for this region is used to illustrate the inventory integration methodology presented in Chapter 4. A subset of the inventory is used to compute preliminary estimates of earthquake damage and losses in the region. A summary of the procedures and results of the GIS-based regional analysis is presented in Section 5.4.

## 5.2 Seismic Hazard Analysis

Chapter 2 of this dissertation presented a discussion of regional seismic hazard analysis. The background of the various steps in the process, as well as the application of GIS technology in a regional study were discussed. Chapter 3 involves a more detailed treatment of local site effects, including soil amplification, liquefaction, landslide, and fault rupture, and the integration of these effects in a GIS-based regional seismic hazard analysis. The case study presented here illustrates several of these concepts in a simplified analysis over a fairly large region. Microzone maps are shown to help describe the hazard estimation methodology which is illustrated in the left half of Figure 1.2.

## 5.2.1 Surface Ground Shaking

As discussed in Section 5.1, this case study presents a regional seismic hazard and risk analysis for a scenario event, a magnitude 7.5 event on the Salt Lake Segment of the Wasatch Fault in Salt Lake County, Utah. Figure 5.1 shows a fault map of the region, with the assumed scenario break needed to generate a magnitude 7.5 event on this fault trace. In order to estimate the surface ground shaking in the region, the attenuation relationship developed by Boore, Joyner, and Fumal (1993) for peak ground accelerations from western North American earthquakes is used. This relationship is given in the form:

$$\log(\text{PGA}) = -0.038 + 0.216(M-6) - 0.777\log(r) + 0.158G_b + 0.254G_c \quad (5.1)$$

where:

$$r = (d_2 + 30.03)^{1/2}$$

PGA = the larger of two horizontal peak ground acceleration values in g

d = distance to the rupture zone in km

M = the assumed magnitude of the earthquake (7.5 in this study)

$G_b = 0$  and  $G_c = 0$  for soil type A (shear wave velocity > 750 m/s)

$G_b = 1$  and  $G_c = 0$  for soil type B (shear wave velocity = 360-750 m/s)

$G_b = 0$  and  $G_c = 1$  for soil type C (shear wave velocity < 360 m/s)

A map of buffer zones of PGA values located at one kilometer intervals from the assumed scenario break is shown in Figure 5.2. Also shown in this figure is an example of the attributes associated with each buffer zone. PGA and Modified Mercalli Intensity (MMI) values are given for the three soil types of A, B, and C as defined above. The equation used to compute MMI from PGA is that of Trifunac and Brady (1975) given in Equation (1) from Table 3.4 as:

$$\log(\text{PGA}) = 0.014 + 0.3(\text{MMI}) \quad (5.2)$$

A map of the local site geology is required to define the areas of A, B, and C soil types in the study region. Figure 5.3 shows a map of A, B, and C soil types, derived from various maps of regional soil conditions. To estimate the final surface ground shaking in the region, the map of ground motion buffer zones is combined with the soil type map to produce the final map of surface ground shaking as illustrated in Figure 5.4 for PGA and Figure 5.5 for MMI values. An example list of the attributes associated with each polygon



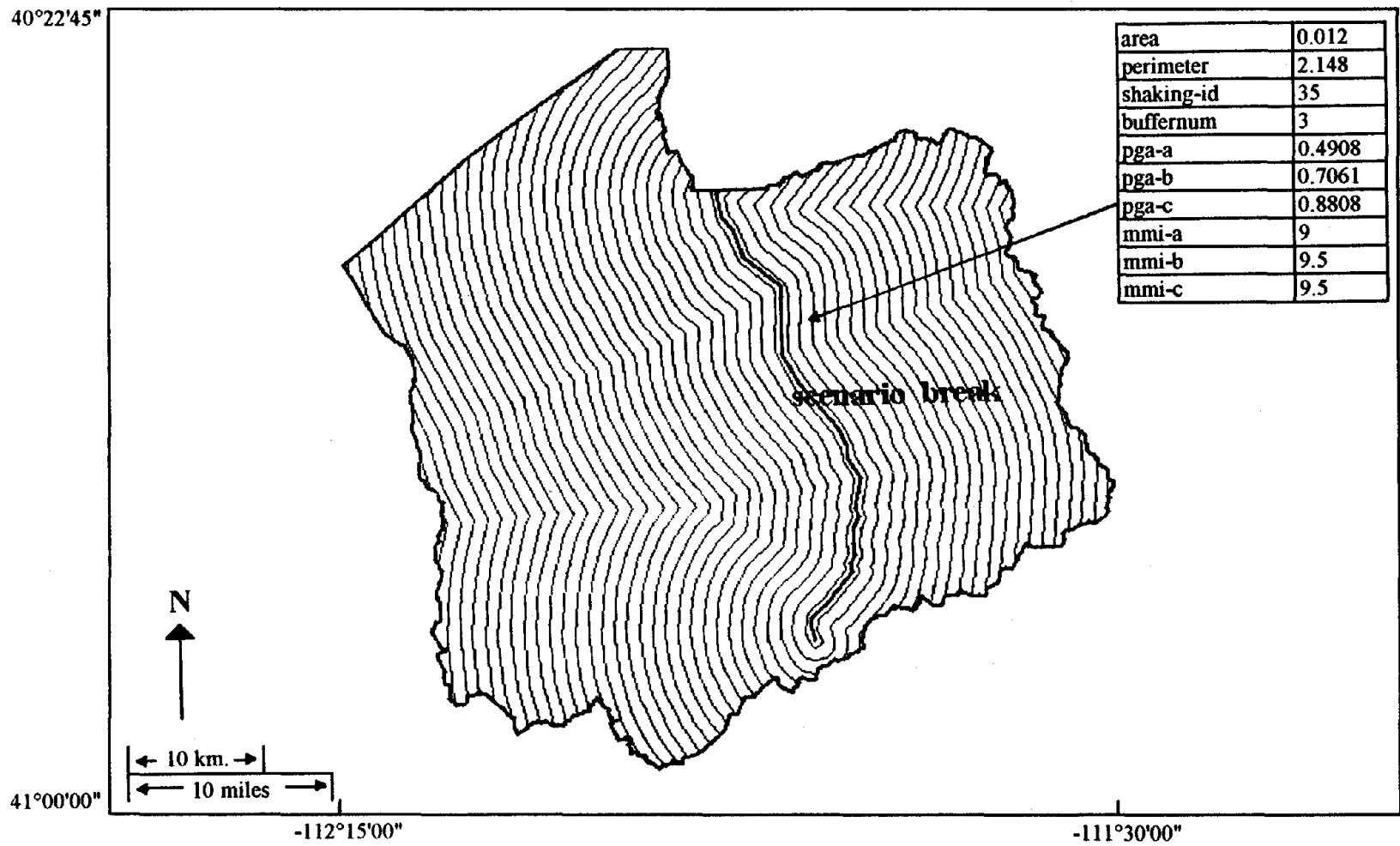


Figure 5.2. Map showing buffer zones of ground shaking in Salt Lake County, Utah.

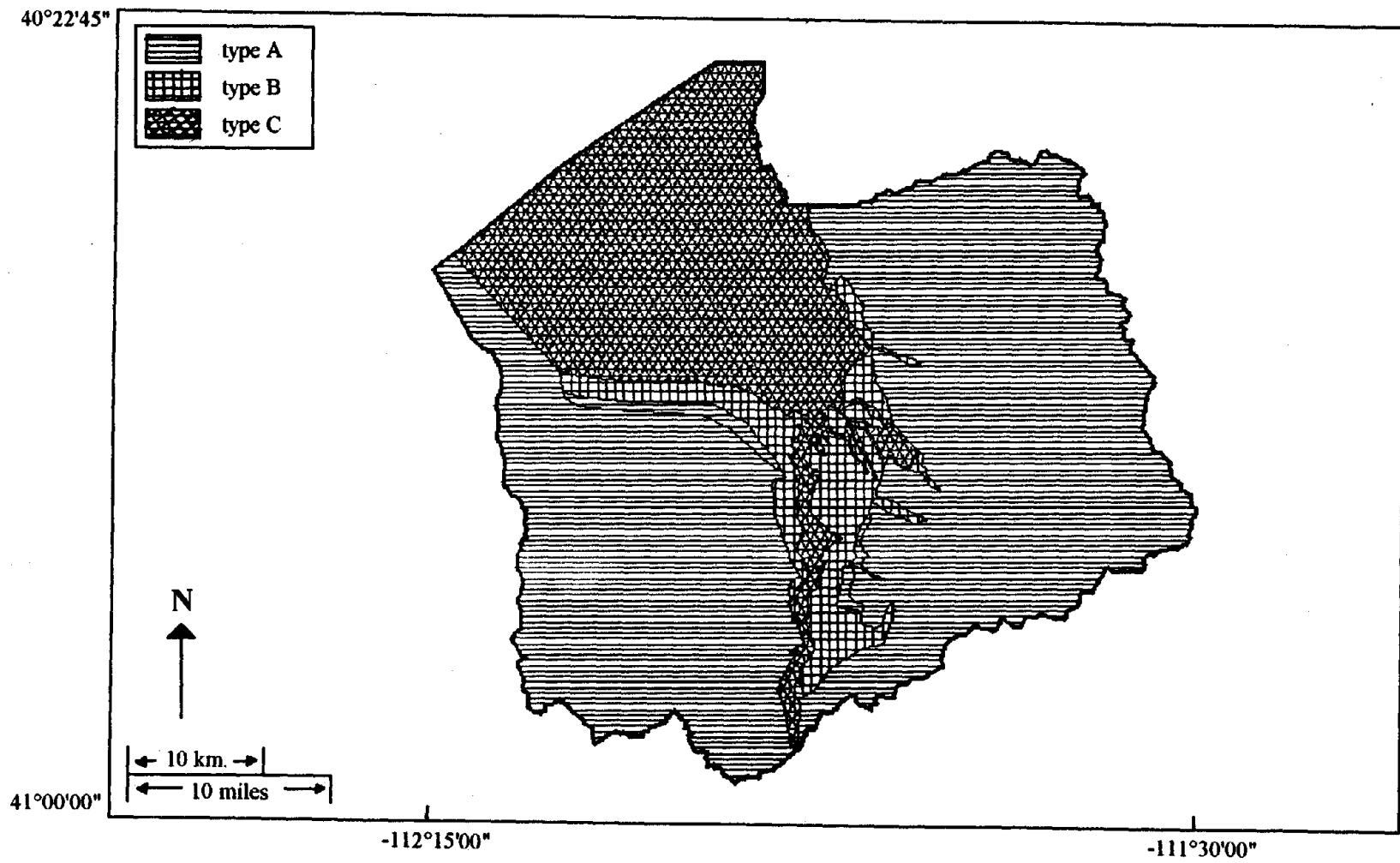


Figure 5.3. Map showing regional distribution of general soil types in Salt Lake County, Utah.

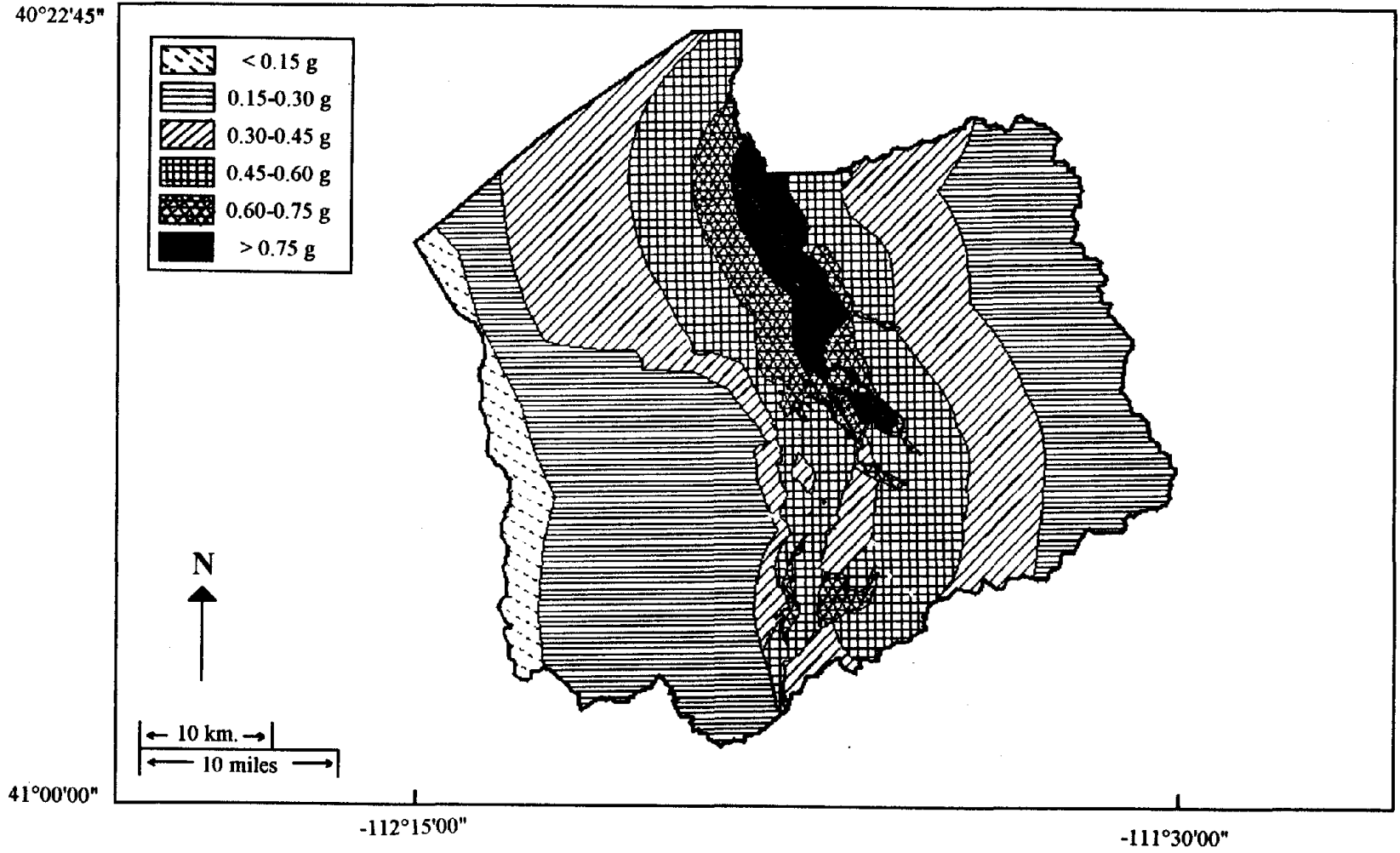


Figure 5.4. Map showing regional distribution of peak ground acceleration values in Salt Lake County, Utah.

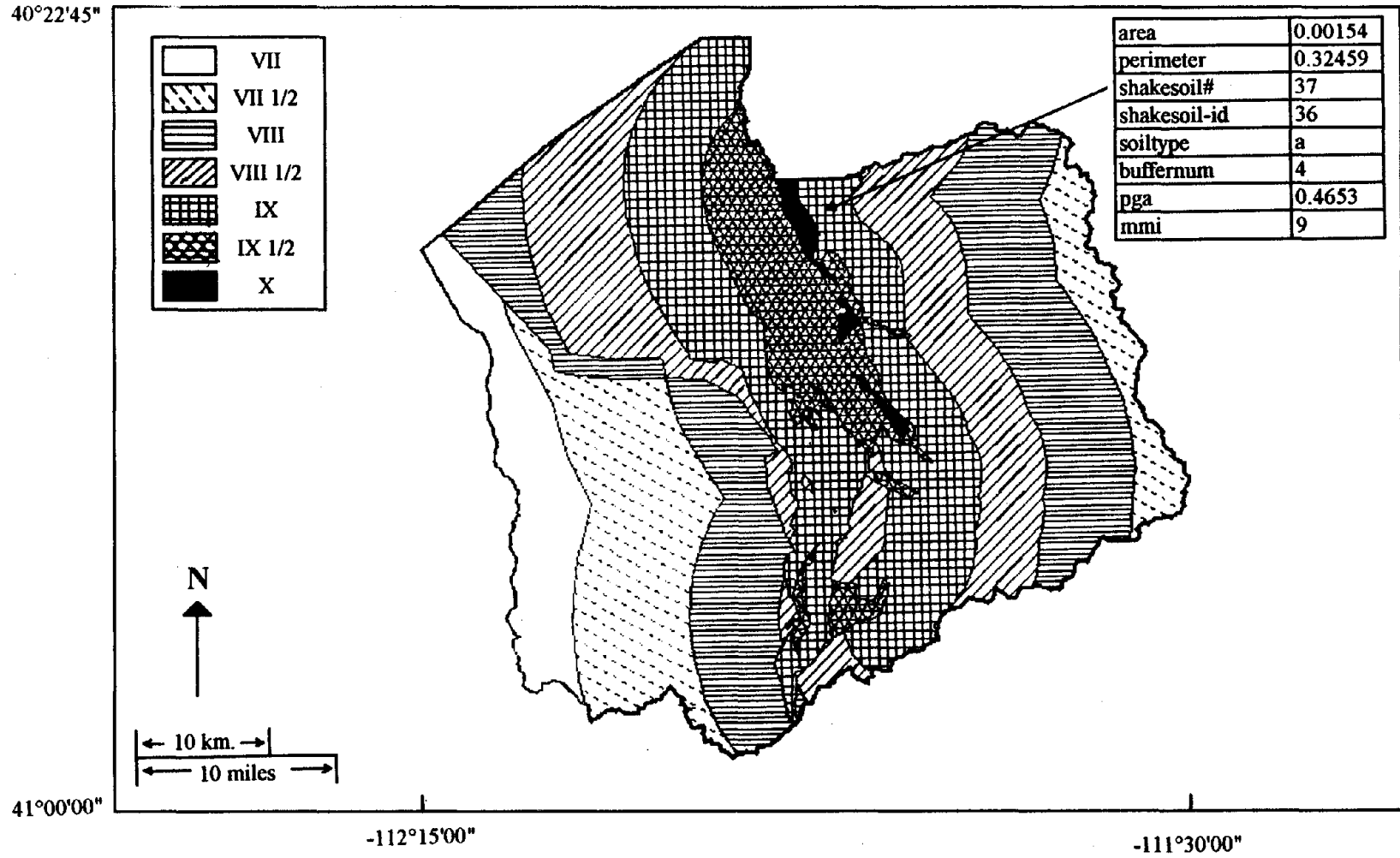


Figure 5.5. Map showing regional distribution of ground shaking hazard ( $MMI_{GS}$ ) in Salt Lake County, Utah.

on the map is also shown in Figure 5.5. High ground motion values are shown to occur through the middle portion of the county. This is due to the close proximity of the fault in these regions, as well as the presence of softer soil deposits (soil type C).

### 5.2.2 Local Site Effects

The local site conditions to be considered in this case study include liquefaction, landslide, and surface fault rupture. The hazards associated with liquefaction and landslide are defined in terms of 'high', 'moderate', 'low', and 'very low' potential of occurrence as discussed in Chapter 3. These two maps were obtained in digital format from the State Office of Emergency Services and were edited in the GIS to those shown in Figures 5.6 and 5.7, respectively. The hazard due to surface fault rupture is defined in terms of 100 and 200 meter buffer zones around the assumed scenario fault break as discussed in Figure (f) of Table 3.4. The surface fault rupture map is shown in Figure 5.8, with only the 200 meter zone drawn for clarity.

In order to integrate the various seismic hazards due to ground shaking, liquefaction, landslide, and surface fault rupture as illustrated in the next section, each hazard must be quantified in terms of the same hazard parameter. Section 3.4 presents a methodology, as well as an example of the methodology, for performing this task in the GIS environment. MMI is chosen to be the seismic hazard parameter and the heuristic rules used to quantify the various hazards are taken as those used in Table 3.4, the illustrative example. The rules for quantifying surface fault rupture hazard are given as Equations (2a) through (2c) in Table 3.4, and for quantifying landslide hazard as Equations (4a) through (4c). The description of liquefaction hazard in this case study is different from that used in the example in Table 3.4, but is very similar to the description of landslide hazard. Therefore, the rules for quantifying the liquefaction hazard are given in the form of Equations (4a) through (4c) in Table 3.4, with 'MMI<sub>LIQ</sub>' replacing 'MMI<sub>LAN</sub>'.

The hazard maps for liquefaction, landslide, and surface fault rupture are shown in Figures 5.9, 5.10, and 5.11, respectively. The hazards are quantified in terms of MMI, according to the rules discussed in Table 3.4 and in the previous paragraph. Figure 5.9 shows an example attribute listing for one of the polygons. The next section details the integration of the various seismic hazards to produce a final combined seismic hazard map that will then be used to compute damage and loss in the study region.

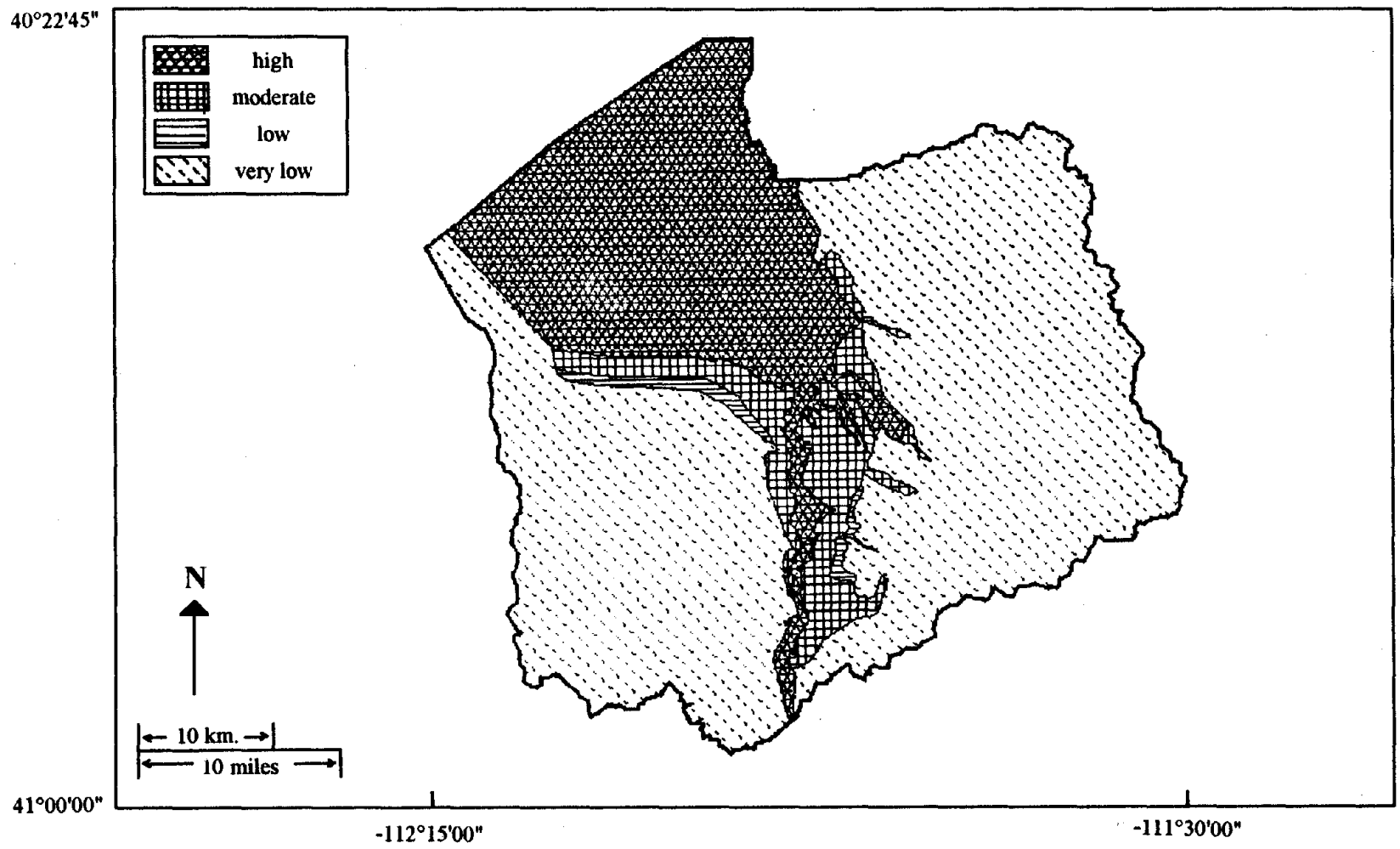


Figure 5.6. Map showing liquefaction potential in Salt Lake County, Utah.

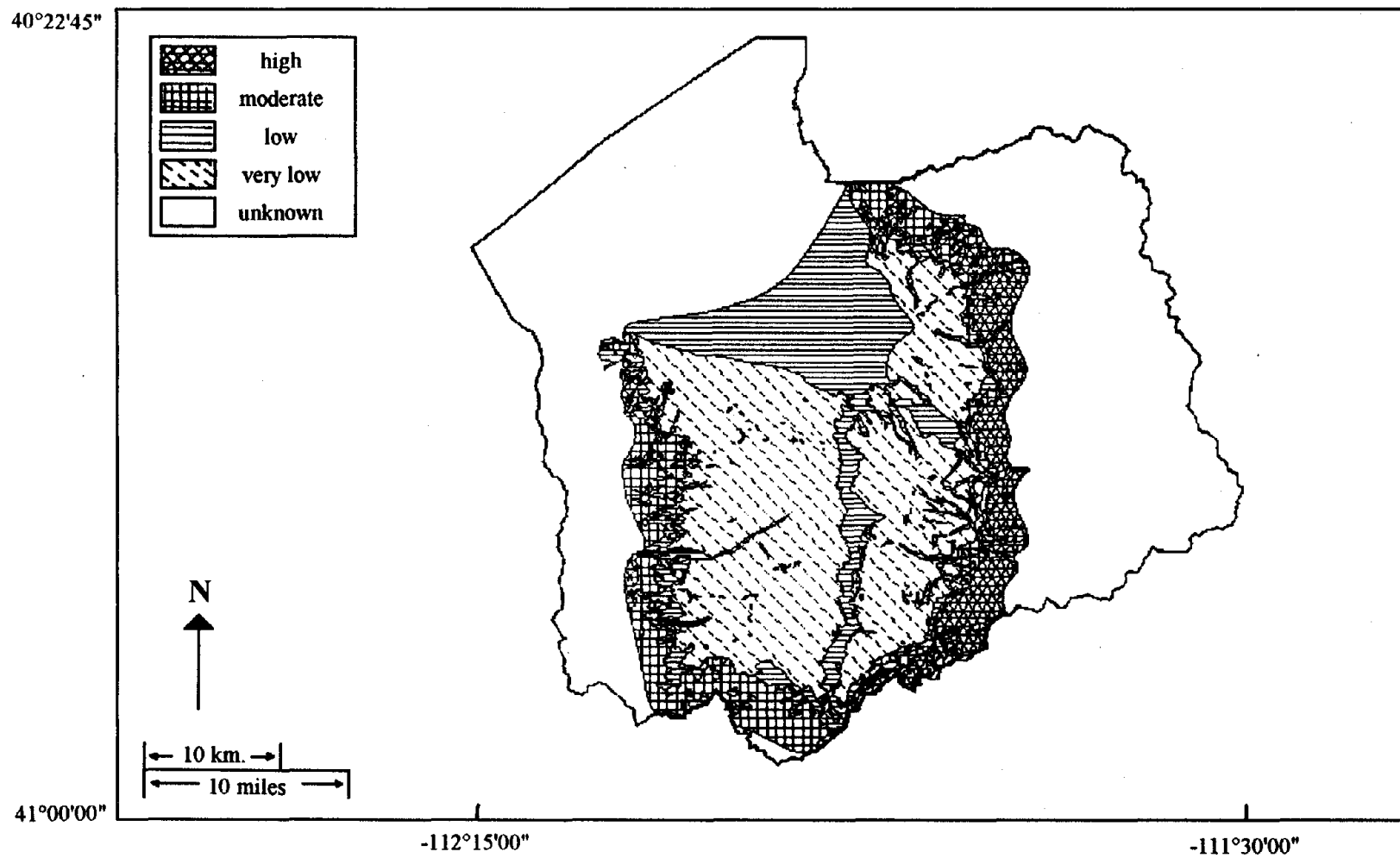


Figure 5.7. Map showing landslide potential in Salt Lake County, Utah.

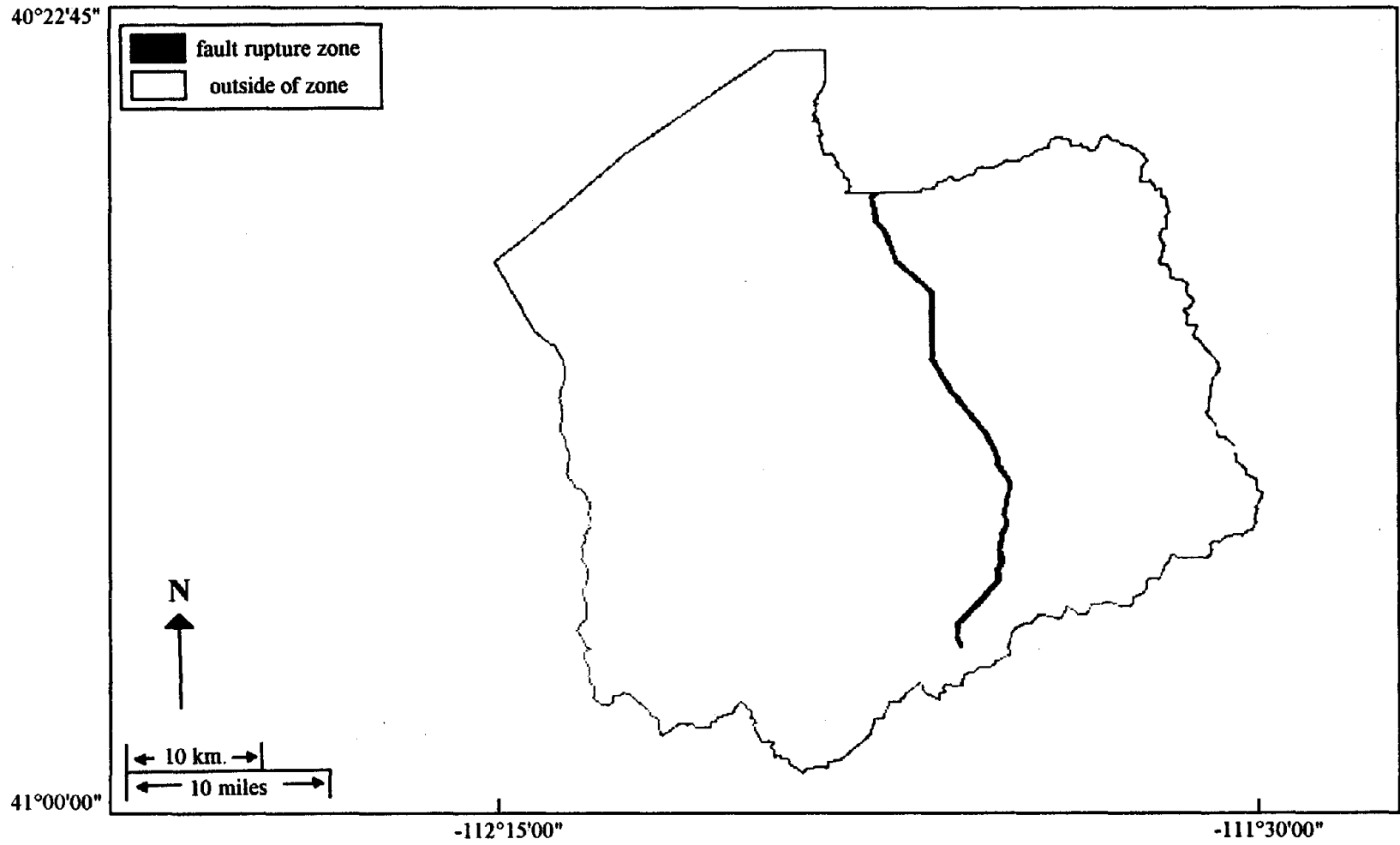


Figure 5.8. Map showing fault rupture zones in Salt Lake County, Utah.



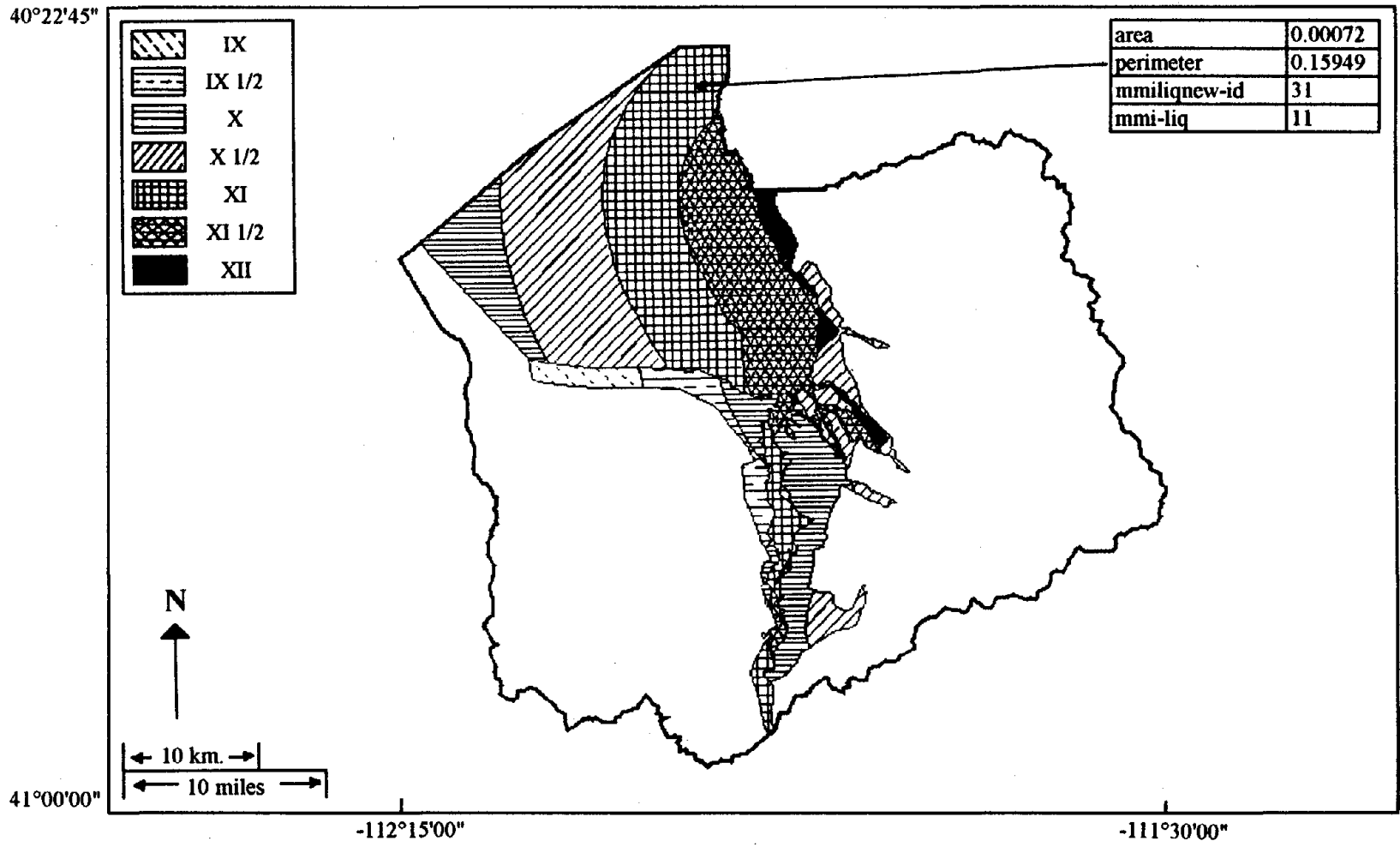


Figure 5.9. Map showing regional distribution of liquefaction hazard ( $MMI_{LIQ}$ ) in Salt Lake County, Utah.

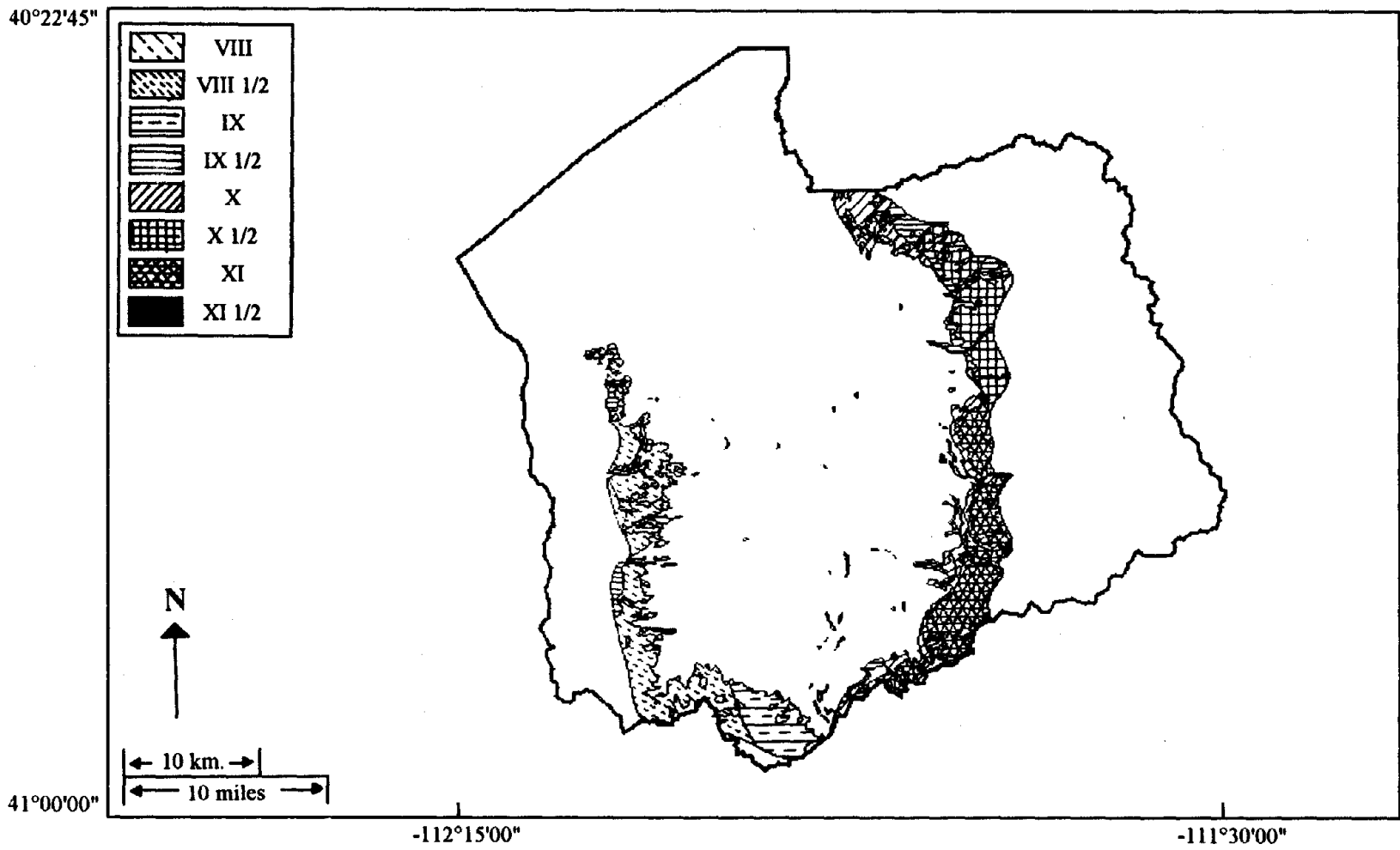


Figure 5.10. Map showing regional distribution of landslide hazard ( $MMI_{LAN}$ ) in Salt Lake County, Utah.

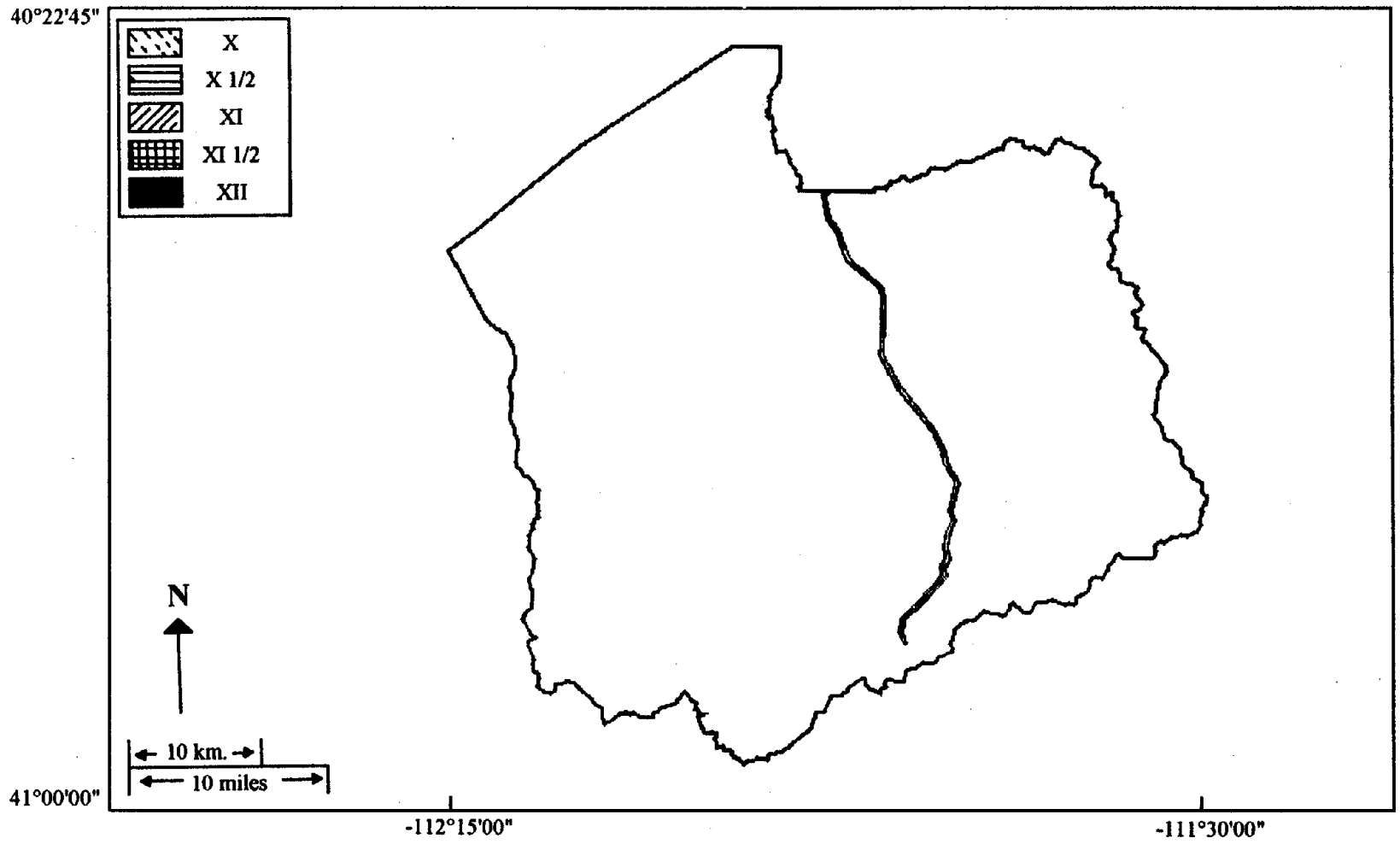


Figure 5.11. Map showing regional distribution of fault rupture hazard ( $MMI_{FR}$ ) in Salt Lake County, Utah.

### 5.2.3 Hazard Integration

The previous section discussed the quantification of the various seismic hazards leading to the maps shown in Figure 5.5 ( $MMI_{GS}$  due to ground shaking), Figure 5.9 ( $MMI_{LIQ}$  due to liquefaction), Figure 5.10 ( $MMI_{LAN}$  due to landslide), and Figure 5.11 ( $MMI_{FR}$  due to surface fault rupture). The integration of these four hazards is assumed to follow the weighted average methodology described in Section 3.4. The heuristic hazard combination rules used for the region in this case study are those listed in Table 3.5. Figure 5.12 shows the final combined seismic hazard for the scenario event in the study region, with a list of attributes shown for one of the polygons.

Similar to the ground shaking hazard map, high values of MMI are found to occur through the middle portion of the county. This is due to the high ground shaking in this area, as well as the high hazards due to liquefaction and fault rupture. It is again emphasized that the results of this case study are only preliminary and are based on several simplifying assumptions. The analysis method and integration rules are chosen with the intent of illustrating the use of GIS technology in a regional seismic hazard analysis and can easily be modified as additional information becomes available. The rest of this case study deals with the estimation of damage and loss due to the scenario event. In order to illustrate the effects of local site conditions, values are computed for the combined final seismic hazard and for the hazard due to ground shaking alone.

## 5.3 Earthquake Damage and Loss Estimation

Chapter 4 of this dissertation deals with structural inventory development and the estimation of earthquake damage and loss. This section of the case study is used to illustrate these concepts in the GIS environment. A simplified version of the methodology outlined in the right half of Figure 1.2 is used here to compute damage and loss for a subset of the complete inventory due to the scenario event in the region. Although the analysis presented in this case study is simplified with many assumptions, the GIS-based methodology can easily be extended to include more complex models as well as other inventory data.

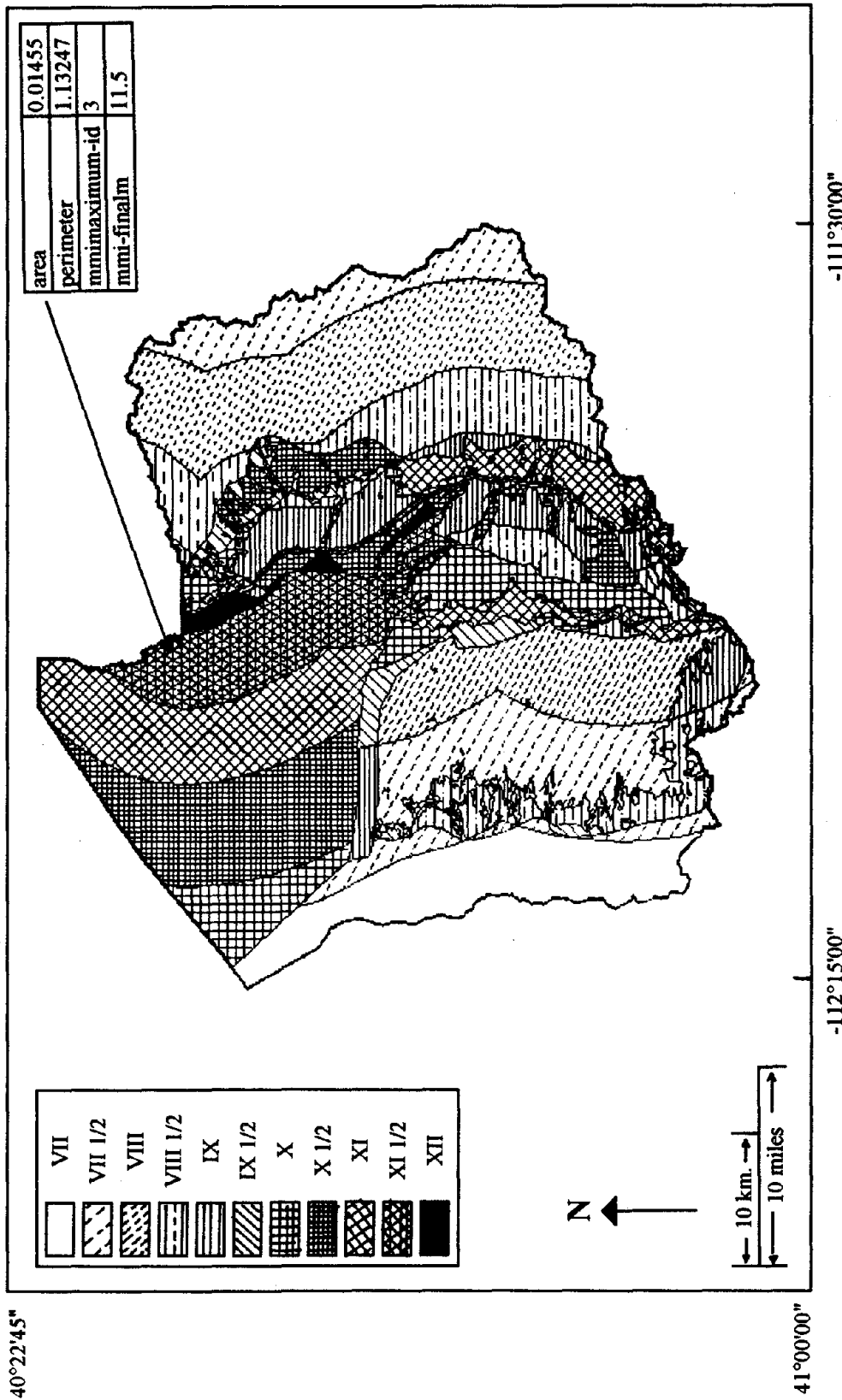


Figure 5.12. Map showing regional distribution of combined seismic hazard (MMI<sub>F</sub>) in Salt Lake County, Utah.

### 5.3.1 Structural Inventory Development

Section 4.1 provides an overview of structural inventories, including the required information, the sources of inventory data, and the classification and inference schemes. The methodology presented in Section 4.1.4 for compiling a complete inventory of structures in a region is implemented in this case study. The first step is to determine the data attributes to be included in each table and the interaction among the various tables in the final inventory. Figure 5.13 illustrates the inter-related database structure used in this simplified case study. The next two steps involve the development of the social function and earthquake engineering classification schemes to be used in the inventory. The two classifications used here are based on those given in ATC-13 (Applied Technology Council, 1985) with modifications for use in Utah (Applied Technology Council, ATC-36, in progress). The social function classification is given in Table 5.1 and the earthquake engineering classification is given in Table 5.2.

The next step in the inventory compilation is to develop a list of available sources of inventory data for each major social function class. For this case study, the list shown in Table 5.3 is developed. Once these data sources have been collected and analyzed, heuristic rules are developed to infer the earthquake engineering classification, the minor social function classifications, and the missing data attributes. The rest of the methodology for inventory development involves the compilation of the various tables from all sources. Figure 5.14 illustrates the process used in this case study to analyze the attributes in the Salt Lake County Tax Assessor Datafile, develop inference rules, and fill-in the final inventory tables.

Although all of the sources listed in Table 5.3 have been collected and analyzed, less than half of them have actually been used in the current inventory for structures in the region. The final inventory has not yet been completely compiled, therefore, only a portion of the inventory for the region is used in the case study presented in this chapter. Table 5.4 presents a summary of the current state of the regional inventory. The buildings used in this analysis comprise about 95% of the total buildings located in the county, therefore it is assumed that the results computed from these roughly 195,000 buildings will be reasonable.

Once each facility in the county is address matched and assigned a longitude and latitude as shown in Figure 5.14, point maps of the facilities are generated in order to

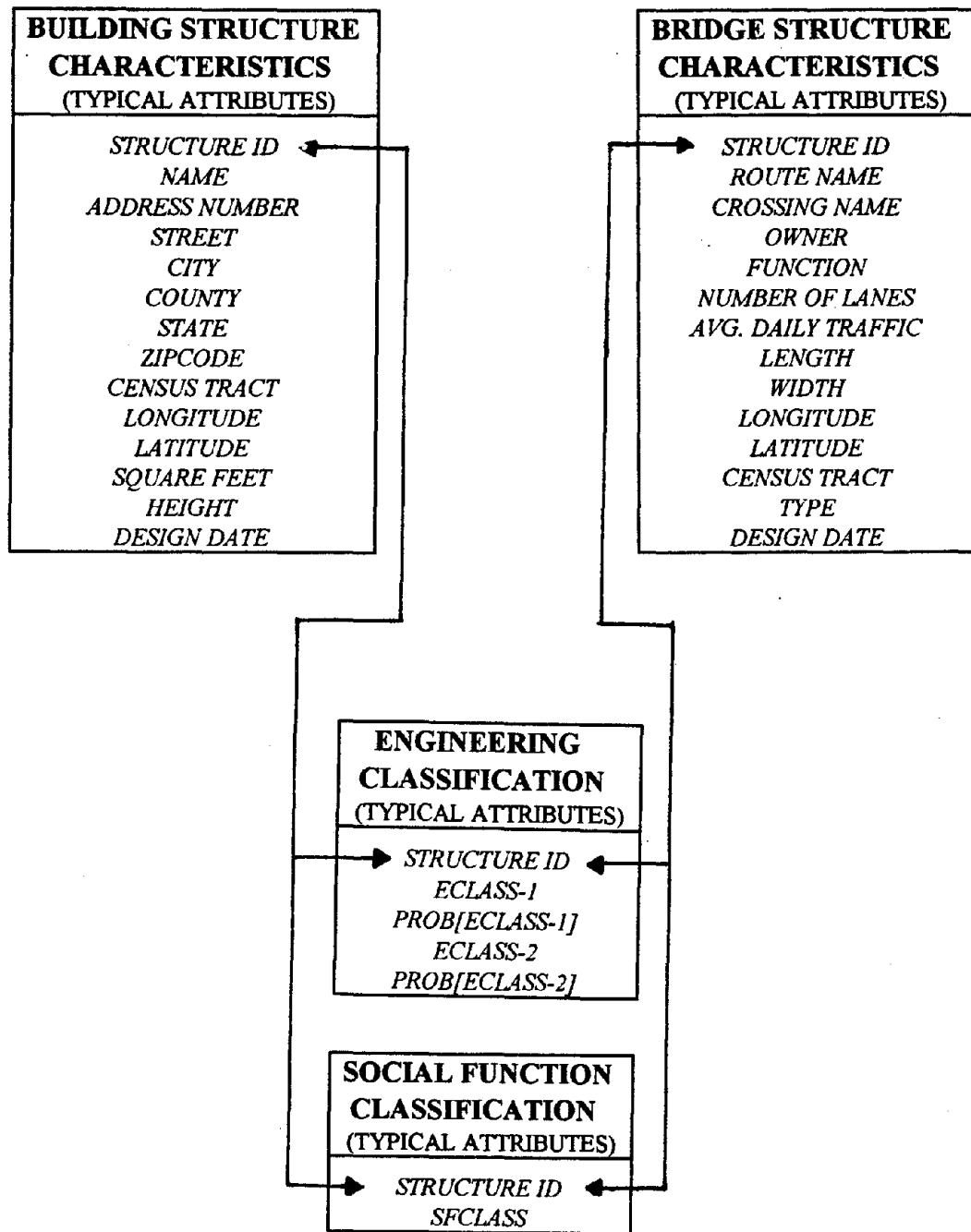


Figure 5.13. Interrelated database tables at inventory development stage (from Applied Technology Council, ATC-36, in progress).

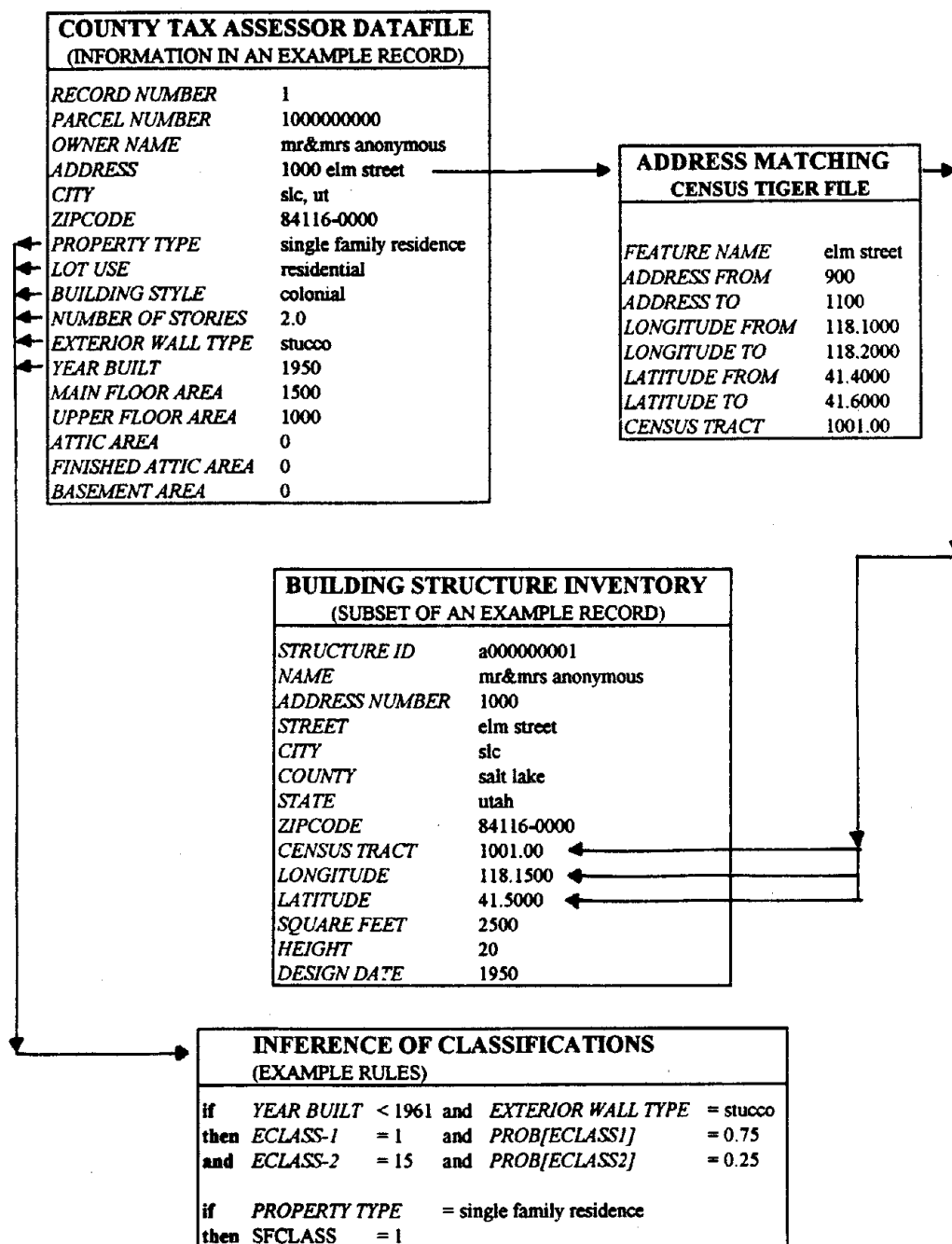


Figure 5.14. Use of County Tax Assessor datafile in structural inventory development.



**Table 5.1.** Social function classification for Salt Lake County, Utah (from Applied Technology Council, ATC-36, in progress).

DESCRIPTION	SOCIAL FUNCTION CLASS
<b>A. RESIDENTIAL</b>	
Permanent Dwelling	1
Temporary Lodging	2
Group Institutional Housing	3
<b>B. COMMERCIAL</b>	
Retail Trade	4
Wholesale Trade	5
Financial Services	36
Personal Services	6
Professional Services	7
Entertainment and Recreation	9
Parking	10
<b>C. INDUSTRIAL</b>	
Heavy Manufacturing	11
Light Manufacturing	12
Food and Drug Processing	13
Chemical Processing	14
Metal and Mineral Processing	15
High Technology	16
Construction	17
Petroleum Refining and Distribution	18
<b>D. AGRICULTURE</b>	
Livestock	47
Harvest	48
Forestry	49
Fisheries	50
<b>E. MINING</b>	
	20
<b>F. RELIGION AND NON-PROFIT</b>	
	21
<b>G. GOVERNMENT</b>	
General Services	22
Emergency Response Centers	23
Police	37
Fire	38
National Guard/Reserve Armories	39

**Table 5.1.** Social function classification for Salt Lake County, Utah (from Applied Technology Council, ATC-36, in progress), continued.

<b>DESCRIPTION</b>	<b>SOCIAL FUNCTION CLASS</b>
<b>H. MEDICAL FACILITIES AND SERVICES</b>	
Hospitals	40
Ambulance Services	41
Nursing Homes	42
Health Care Services	8
<b>I. EDUCATION</b>	
Elementary	24
Secondary & Junior Colleges	43
Colleges and Universities	44
<b>J. TRANSPORTATION (Freight and Passenger)</b>	
Highway	25
Railway	26
Air	27
Sea/Water (Port, Harbor, Canals, etc.)	28
Mass Transit (Bus/Rail)	46
<b>K. UTILITIES</b>	
Electric Power	29
Water	30
Sanitary Sewer	31
Natural Gas	32
<b>L. COMMUNICATION</b>	
Radio and TV	34
Hard-wire Telephone and Telegraph	33
Cellular Telephone	45
<b>M. FLOOD CONTROL</b>	
	35

**Table 5.2.** Earthquake engineering classification for Salt Lake County, Utah (from Applied Technology Council, ATC-36, in progress).

<b>EARTHQUAKE ENGINEERING CLASS</b>	<b>DESCRIPTION</b>
1	Wood, Light Frame
2	Wood, Commercial & Industrial
3	Steel, Moment Frame
4	Steel, Braced Frame
5	Steel, Light Frame
6	Steel Frame with Concrete Shear Wall
7	Steel Frame with URM Infill
8	Concrete, Moment Frame
9	Concrete, Shear Wall
10	Concrete Frame with URM Infill
11	Precast/Tilt-up with Flexible Diaphragm
12	Precast Frame
13	Reinforced Masonry with Flexible Diaphragm
14	Reinforced Masonry with Precast Diaphragm
15	URM Bearing Wall
16	Mobile Homes
24	Conventional Bridges (< 500' spans)
25	Continuous/Monolithic Bridges
30	Major Bridges (> 500' spans)
31	Underground Pipelines
32	At Grade Pipelines
35	Concrete Dams
36	Earthfill and Rockfill Dams
38	Alluvium Tunnels
39	Rock Tunnels
40	Cut and Cover Tunnels
41	Underground Liquid Storage Tanks
42	Underground Solid Storage Tanks
43	On Ground Liquid Storage Tanks
44	On Ground Solid Storage Tanks
45	Elevated Liquid Storage Tanks
46	Elevated Solid Storage Tanks

**Table 5.2.** Earthquake engineering classification for Salt Lake County, Utah (from Applied Technology Council, ATC-36, in progress), continued.

<b>EARTHQUAKE ENGINEERING CLASS</b>	<b>DESCRIPTION</b>
47	Railroad Lines
48	Highways
49	Runways
50	Masonry Chimneys
51	Concrete Chimneys
52	Steel Chimneys
53	Cranes
54	Conveyor Systems
55	Conventional Electrical Transmission Towers (< 100' high)
56	Major Electrical Transmission Towers (> 100' high)
57	Broadcast Towers
58	Observation Towers
59	Offshore Towers
61	Canals
62	Earth Retaining Structures (> 20' high)
63	Waterfront Structures
64	Residential Equipment
65	Office Equipment
66	Electrical Equipment
68	Mechanical Equipment
70	High Technology and Laboratory Equipment
90	Trains, Trucks, and Other Vehicles

**Table 5.3.** Sources of inventory data for Salt Lake County, Utah (from Applied Technology Council, ATC-36, in progress).

DESCRIPTION	PRIMARY SOURCE	SECONDARY SOURCE
<b>A. RESIDENTIAL</b>		
Permanent Dwelling	CTA	CFE
Temporary Lodging	CTA	CFE
Group Institutional Housing	CTA	CFE
<b>B. COMMERCIAL</b>		
Retail Trade	CTA	DNB
Wholesale Trade	CTA	DNB
Financial Services	CTA	DNB
Personal Services	CTA	DNB
Professional Services	CTA	DNB
Entertainment and Recreation	CTA	DNB
Parking	CTA	DNB
<b>C. INDUSTRIAL</b>		
Heavy Manufacturing	CTA	DFAD
Light Manufacturing	CTA	DFAD
Food and Drug Processing	CTA	DFAD
Chemical Processing	CTA	DFAD
Metal and Mineral Processing	CTA	DFAD
High Technology	CTA	DFAD
Construction	CTA	DFAD
Petroleum Refining and Distribution	CTA	DFAD
<b>D. AGRICULTURE</b>		
Livestock	DFAD	CRD
Harvest	DFAD	CRD
Forestry	DFAD	CRD
Fisheries	DFAD	CRD
<b>E. MINING</b>		
	DFAD	CRD
<b>F. RELIGION AND NON-PROFIT</b>		
	LPD	DFAD
<b>G. GOVERNMENT</b>		
General Services	LPD	SES
Emergency Response Centers	SES	CRD
Police	LPD	SES
Fire	LPD	SES
National Guard/Reserve Armories	CRD	DFAD

**Table 5.3.** Sources of inventory data for Salt Lake County, Utah (from Applied Technology Council, ATC-36, in progress), continued.

DESCRIPTION	PRIMARY SOURCE	SECONDARY SOURCE
<b>H. MEDICAL FACILITIES AND SERVICES</b>		
Hospitals	LPD	CRD
Ambulance Services	CTA	CRD
Nursing Homes	CTA	CRD
Health Care Services	CTA	CRD
<b>I. EDUCATION</b>		
Elementary	LPD	DFAD
Secondary & Junior Colleges	LPD	DFAD
Colleges and Universities	LPD	DFAD
<b>J. TRANSPORTATION (Freight and Passenger)</b>		
Highway	CTF	SES
Railway	CTF	SES
Air	SES	DFAD
Sea/Water (Port, Harbor, Canals, etc.)	SES	DFAD
Mass Transit (Bus/Rail)	SES	DFAD
<b>K. UTILITIES</b>		
Electric Power	PCD	SES
Water	PCD	SES
Sanitary Sewer	PCD	SES
Natural Gas	PCD	SES
<b>L. COMMUNICATION</b>		
Radio and TV	DFAD	CRD
Hard-wire Telephone and Telegraph	SES	CRD
Cellular Telephone	DFAD	CRD
<b>M. FLOOD CONTROL</b>	<b>SES</b>	<b>DFAD</b>

CTA = County Tax Assessor  
 CFF = Census Flat Files  
 DNB = Dun and Bradstreet Data  
 DFAD = Digital Feature Analysis Data  
 CRD = Critical Resources Database  
 LPD = Local Practitioner Databases  
 SES = State Emergency Services  
 CTF = Census TIGER Files  
 PCD = Private Company Databases

**Table 5.4.** Summary of current status of inventory data for Salt Lake County, Utah  
(from Applied Technology Council, ATC-36, in progress).

<b>BUILDINGS</b>	
Total number of all buildings	195,785
Total number of residential buildings	176,657
% of total that are residential buildings	90.2
Total number of commercial buildings	19,128
% of total that are commercial buildings	9.8
Total number of buildings with wood frame construction	111,732
% of total with wood frame construction	57.1
Total number of buildings with unreinforced masonry construction	52,519
% of total with unreinforced masonry construction	26.8
Total number of buildings with steel construction	555
% of total with steel construction	0.28
Total number of buildings with concrete construction	156
% of total with concrete construction	0.08
Total number of buildings with mixed construction	30,823
% of total with mixed construction	15.7
<b>BRIDGES</b>	
Total number of bridges	279
Total number of conventional bridges	172
% of total that are conventional bridges	61.6
Total number of continuous bridges	107
% of total that are continuous bridges	38.4
Total number of interchanges or ramps	102
% of total that are interchanges or ramps	36.6
Total number of minor bridges	177
% of total that are minor bridges	63.4

conduct the overlay analysis procedure illustrated in Figure 1.2. The large number of buildings in this case study requires the inventory to be subdivided into files of about 30,000 buildings each to facilitate the analysis. One of these files, containing the 20,000 commercial buildings in the county, is shown in Figure 5.15. An example list of attributes associated with one of the buildings is shown as well. Figure 5.16 illustrates the same concept for the bridges in the county.

At this stage in the analysis, summary maps may also be generated that help to describe the characteristics of the inventory in the study region. For example, the percentage of unreinforced masonry buildings in each Census tract can be displayed as shown in Figure 5.17. Figure 5.18 illustrates another summary statistic, the average design date of the buildings in each Census tract. These summaries help to indicate those areas that contain relatively older and more hazardous buildings. Perhaps if resources were limited, a detailed analysis might be conducted only in the most hazardous areas, while the remainder of the county can be analyzed when more funding is available.

### 5.3.2 Damage Estimation

The definitions of damage and the various ways to compute damage due to earthquakes have been discussed in Section 4.2. In this case study, the damage is represented as a damage factor as defined in Equation (4.3), and is computed through expected damage factor curves as illustrated in Figure 4.5. These curves give the expected damage factor and the standard deviation of the damage factor at different levels of intensity for a given earthquake engineering class. The curves used in this case study were modified for Utah construction from the ATC-13 (Applied Technology Council, 1985) curves for California construction by local experts on the ATC-36 (Applied Technology Council, in progress) project panel.

The analysis procedure for estimating damage involves overlaying the point maps of facility data, such as Figures 5.15 and 5.16, on the seismic hazard maps shown in Figures 5.5 and 5.12 to assign values of seismic hazard to each facility in the inventory. At this stage, Table 5.5, the table of values for expected damage as a function of intensity for each engineering class, must be included in the scheme of inter-related tables shown previously in Figure 5.13. Figure 5.19 illustrates the procedure of overlaying the point map of buildings shown in Figure 5.15 on top of the final combined seismic hazard map, with an example listing of the attributes now associated with each building. Figure 5.20



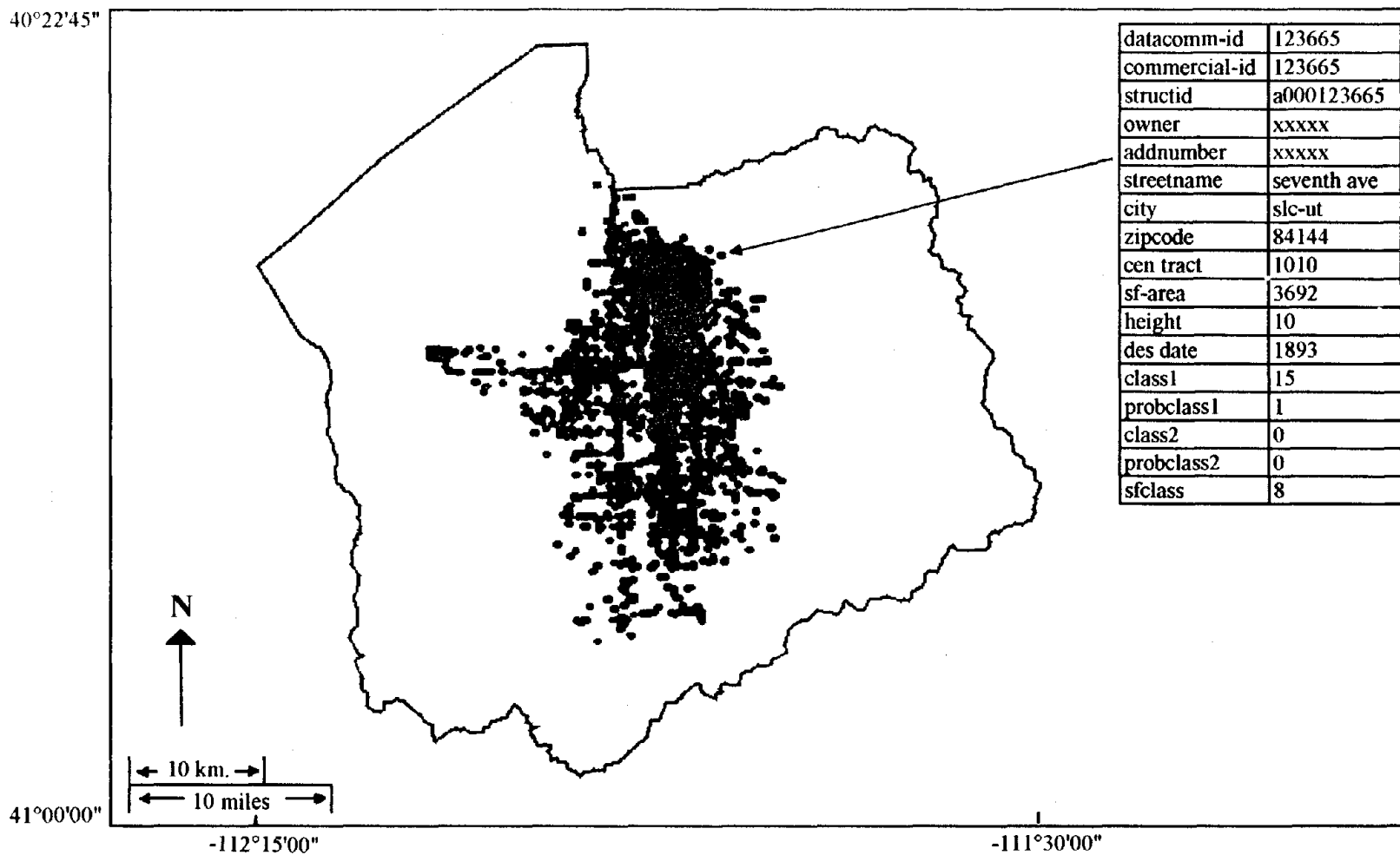


Figure 5.15. Map showing commercial building inventory in Salt Lake County, Utah.

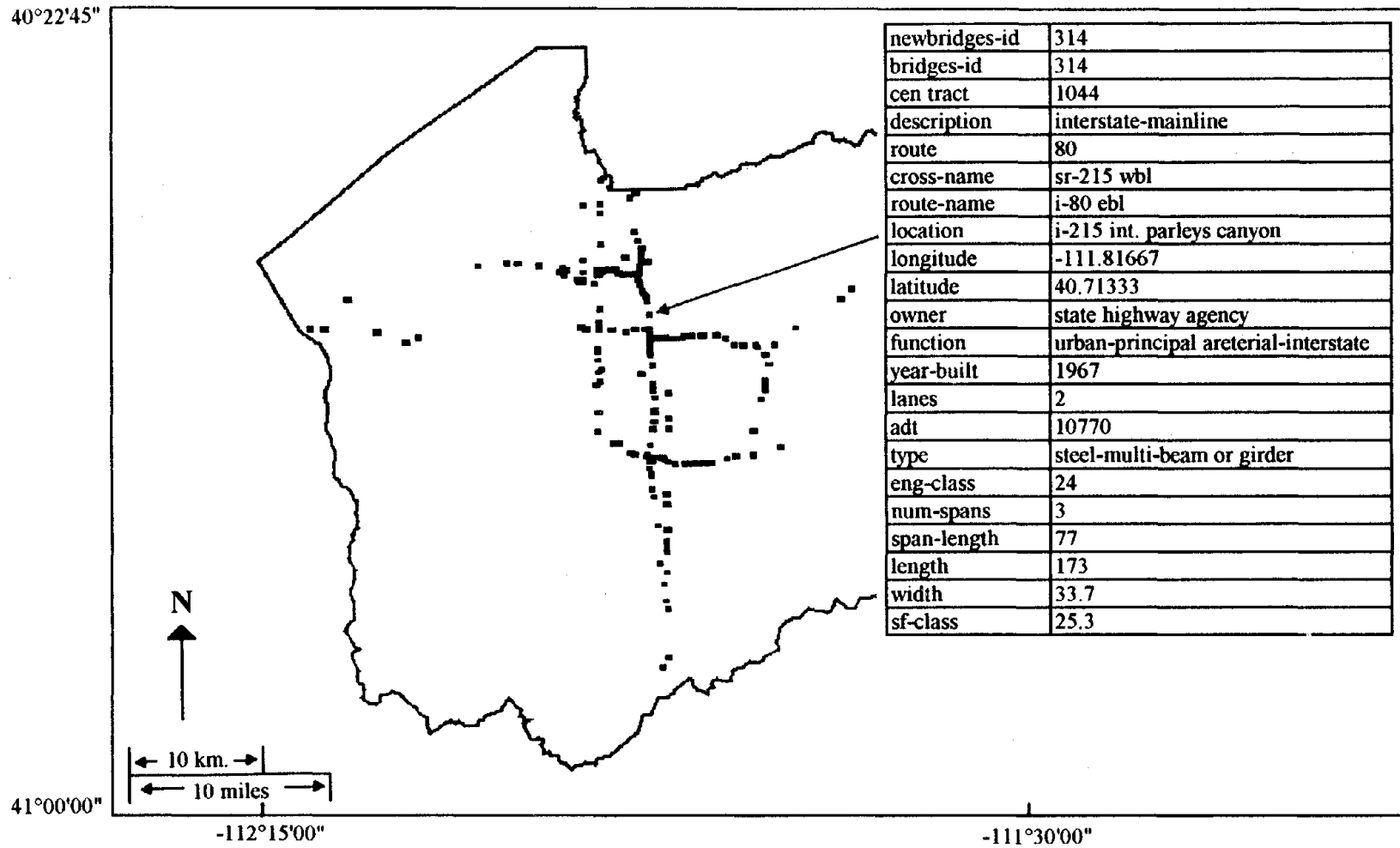


Figure 5.16. Map showing highway bridge inventory in Salt Lake County, Utah.

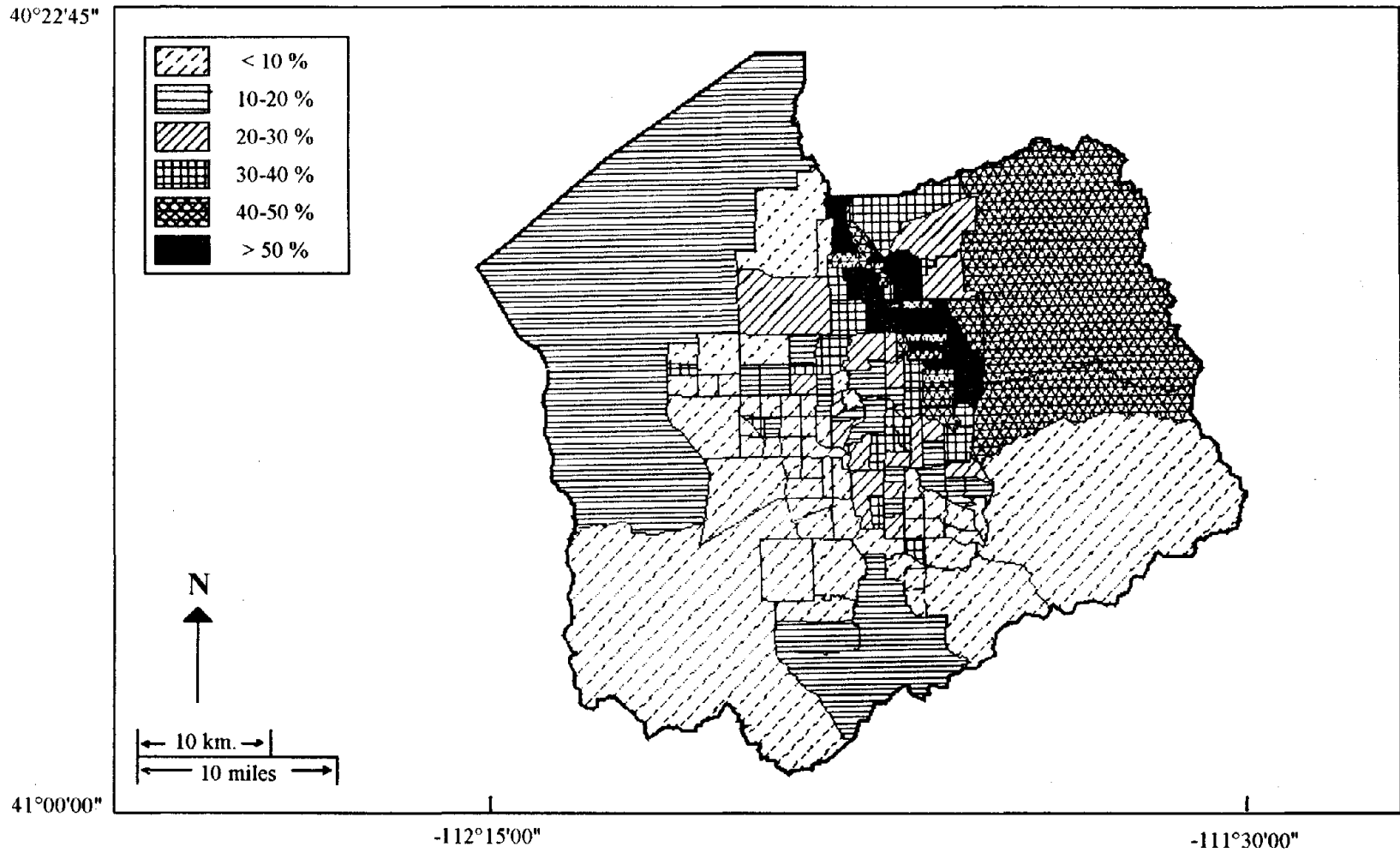
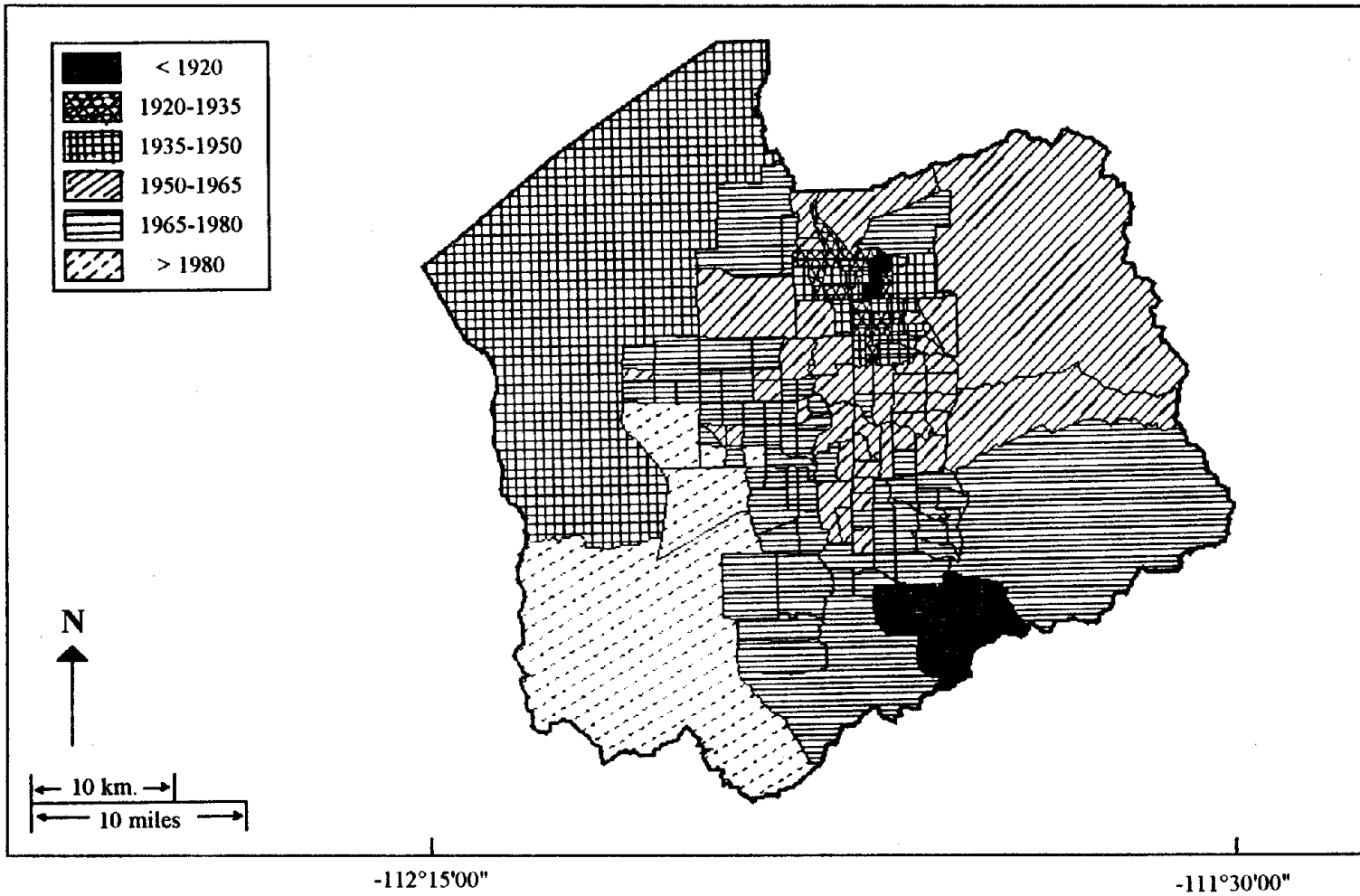


Figure 5.17. Map showing percentage of unreinforced masonry buildings in each Census tract in Salt Lake County, Utah.

40°22'45"



**Figure 5.18.** Map showing average design date of buildings in each Census tract in Salt Lake County, Utah.

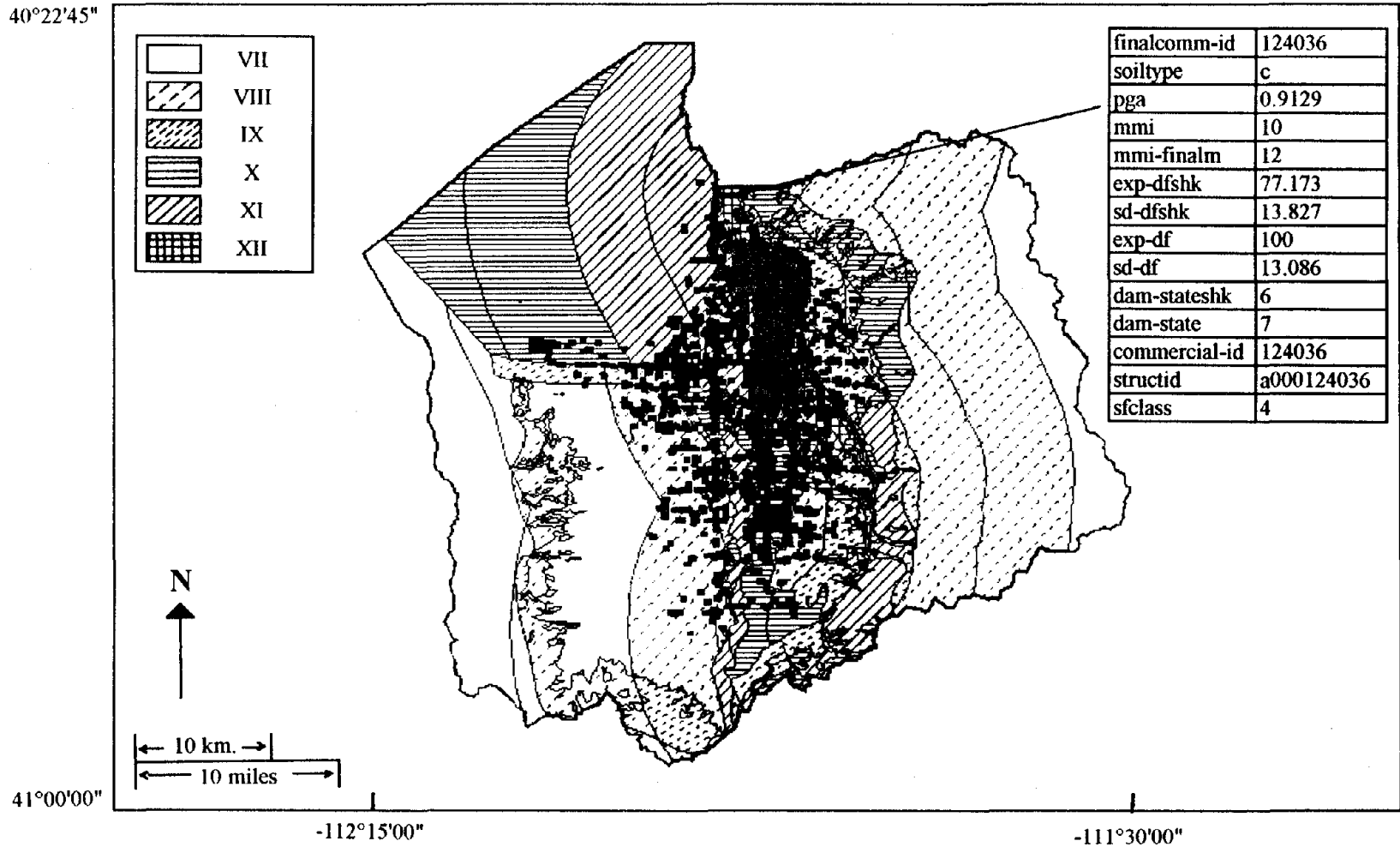


Figure 5.19. Map showing intermediate results for commercial buildings on top of combined seismic hazard ( $MMI_F$ ) in Salt Lake County, Utah.

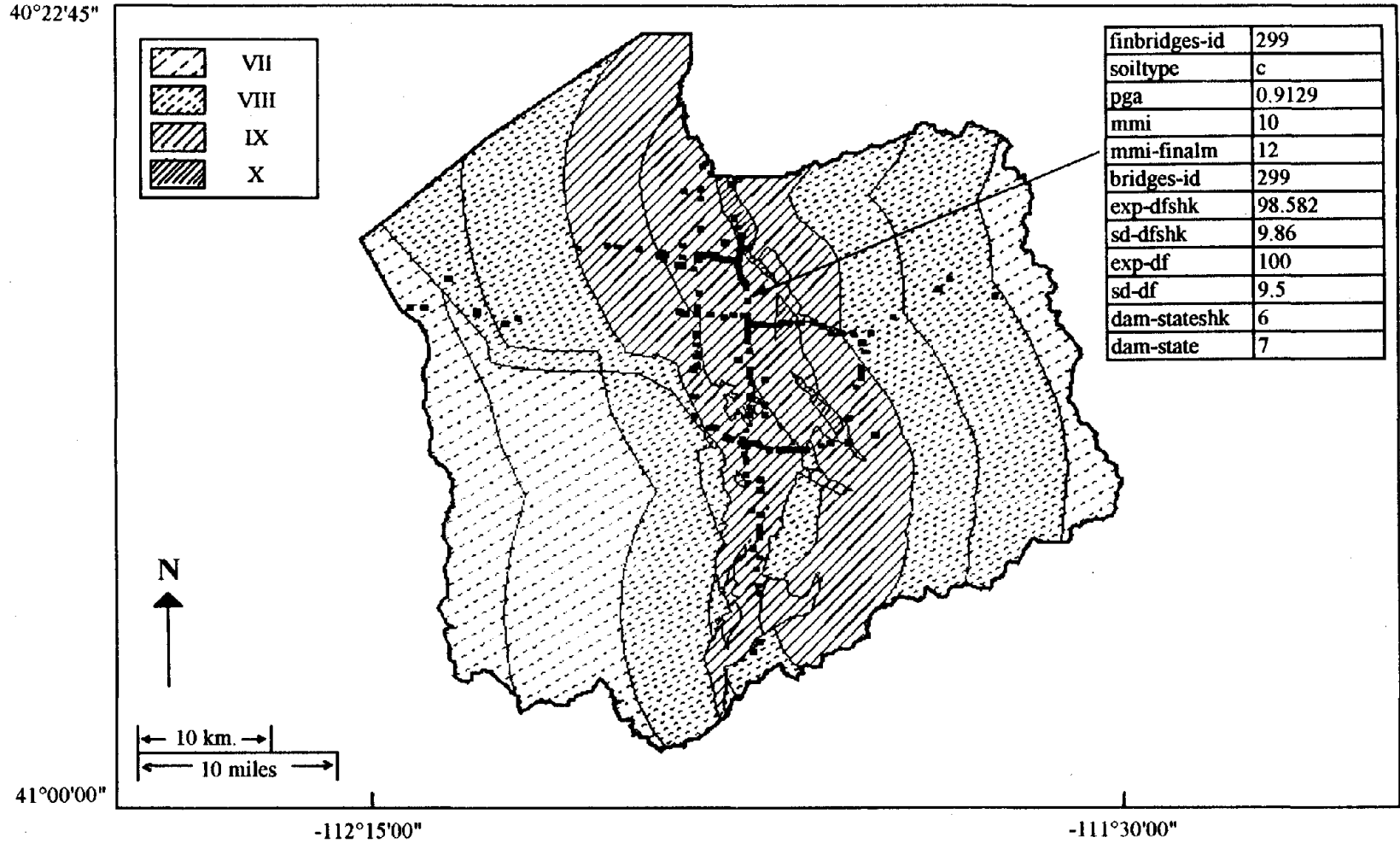


Figure 5.20. Map showing intermediate results for highway bridges on top of ground shaking hazard ( $MMI_{GS}$ ) in Salt Lake County, Utah.

**Table 5.5.** Expected values and standard deviation of damage factor (%) as a function of MMI for earthquake engineering classes in Salt Lake County, Utah (from Applied Technology Council, ATC-36, in progress).

MMI	CLASS 1		CLASS 2		CLASS 3		CLASS 4	
	E[DF]	SD[DF]	E[DF]	SD[DF]	E[DF]	SD[DF]	E[DF]	SD[DF]
6.0	0.78	0.58	0.78	0.58	0.71	1.01	0.69	1.10
7.0	1.54	0.78	1.54	0.78	0.98	0.59	1.29	0.70
8.0	4.71	2.46	4.71	2.46	1.50	0.39	2.99	0.58
9.0	9.24	3.84	9.24	3.84	2.42	0.34	4.14	0.41
10.0	19.79	8.54	19.79	8.54	4.36	0.32	5.78	0.37
11.0	24.37	7.94	24.37	7.94	6.76	0.30	8.89	0.33
12.0	37.33	10.20	37.33	10.20	8.31	0.26	10.27	0.27

MMI	CLASS 5		CLASS 6		CLASS 7		CLASS 8	
	E[DF]	SD[DF]	E[DF]	SD[DF]	E[DF]	SD[DF]	E[DF]	SD[DF]
6.0	2.00	1.94	0.54	0.49	1.55	1.32	1.27	1.07
7.0	5.00	2.50	2.81	1.63	5.66	4.28	4.21	2.16
8.0	8.00	3.88	6.55	2.96	16.11	9.89	12.21	4.86
9.0	13.00	5.95	13.02	5.08	30.81	13.17	23.00	8.10
10.0	20.00	8.00	23.61	6.95	44.92	14.38	34.23	10.44
11.0	27.00	9.26	35.54	9.46	66.11	16.38	47.63	11.91
12.0	34.00	8.77	47.63	9.23	77.79	16.25	60.00	6.66

MMI	CLASS 9		CLASS 10		CLASS 11		CLASS 12	
	E[DF]	SD[DF]	E[DF]	SD[DF]	E[DF]	SD[DF]	E[DF]	SD[DF]
6.0	0.54	0.49	1.55	1.32	1.45	0.96	5.00	5.91
7.0	2.81	1.63	5.66	4.28	4.81	2.51	20.00	18.36
8.0	6.55	2.96	16.11	9.89	10.54	4.43	33.00	18.94
9.0	13.02	5.08	30.81	13.17	18.65	7.00	45.00	14.58
10.0	23.61	6.95	44.92	14.38	30.05	10.33	54.00	16.25
11.0	35.54	9.46	66.11	16.38	46.81	13.10	64.00	16.96
12.0	47.63	9.23	77.79	16.25	64.50	13.25	73.00	18.98

MMI	CLASS 13		CLASS 14		CLASS 15		CLASS 16	
	E[DF]	SD[DF]	E[DF]	SD[DF]	E[DF]	SD[DF]	E[DF]	SD[DF]
6.0	0.84	0.60	7.00	4.21	8.96	5.39	0.97	1.60
7.0	2.90	1.74	10.00	5.19	22.63	11.75	2.88	1.94
8.0	5.97	3.17	20.00	5.84	39.53	11.56	6.26	3.86
9.0	13.50	6.77	28.00	6.55	64.78	15.15	15.01	7.20
10.0	23.24	8.29	45.00	8.06	77.17	13.83	28.47	7.90
11.0	41.93	12.38	62.00	9.05	89.41	13.09	38.67	10.46
12.0	52.34	12.48	80.00	10.48	100.00	13.09	57.24	9.42

**Table 5.5.** Expected value and standard deviation of damage factor (%) as a function of MMI for earthquake engineering classes in Salt Lake County, Utah (from Applied Technology Council, ATC-36, in progress), continued.

MMI	CLASS 24		CLASS 25		CLASS 30		CLASS 31	
	E[DF]	SD[DF]	E[DF]	SD[DF]	E[DF]	SD[DF]	E[DF]	SD[DF]
6.0	8.80	5.37	4.01	3.61	0.20	0.10	0.00	0.00
7.0	26.40	9.50	3.07	2.64	1.50	0.78	0.40	0.20
8.0	48.40	12.58	9.90	4.36	1.97	1.24	0.70	0.62
9.0	81.60	14.69	41.20	4.94	28.50	12.54	2.90	1.80
10.0	98.58	0.99	63.80	14.04	69.10	0.00	7.80	4.13
11.0	100.00	9.50	89.40	12.52	100.00	22.00	19.20	7.10
12.0	100.00	9.50	100.00	18.00	100.00	22.00	30.60	13.77

MMI	CLASS 32		CLASS 35		CLASS 36		CLASS 38	
	E[DF]	SD[DF]	E[DF]	SD[DF]	E[DF]	SD[DF]	E[DF]	SD[DF]
6.0	0.00	0.00	0.50	0.20	2.30	1.56	0.19	0.29
7.0	0.50	0.20	3.40	1.73	5.80	3.13	0.80	0.73
8.0	1.10	0.72	6.30	3.02	9.20	3.77	1.90	1.31
9.0	2.30	1.13	17.00	7.82	22.57	9.71	5.50	3.52
10.0	5.10	2.55	29.80	9.24	39.60	11.48	12.00	6.48
11.0	14.10	5.08	42.60	16.40	56.63	20.39	23.80	12.14
12.0	23.10	9.93	55.40	21.33	73.65	26.51	35.60	18.69

MMI	CLASS 39		CLASS 40		CLASS 41		CLASS 42	
	E[DF]	SD[DF]	E[DF]	SD[DF]	E[DF]	SD[DF]	E[DF]	SD[DF]
6.0	0.20	0.25	0.30	0.47	0.10	0.15	0.00	0.00
7.0	0.50	0.70	1.00	0.80	0.60	1.02	0.50	0.38
8.0	1.80	0.86	2.80	1.99	2.50	1.58	0.10	0.15
9.0	4.90	2.40	9.20	5.70	6.20	4.03	2.10	1.53
10.0	9.00	3.69	17.60	9.15	15.30	10.40	3.50	2.28
11.0	16.40	5.74	29.20	15.48	27.80	26.41	14.40	10.80
12.0	23.80	9.04	40.80	21.42	40.30	32.84	25.30	17.71

MMI	CLASS 43		CLASS 44		CLASS 45		CLASS 46	
	E[DF]	SD[DF]	E[DF]	SD[DF]	E[DF]	SD[DF]	E[DF]	SD[DF]
6.0	1.70	1.05	2.00	0.86	4.70	2.59	4.70	2.54
7.0	4.60	2.48	5.10	2.55	10.40	5.20	9.50	3.90
8.0	15.60	7.80	17.10	8.04	23.80	9.04	20.00	7.40
9.0	27.90	10.60	35.32	12.36	38.80	17.85	31.40	10.36
10.0	37.40	11.59	43.80	14.89	58.58	16.40	55.10	15.98
11.0	46.90	16.18	52.27	18.03	78.37	29.00	78.80	24.43
12.0	56.40	19.46	60.75	20.96	98.16	36.32	100.00	31.00



**Table 5.5.** Expected value and standard deviation of damage factor (%) as a function of MMI for earthquake engineering classes in Salt Lake County, Utah (from Applied Technology Council, ATC-36, in progress), continued.

MMI	CLASS 47		CLASS 48		CLASS 49		CLASS 50	
	E[DF]	SD[DF]	E[DF]	SD[DF]	E[DF]	SD[DF]	E[DF]	SD[DF]
6.0	0.10	0.15	0.10	0.14	0.00	0.00	6.10	2.01
7.0	0.90	0.81	0.60	0.97	0.30	0.17	9.60	4.51
8.0	3.00	7.17	2.50	2.40	3.60	2.95	20.60	5.15
9.0	7.80	3.90	4.60	4.05	9.30	4.46	38.80	8.15
10.0	12.50	5.25	9.60	6.05	15.70	6.75	58.20	9.89
11.0	19.10	4.78	19.90	5.57	27.00	5.94	81.10	9.73
12.0	39.10	7.82	29.60	13.02	55.30	9.40	100.00	14.50

MMI	CLASS 51		CLASS 52		CLASS 53		CLASS 54	
	E[DF]	SD[DF]	E[DF]	SD[DF]	E[DF]	SD[DF]	E[DF]	SD[DF]
6.0	2.10	1.16	2.70	1.51	1.40	0.99	2.10	1.01
7.0	6.80	3.40	6.30	2.90	5.50	2.64	5.80	2.20
8.0	15.10	6.19	16.40	5.25	11.70	5.03	10.10	3.53
9.0	30.30	3.94	30.00	8.70	25.30	8.35	15.70	5.34
10.0	45.90	13.77	45.20	14.01	40.60	7.71	30.90	4.64
11.0	64.10	14.74	60.41	18.12	53.50	8.56	40.90	10.23
12.0	82.31	21.81	75.61	22.68	66.40	11.62	50.90	10.18

MMI	CLASS 55		CLASS 56		CLASS 57		CLASS 58	
	E[DF]	SD[DF]	E[DF]	SD[DF]	E[DF]	SD[DF]	E[DF]	SD[DF]
6.0	0.60	0.48	0.10	0.15	1.00	0.43	2.70	2.70
7.0	1.10	0.75	0.70	0.58	2.40	1.34	4.92	3.30
8.0	3.80	1.94	1.10	0.76	4.90	2.74	10.31	15.98
9.0	9.10	4.10	3.10	1.77	10.70	5.89	15.00	7.95
10.0	18.50	7.21	8.00	4.00	27.90	10.88	25.00	11.00
11.0	33.60	11.09	16.60	6.81	49.10	14.73	41.40	16.15
12.0	48.70	17.53	34.21	11.97	70.30	24.25	57.80	23.99

MMI	CLASS 59		CLASS 61		CLASS 62		CLASS 63	
	E[DF]	SD[DF]	E[DF]	SD[DF]	E[DF]	SD[DF]	E[DF]	SD[DF]
6.0	1.10	1.73	0.30	0.41	1.70	1.67	0.50	0.25
7.0	2.30	2.28	0.60	0.52	7.10	2.98	1.70	0.77
8.0	3.80	3.42	2.80	2.44	12.60	4.66	4.90	1.96
9.0	9.70	7.66	7.50	4.95	21.50	5.59	12.50	4.25
10.0	19.40	11.64	17.20	8.60	45.00	10.80	25.10	6.78
11.0	34.80	15.31	33.80	14.53	72.20	10.83	40.20	7.64
12.0	50.19	26.10	50.40	23.44	99.40	19.38	53.10	8.50

**Table 5.5.** Expected value and standard deviation of damage factor (%) as a function of MMI for earthquake engineering classes in Salt Lake County, Utah (from Applied Technology Council, ATC-36, in progress), continued.

MMI	CLASS 64		CLASS 65		CLASS 66		CLASS 68	
	E[DF]	SD[DF]	E[DF]	SD[DF]	E[DF]	SD[DF]	E[DF]	SD[DF]
6.0	0.80	0.56	3.70	2.63	8.70	5.66	2.50	1.70
7.0	2.20	1.19	8.70	5.66	18.70	8.98	6.10	4.27
8.0	5.40	2.16	18.70	8.98	31.80	9.54	11.31	7.13
9.0	13.70	5.34	31.80	9.54	42.90	9.87	22.00	11.66
10.0	25.70	7.97	42.90	9.87	59.00	17.11	33.10	14.23
11.0	43.10	9.91	59.00	17.11	75.10	19.53	48.31	25.12
12.0	57.60	9.22	75.10	19.53	91.21	23.71	63.52	30.17

MMI	CLASS 70		CLASS 90	
	E[DF]	SD[DF]	E[DF]	SD[DF]
6.0	1.40	1.13	0.50	0.75
7.0	4.66	2.94	1.00	1.54
8.0	13.00	6.50	2.10	0.97
9.0	24.40	11.22	6.20	3.22
10.0	40.80	14.28	12.00	5.04
11.0	59.10	20.10	25.00	10.50
12.0	74.90	12.73	35.00	13.30

illustrates this same concept for bridges being overlaid on the map of seismic hazard due to ground shaking alone.

Several types of summary maps may be generated at this point. Damage estimates may be averaged or summed by earthquake engineering class, by social function class, by zip code, by ranges of design date, or by any other data attribute associated with each facility. As an example, Figure 5.21 shows the average damage factor of the buildings in each Census tract due to ground shaking hazard alone, while Figure 5.22 shows the average damage factor of the buildings in each Census tract due to the combined seismic hazards. These two figures illustrate the increase in expected damage when the local site effects are considered in the analysis. As another example, Figure 5.23 shows the percentage of buildings in each Census tract that have an expected damage factor greater than or equal to 60% due to the combined seismic hazards. The patterns of high damage shown here are consistent with the high intensity values shown in Figure 5.12 and the areas with higher percentages of hazardous buildings shown in Figure 5.17.

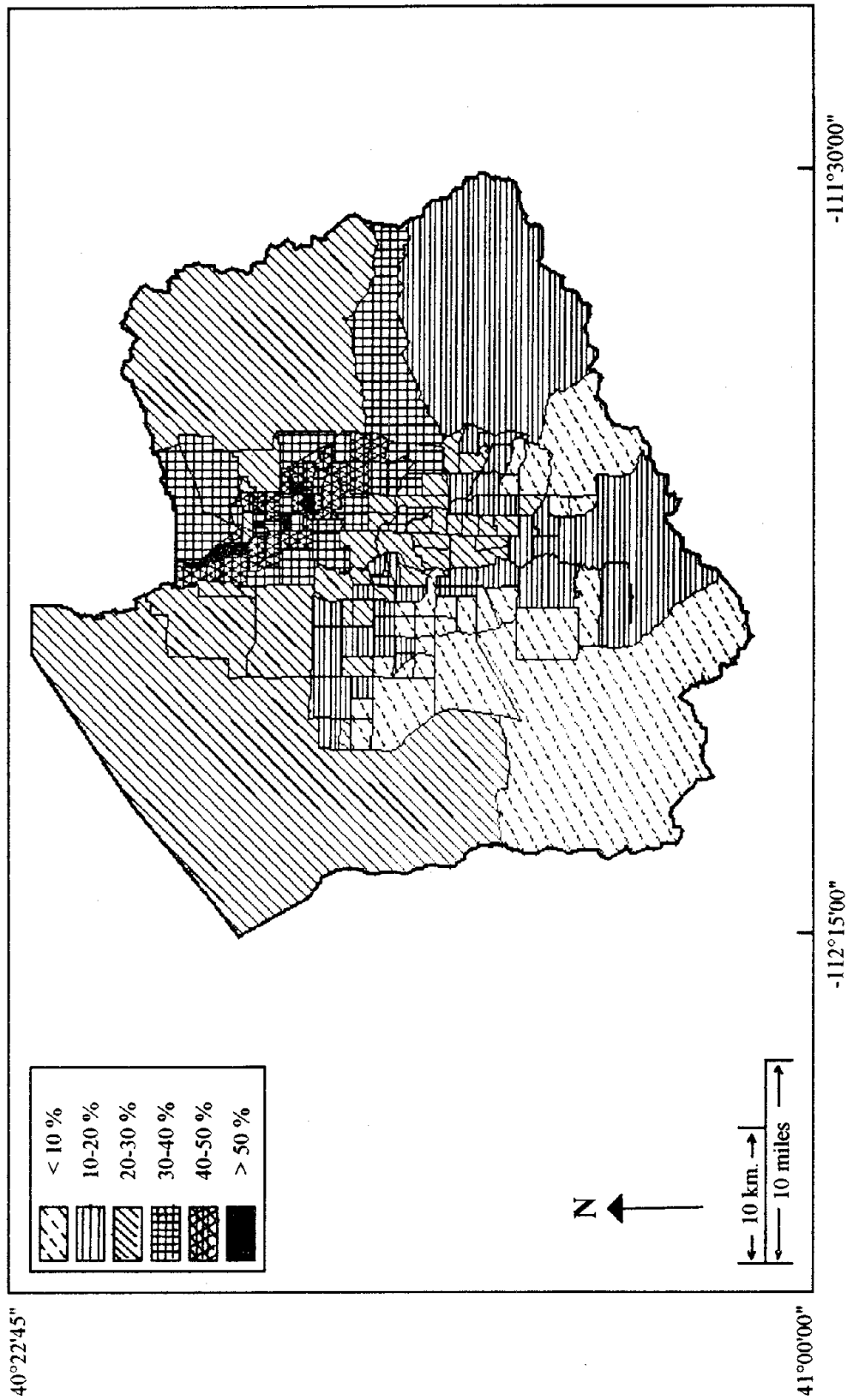


**Figure 5.21.** Map showing average expected damage factor (%) due to ground shaking hazard ( $MMI_{GS}$ ) in each Census tract in Salt Lake County, Utah.

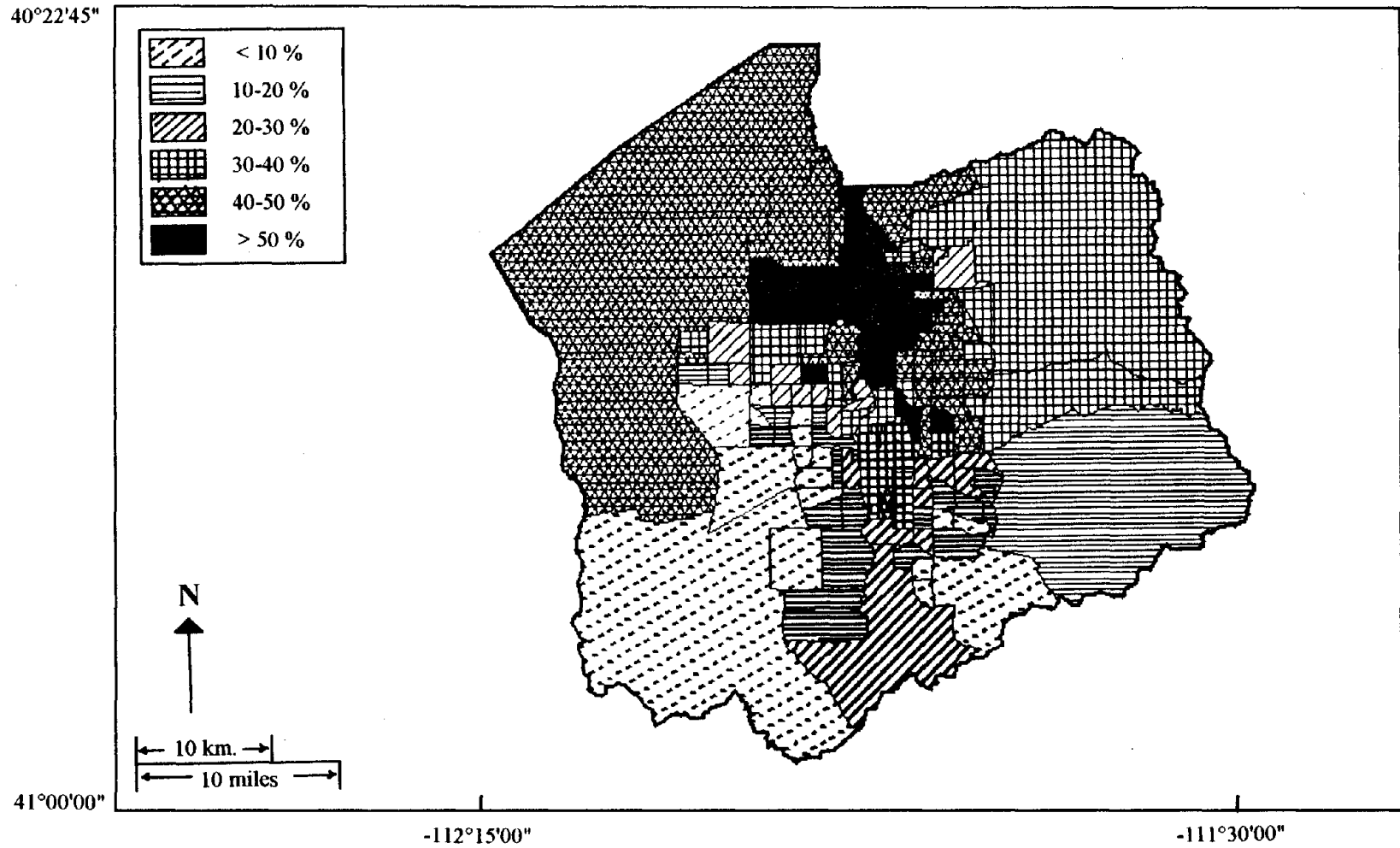


**Figure 5.22.** Map showing average expected damage factor (%) due to combined seismic hazard ( $MMI_F$ ) in each Census tract in Salt Lake County, Utah.

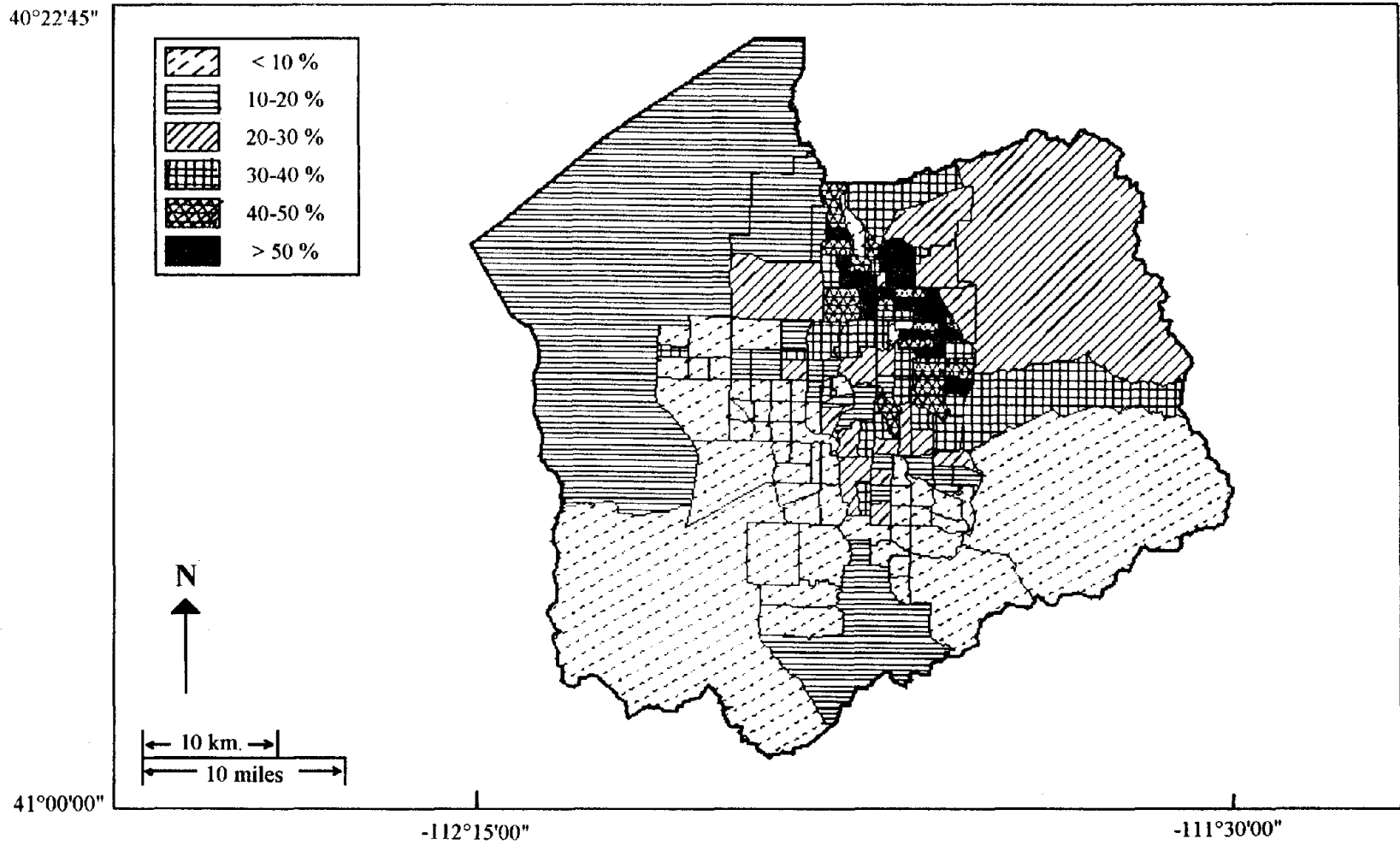


**Figure 5.23.** Map showing percentage of buildings with expected damage factor greater than 60% due to combined seismic hazard ( $MMI_F$ ) in Salt Lake County, Utah.

### 5.3.3 Loss Estimation

The different definitions of loss and the various ways to compute these losses due to earthquakes have been discussed in Section 4.3. In a GIS-based earthquake damage and loss study, the losses are generally computed by adding more tables to the database of inter-related tables, not by performing further map overlays. In this case study, the loss estimates are limited to direct structural dollar loss, loss of facility use, and casualties. In order to compute these estimates, four new tables must be added to the scheme of inter-related tables. These tables are the occupancy values and facility replacement costs shown in Tables 5.6 and 5.7, the loss of function estimates shown in Tables 5.8 and 5.9, and the casualty estimates shown in Table 5.10. Figure 5.24 shows the final database of inter-related tables used in the analysis in this case study. This figure helps to illustrate the modular design of a GIS-based regional analysis. Models in the form of database tables can be easily added or modified at any stage in the analysis. Data in the form of maps or flat tables can also be easily added or modified to improve the analysis and keep the inventory up to date.

In the same manner as previously shown in Figures 5.15 and 5.16, the final results of the analysis for the commercial buildings and the bridges are shown in Figures 5.25 and 5.26, respectively. Example attribute listings are also shown to illustrate the types of results that can be reported. As with the damage estimates, the loss estimates may also be summarized at any level or over any selected attribute. Figures 5.27 through 5.29 illustrate three examples of loss statistics due to the scenario event with all collateral hazards included. Figure 5.27 shows the total expected dollar loss due to structural damage to buildings in each Census tract, Figure 5.28 shows the average number of days to restore the buildings in each Census tract to 100% of their full functionality, and Figure 5.29 shows the total expected number of deaths in each Census tract. An earthquake has not occurred in this region in recent history, therefore verification of these results on any quantitative basis is not possible. However, these results can be compared to such recent events as the 1989 Loma Prieta and the 1994 Northridge earthquakes. In this sense, the dollar loss estimates appear to be reasonable but the loss of function and casualty estimates appear to be high, indicating the need for further study to improve these models.

**Table 5.6.** Occupancy rates for social function classes in Salt Lake County, Utah (from Applied Technology Council, ATC-36, in progress).

DESCRIPTION	CLASS	TYPE	OCCUPANTS per 1000 sf	
			day	night
<b>A. RESIDENTIAL</b>				
Permanent Dwelling	1	Houses/Condos/Apartments	1.2	3.1
		Mobile Homes	1.2	3.1
Temporary Lodging	2	Hotels/Motels	0.6	2.5
Group Institutional Housing	3	Dormitories	2.0	3.0
<b>B. COMMERCIAL</b>				
Retail Trade	4	Stores	10.0	-
Wholesale Trade	5	Warehouses	1.0	-
Financial Services	36	Banks	4.0	-
Personal Services	6	Service Stations/Shops	4.0	0.1
Professional Services	7	Offices	4.0	-
Entertainment and Recreation	9	Restaurants/Bars/Theaters	6.0	-
Parking	10	Garages	0.2	-
<b>C. INDUSTRIAL</b>				
Heavy Manufacturing	11	Factories/Offices	3.0	0.3
Light Manufacturing	12	Light Factories/Offices	5.0	0.3
Food and Drug Processing	13	Factories/Offices	2.5	0.3
Chemical Processing	14	Factories/Offices	2.5	0.3
Metal and Mineral Processing	15	Factories/Offices	1.2	0.1
High Technology	16	Factories/Offices	3.0	0.3
Construction	17	Offices	4.0	0.1
Petroleum Refining and Distribution	18	Factories/Offices	2.5	0.3
<b>D. AGRICULTURE</b>	19	Farm Buildings	0.2	-
<b>E. MINING</b>	20	Mine Buildings	4.0	-
<b>F. RELIGION AND NON-PROFIT</b>	21	Churches	65.0	-
		Offices	4.0	-
		Stores	10.0	-
<b>G. GOVERNMENT</b>				
General Services	22	Offices	4.0	-
Emergency Response Centers	23	Response Stations	3.0	0.4
Police	37	Stations	2.0	0.5
Fire	38	Stations	1.0	1.0
National Guard/Reserve Armories	39	Armories	10.0	-

**Table 5.6.** Occupancy rates for social function classes in Salt Lake County, Utah (from Applied Technology Council, ATC-36, in progress), continued.

DESCRIPTION	CLASS	TYPE	OCCUPANTS per 1000 sf	
			day	night
<b>H. MEDICAL FACILITIES AND SERVICES</b>				
Hospitals	40	Hospitals	4.0	2.0
Ambulance Services	41	Offices/Garages	2.0	1.0
Nursing Homes	42	Convalescent Centers	4.0	2.0
Health Care Services	8	Medical Offices/Clinics	5.0	-
<b>I. EDUCATION</b>				
Elementary	24	Schools	20.0	-
Secondary & Junior Colleges	43	Schools	10.0	-
Colleges and Universities	44	Colleges/Universities	5.0	0.1
<b>J. TRANSPORTATION (Freight and Passenger)</b>				
Highway	25	Offices	4.0	0.2
		Freeway Interchanges	-	-
		Minor Bridges	-	-
Railway	26	Terminals	10.0	0.2
Air	27	Terminals	10.0	0.2
Sea/Water (Port, Harbor, Canals, etc.)	28	Terminals	3.0	0.2
Mass Transit (Bus/Rail)	46	Terminals	3.0	0.2
<b>K. UTILITIES</b>				
Electric Power	29	Offices	4.0	0.2
Water	30	Offices	4.0	0.2
Sanitary Sewer	31	Offices	4.0	0.2
Natural Gas	32	Offices	4.0	0.2
<b>L. COMMUNICATION</b>				
Radio and TV	34	Offices	4.0	0.5
		Broadcast Stations	6.0	1.0
Hard-wire Telephone and Telegraph	33	Offices	4.0	0.5
Cellular Telephone	45	Offices	4.0	0.5



**Table 5.7.** Replacement costs for social function classes in Salt Lake County, Utah  
(from Applied Technology Council, ATC-36, in progress).

DESCRIPTION	CLASS	TYPE	REPLACEMENT COST (1993 \$)			
			lowrise (\$/sf)	midrise (\$/sf)	highrise (\$/sf)	each (\$)
<b>A. RESIDENTIAL</b>						
Permanent Dwelling	1	Houses/Condos/Apts.	45	65	70	-
		Mobile Homes	30	-	-	-
Temporary Lodging	2	Hotels/Motels	65	70	80	-
Group Institutional Housing	3	Dormitories	55	60	55	-
<b>B. COMMERCIAL</b>						
Retail Trade	4	Stores	45	55	65	-
Wholesale Trade	5	Warehouses	30	45	60	-
Financial Services	36	Banks	80	85	90	-
Personal Services	6	Service Stations/Shops	70	75	80	-
Professional Services	7	Offices	65	70	80	-
Entertainment and Recreation	9	Rests./Bars/Theaters	80	85	90	-
Parking	10	Garages	25	30	40	-
<b>C. INDUSTRIAL</b>						
Heavy Manufacturing	11	Factories/Offices	100	120	130	-
Light Manufacturing	12	Light Factories/Offices	50	60	-	-
Food and Drug Processing	13	Factories/Offices	100	120	130	-
Chemical Processing	14	Factories/Offices	100	-	-	-
Metal & Mineral Processing	15	Factories/Offices	100	-	-	-
High Technology	16	Factories/Offices	100	-	-	-
Construction	17	Offices	60	65	75	-
Petroleum Ref. and Dist.	18	Factories/Offices	100	120	130	-
<b>D. AGRICULTURE</b>						
	19	Farm Buildings	45	-	-	-
<b>E. MINING</b>						
	20	Mine Buildings	50	60	70	-
<b>F. RELIGION &amp; NON-PROFIT</b>						
	21	Churches	85	-	-	-
		Offices	65	70	80	-
		Stores	45	55	65	-
<b>G. GOVERNMENT</b>						
General Services	22	Offices	75	80	90	-
Emergency Response Centers	23	Response Stations	85	-	-	-
Police	37	Stations	85	-	-	-
Fire	38	Stations	85	-	-	-
National Guard/Reserve	39	Armories	60	-	-	-

**Table 5.7.** Replacement costs for social function classes in Salt Lake County, Utah  
(from Applied Technology Council, ATC-36, in progress), continued.

DESCRIPTION	CLASS	TYPE	REPLACEMENT COST (1993 \$)			
			lowrise (\$/sf)	midrise (\$/sf)	highrise (\$/sf)	each (\$)
<b>H. MEDICAL FACILITIES AND SERVICES</b>						
Hospitals	40	Hospitals	110	115	120	-
Ambulance Services	41	Offices/Garages	50	-	-	-
Nursing Homes	42	Convalescent Centers	80	85	90	-
Health Care Services	8	Medical Offices/Clinics	90	95	100	-
<b>I. EDUCATION</b>						
Elementary	24	Schools	65	75	-	-
Secondary & Junior Colleges	43	Schools	65	75	-	-
Colleges and Universities	44	Colleges/Universities	85	90	95	-
<b>J. TRANSPORTATION (Freight and Passenger)</b>						
Highway	25	Offices	65	70	80	-
		Freeway Interchanges	-	-	-	15 mil.
		Minor Bridges	-	-	-	2 mil.
Railway	26	Terminals	60	65	70	-
Air	27	Terminals	80	85	90	-
Sea/Water	28	Terminals	60	65	70	-
Mass Transit (Bus/Rail)	46	Terminals	60	65	70	-
<b>K. UTILITIES</b>						
Electric Power	29	Offices	65	70	80	-
Water	30	Offices	65	70	80	-
Sanitary Sewer	31	Offices	65	70	80	-
Natural Gas	32	Offices	65	70	80	-
<b>L. COMMUNICATION</b>						
Radio and TV	34	Offices	65	70	80	-
		Broadcast Stations	60	65	70	-
Hard-wire Tel.	33	Offices	65	70	80	-
Cellular Telephone	45	Offices	65	70	80	-

**Table 5.8.** Loss-of-function parameters for social function classes in Salt Lake County, Utah for damage states 2, 3, and 4 (from Applied Technology Council, ATC-36, in progress).

DESCRIPTION	CLASS	TYPE	Dam. State 2 E[DF] < 1%		Dam. State 3 E[DF]=1-10%		Dam. State 4 E[DF]=10-30%	
			days to 100%	% fun @3 day	days to 100%	% fun @3 day	days to 100%	% fun @3 day
<b>A. RESIDENTIAL</b>								
Permanent Dwelling	1	Houses/Apts.	0.8	100	3.3	93.6	10.5	39.5
		Mobile Homes	0.8	100	3.3	93.6	10.5	39.5
Temporary Lodging	2	Hotels/Motels	0.8	100	3.3	93.6	10.5	39.5
Group Institutional Housing	3	Dormitories	0.8	100	3.3	93.6	10.5	39.5
<b>B. COMMERCIAL</b>								
Retail Trade	4	Stores	5.8	61.4	20	28.8	71	19.5
Wholesale Trade	5	Warehouses	5.8	61.4	20	28.8	71	19.5
Financial Services	36	Banks	5.8	61.4	20	28.8	71	19.5
Personal Services	6	Service Sta./Shops	5.8	61.4	20	28.8	71	19.5
Professional Services	7	Offices	5.8	61.4	20	28.8	71	19.5
Entertainment & Recreation	9	Rests./Bars/Theat.	5.8	61.4	20	28.8	71	19.5
Parking	10	Garages	0.4	100	6.5	64.1	24.4	19.09
<b>C. INDUSTRIAL</b>								
Heavy Manufacturing	11	Factories/Offices	5.6	53.2	22.6	17.2	99.3	7.7
Light Manufacturing	12	Factories/Offices	5.6	53.2	22.6	17.2	99.3	7.7
Food and Drug Processing	13	Factories/Offices	4.4	72.8	16.1	35.4	72.7	13.9
Chemical Processing	14	Factories/Offices	5.6	53.2	22.6	17.2	99.3	7.7
Metal & Mineral Processing	15	Factories/Offices	5.6	53.2	22.6	17.2	99.3	7.7
High Technology	16	Factories/Offices	1.1	100	16.5	34.2	111.8	5.7
Construction	17	Offices	6.7	44.1	27.9	24.4	68.1	0
Petroleum Ref. and Dist.	18	Factories/Offices	5.8	61.4	20	28.8	71	19.5
<b>D. AGRICULTURE</b>								
Farm Buildings	19	Farm Buildings	1.7	100	8.9	51.8	25.9	28.2
<b>E. MINING</b>								
Mine Buildings	20	Mine Buildings	6.1	69.1	18.2	22.9	83	9.1
<b>F. RELIGION/NON-PROFIT</b>								
Churches/Offices	21	Churches/Offices	3	98.3	17	26.1	71.7	20.5
<b>G. GOVERNMENT</b>								
General Services	22	Offices	5.1	58.9	28.4	27.3	91.2	0
Emergency Resp. Centers	23	Response Stations	5.1	44.9	18.2	18.8	60.4	0.5
Police	37	Stations	5.1	44.9	18.2	18.8	60.4	0.5
Fire	38	Stations	5.1	44.9	18.2	18.8	60.4	0.5
National Guard/Reserve	39	Armories	5.8	61.4	20	28.8	71	19.5

**Table 5.8.** Loss-of-function parameters for social function classes in Salt Lake County, Utah for damage states 2, 3, and 4 (from Applied Technology Council, ATC-36, in progress), continued.

DESCRIPTION	CLASS	TYPE	Dam. State 2 E[DF] < 1%		Dam. State 3 E[DF]=1-10%		Dam. State 4 E[DF]=10-30%	
			days to 100%	% fun @3 day	days to 100%	% fun @3 day	days to 100%	% fun @3 day
<b>H. MEDICAL FACILITIES AND SERVICES</b>								
Hospitals	40	Hospitals	20.5	37.1	56	10.7	156.8	0
Ambulance Services	41	Offices/Garages	20.5	37.1	56	10.7	156.8	0
Nursing Homes	42	Conv. Centers	20.5	37.1	56	10.7	156.8	0
Health Care Services	8	Offices/Clinics	20.5	37.1	56	10.7	156.8	0
<b>I. EDUCATION</b>								
Elementary	24	Schools	5.7	33.5	15.5	1.5	72.1	4.1
Secondary & Jr. Colleges	43	Schools	5.7	33.5	15.5	1.5	72.1	4.1
Colleges and Universities	44	Colleges/Univs.	5.7	33.5	15.5	1.5	72.1	4.1
<b>J. TRANSPORTATION (Freight and Passenger)</b>								
Highway	25	Offices	6.7	44.1	6.6	55.1	82.5	0
		Fwy. Interchanges	1.1	100	8.4	55.7	84.4	0
		Minor Bridges	0.7	100	7.1	55.8	40.9	6.2
Railway	26	Terminals	0.5	100	5.6	68.5	32.3	16
Air	27	Terminals	0	100	18.3	50.4	112	14.1
Sea/Water	28	Terminals	2.8	100	13.8	43.8	65.6	24.7
Mass Transit (Bus/Rail)	46	Terminals	0.5	100	5.6	68.5	32.3	16
<b>K. UTILITIES</b>								
Electric Power	29	Offices	5.8	61.4	20	28.8	71	19.5
Water	30	Offices	5.8	61.4	20	28.8	71	19.5
Sanitary Sewer	31	Offices	5.8	61.4	20	28.8	71	19.5
Natural Gas	32	Offices	5.8	61.4	20	28.8	71	19.5
<b>L. COMMUNICATION</b>								
Radio and TV	34	Offices	5.8	61.4	20	28.8	71	19.5
		Broadcast Stations	3.9	84.7	9.8	49.5	85	29.9
Hard-wire Tel.	33	Offices	1.1	100	8.6	61.7	56.8	41.4
Cellular Telephone	45	Offices	5.8	61.4	20	28.8	71	19.5

**Table 5.9.** Loss-of-function parameters for social function classes in Salt Lake County, Utah for damage states 5, 6, and 7 (from Applied Technology Council, ATC-36, in progress).

DESCRIPTION	CLASS	TYPE	Dam. State 5 E[DF]=30-60%		Dam. State 6 E[DF]=60-100%		Dam. State 7 E[DF]=100%	
			days to 100%	% fun @3 day	days to 100%	% fun @3 day	days to 100%	% fun @3 day
<b>A. RESIDENTIAL</b>								
Permanent Dwelling	1	Houses/Apts.	71.9	20.7	146.6	0	211.9	0
		Mobile Homes	71.9	20.7	146.6	0	211.9	0
Temporary Lodging	2	Hotels/Motels	71.9	20.7	146.6	0	211.9	0
Group Institutional Housing	3	Dormitories	71.9	20.7	146.6	0	211.9	0
<b>B. COMMERCIAL</b>								
Retail Trade	4	Stores	202.7	15.1	343.1	0	493.3	0
Wholesale Trade	5	Warehouses	202.7	15.1	343.1	0	493.3	0
Financial Services	36	Banks	202.7	15.1	343.1	0	493.3	0
Personal Services	6	Service Sta./Shops	202.7	15.1	343.1	0	493.3	0
Professional Services	7	Offices	202.7	15.1	343.1	0	493.3	0
Entertainment & Recreation	9	Rests./Bars/Theat.	202.7	15.1	343.1	0	493.3	0
Parking	10	Garages	76.1	0	172.2	0	258.3	0
<b>C. INDUSTRIAL</b>								
Heavy Manufacturing	11	Factories/Offices	248	5.4	405.5	0	538.1	0
Light Manufacturing	12	Factories/Offices	248	5.4	405.5	0	538.1	0
Food and Drug Processing	13	Factories/Offices	235.6	0	380.7	0	534.1	0
Chemical Processing	14	Factories/Offices	248	1.6	405.5	0	538.1	0
Metal & Mineral Processing	15	Factories/Offices	248	1.6	405.5	0	538.1	0
High Technology	16	Factories/Offices	258.2	0	429.1	0	612	0
Construction	17	Offices	121	0	257.3	0	330.1	0
Petroleum Ref. and Dist.	18	Factories/Offices	202.7	15.1	343.1	0	493.3	0
<b>D. AGRICULTURE</b>	19	Farm Buildings	77.5	2.3	154.2	0	235	0
<b>E. MINING</b>	20	Mine Buildings	265.3	0	648.6	0	949	0
<b>F. RELIGION/NON-PROFIT</b>	21	Churches/Offices	214.6	18.7	382.6	0	534.9	0
<b>G. GOVERNMENT</b>								
General Services	22	Offices	196.3	0	396.3	0	652	0
Emergency Resp. Centers	23	Response Stations	134.9	0	256.1	0	346.8	0
Police	37	Stations	134.9	0	256.1	0	346.8	0
Fire	38	Stations	134.9	0	256.1	0	346.8	0
National Guard/Reserve	39	Armories	202.7	15.1	343.1	0	493.3	0

**Table 5.9.** Loss-of-function parameters for social function classes in Salt Lake County, Utah for damage states 5, 6, and 7 (from Applied Technology Council, ATC-36, in progress), continued.

DESCRIPTION	CLASS	TYPE	Dam. State 5 E[DF]=30-60%		Dam. State 6 E[DF]=60-100%		Dam. State 7 E[DF]=100%	
			days to 100%	% fun @3 day	days to 100%	% fun @3 day	days to 100%	% fun @3 day
<b>H. MEDICAL FACILITIES AND SERVICES</b>								
Hospitals	40	Hospitals	338.4	0	613.2	0	723.4	0
Ambulance Services	41	Offices/Garages	338.4	0	613.2	0	723.4	0
Nursing Homes	42	Conv. Centers	338.4	0	613.2	0	723.4	0
Health Care Services	8	Offices/Clinics	338.4	0	613.2	0	723.4	0
<b>I. EDUCATION</b>								
Elementary	24	Schools	183	0	362.1	0	562.6	0
Secondary & Jr. Colleges	43	Schools	183	0	362.1	0	562.6	0
Colleges and Universities	44	Colleges/Univs.	183	0	362.1	0	562.6	0
<b>J. TRANSPORTATION (Freight and Passenger)</b>								
Highway	25	Offices	323.6	0	749.7	0	847.4	0
		Fwy. Interchanges	303.6	9.6	686	0	752.9	0
		Minor Bridges	147.2	7.4	291.6	0	437.2	0
Railway	26	Terminals	143.7	7.9	351.7	0	385.9	0
Air	27	Terminals	264.3	0	530.3	1.7	638.7	0
Sea/Water	28	Terminals	191.5	7.8	450.4	0.9	722.5	0
Mass Transit (Bus/Rail)	46	Terminals	143.7	7.9	351.7	0	385.9	0
<b>K. UTILITIES</b>								
Electric Power	29	Offices	202.7	15.1	343.1	0	493.3	0
Water	30	Offices	202.7	15.1	343.1	0	493.3	0
Sanitary Sewer	31	Offices	202.7	15.1	343.1	0	493.3	0
Natural Gas	32	Offices	202.7	15.1	343.1	0	493.3	0
<b>L. COMMUNICATION</b>								
Radio and TV	34	Offices	202.7	15.1	343.1	0	493.3	0
		Broadcast Stations	251.7	22.6	523.5	2.6	629.3	0
Hard-wire Tel.	33	Offices	274.3	36.2	593.2	12.6	701.4	0
Cellular Telephone	45	Offices	202.7	15.1	343.1	0	493.3	0

**Table 5.10.** Casualty rates for damage states in Salt Lake County, Utah (from Applied Technology Council, ATC-36, in progress).

Damage State	E[DF] Range	Number Stories	Fraction Minor Injuries	Fraction Major Injuries	Fraction Dead
1	0%	1+	0	0	0
2	0-1%	1+	0.0003	0.00004	0.00001
3	1-10%	1+	0.0006	0.00008	0.00002
4	10-30%	1+	0.003	0.0004	0.0001
5	30-60%	1	0.03	0.02	0.001
		2+	0.2	0.04	0.002
6	60-100%	1	0.3	0.08	0.01
		2+	0.06	0.16	0.02
7	100%	1	0.2	0.6	0.2
		2	0	0.6	0.4

## 5.4 Summary

This chapter presents a case study to illustrate the GIS-based methodology for regional seismic hazard and risk analysis discussed in this dissertation. The study is part of an on-going project (Applied Technology Council, ATC-36, in progress) sponsored by the Federal Emergency Management Agency for estimating earthquake damage and loss due to a magnitude 7.5 event in Salt Lake County, Utah. This chapter contains a simplified version of the project, but serves to illustrate the role of geographic information systems in all aspects of the analysis, from identifying the potential seismic sources to computing the final loss estimates.

Maps and example database tables are shown at various stages in the analysis to illustrate the overlay procedure and the relationships among the various models and tables of data. The seismic hazard analysis details the estimation of ground shaking, the effects of the various collateral hazards, and the combination of all seismic hazards in the region. The next part of the analysis covers the development of the structural inventory and the estimation of earthquake damage and losses. Results are presented in a preliminary format as point maps of facilities and in a final format as summaries and averages on a Census tract basis.

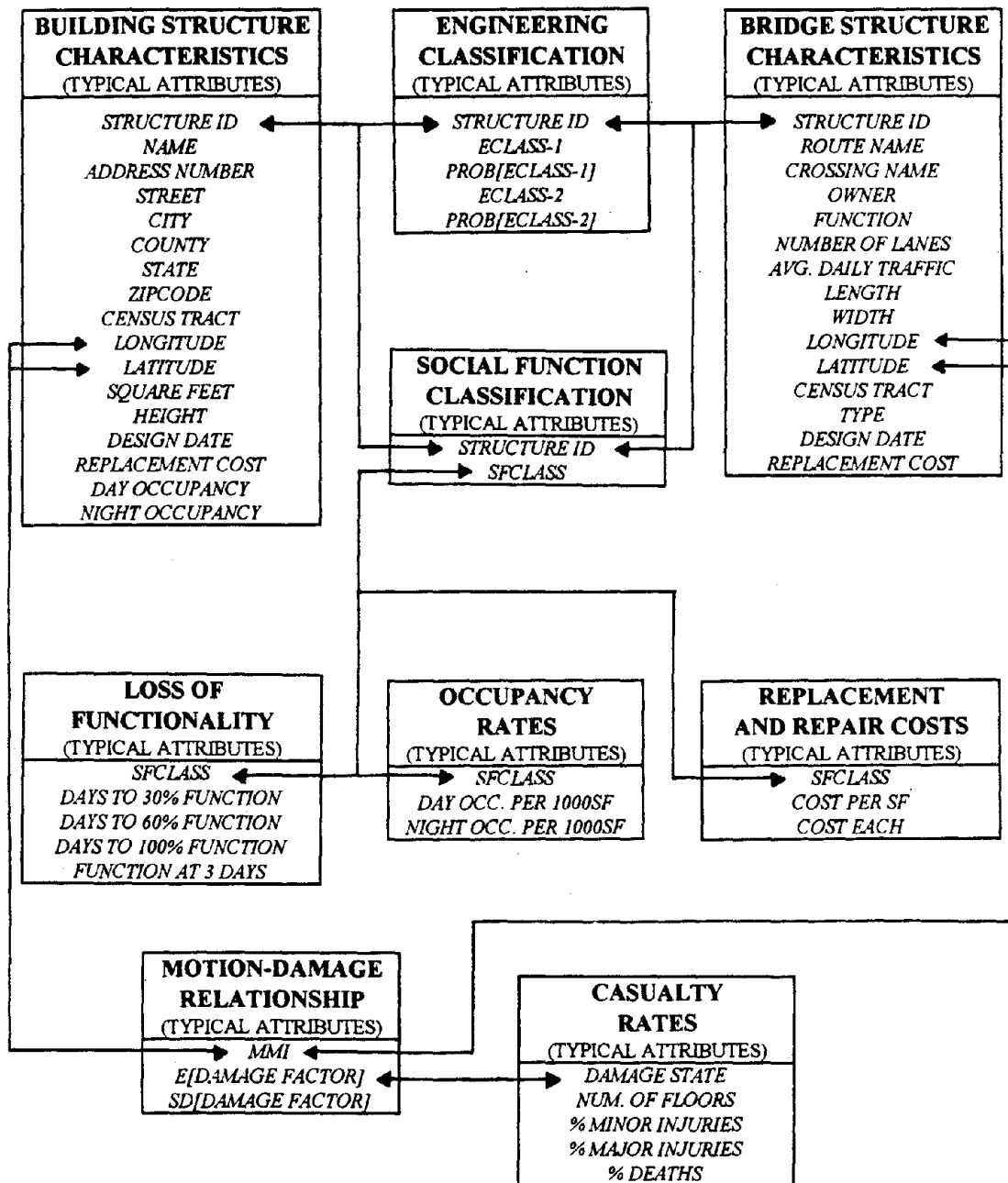


Figure 5.24. Interrelated database tables at final stage of analysis (from Applied Technology Council, ATC-36, in progress).



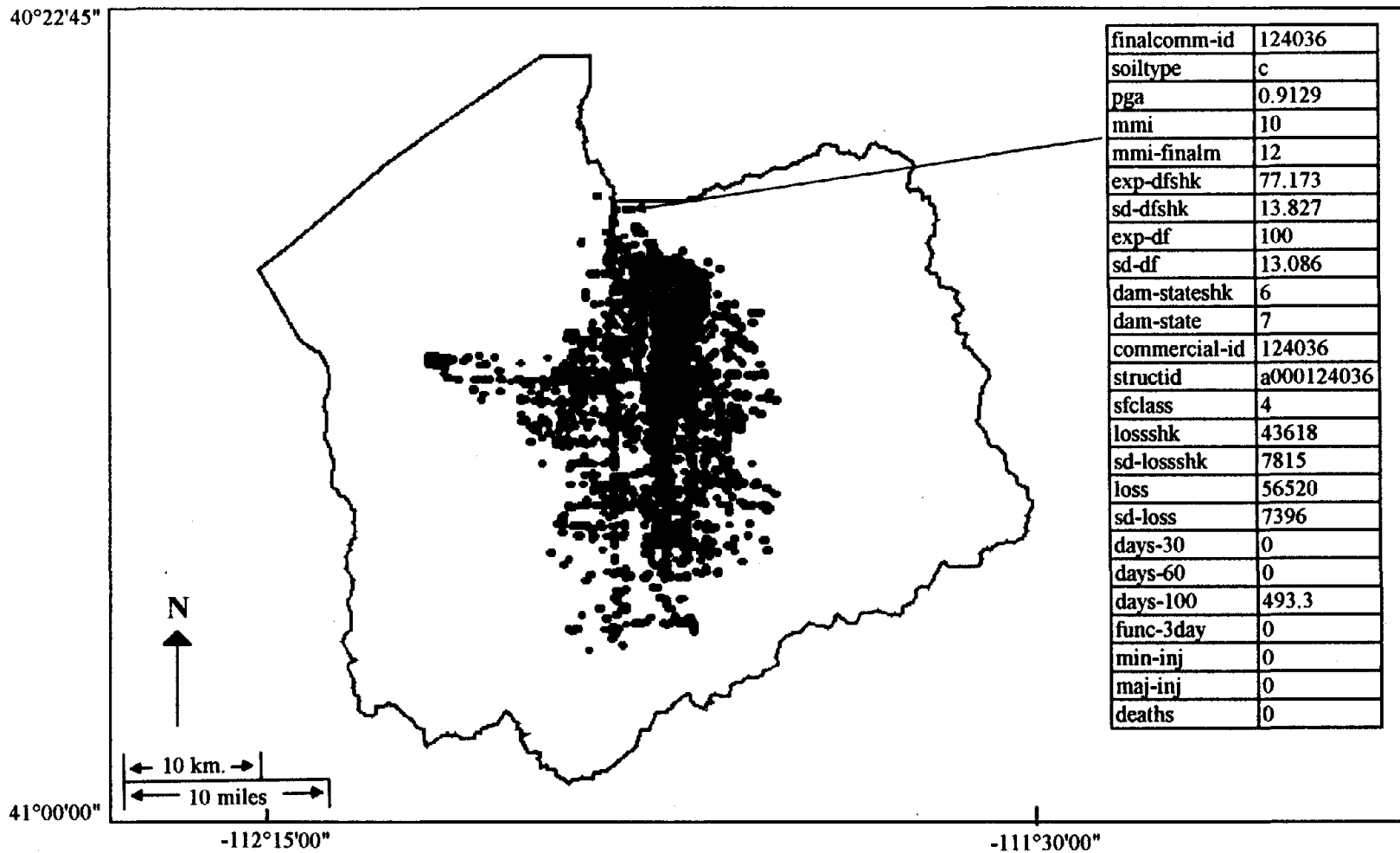


Figure 5.25. Map showing final results for commercial buildings in Salt Lake County, Utah.

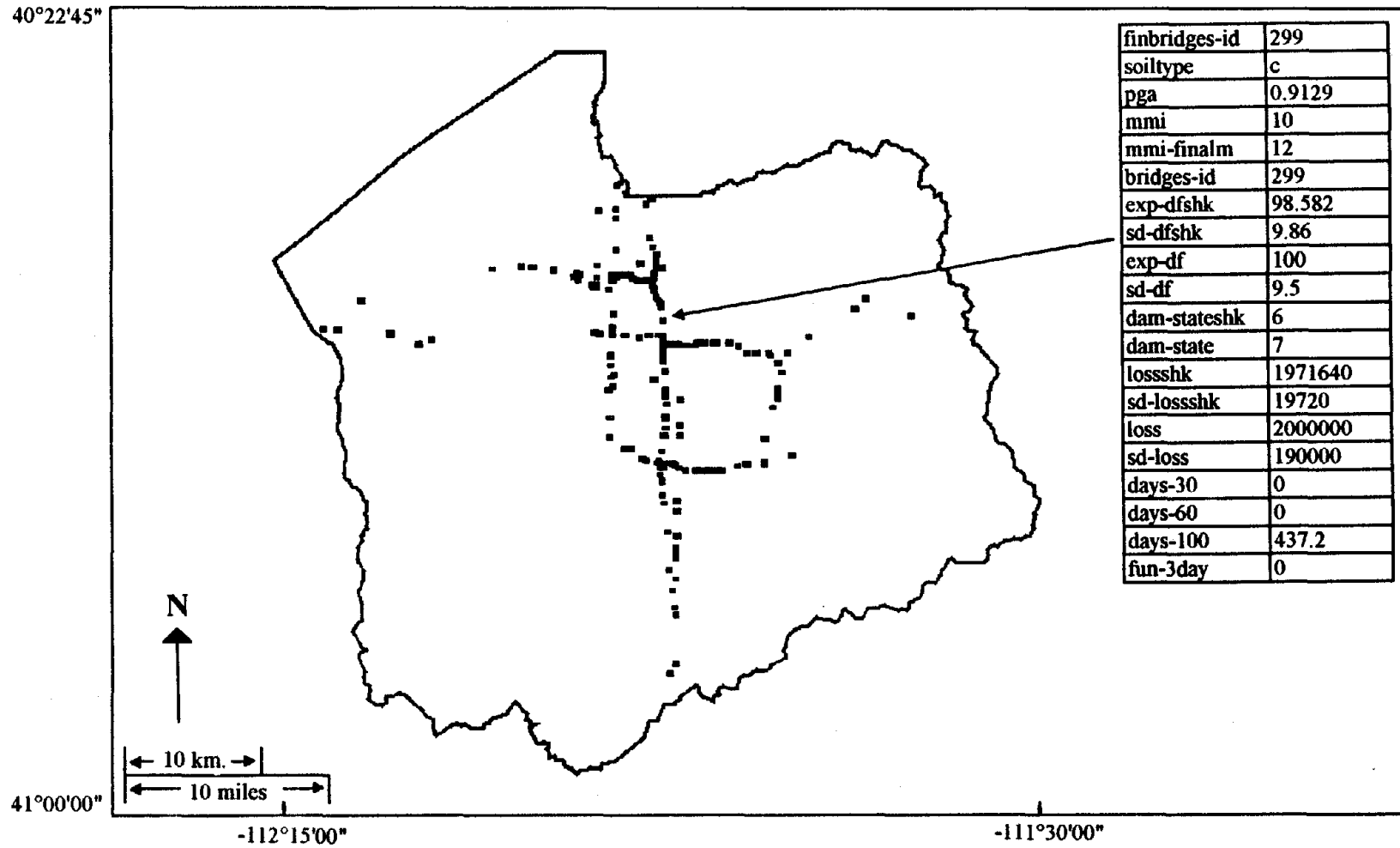


Figure 5.26. Map showing final results for highway bridges in Salt Lake County, Utah.

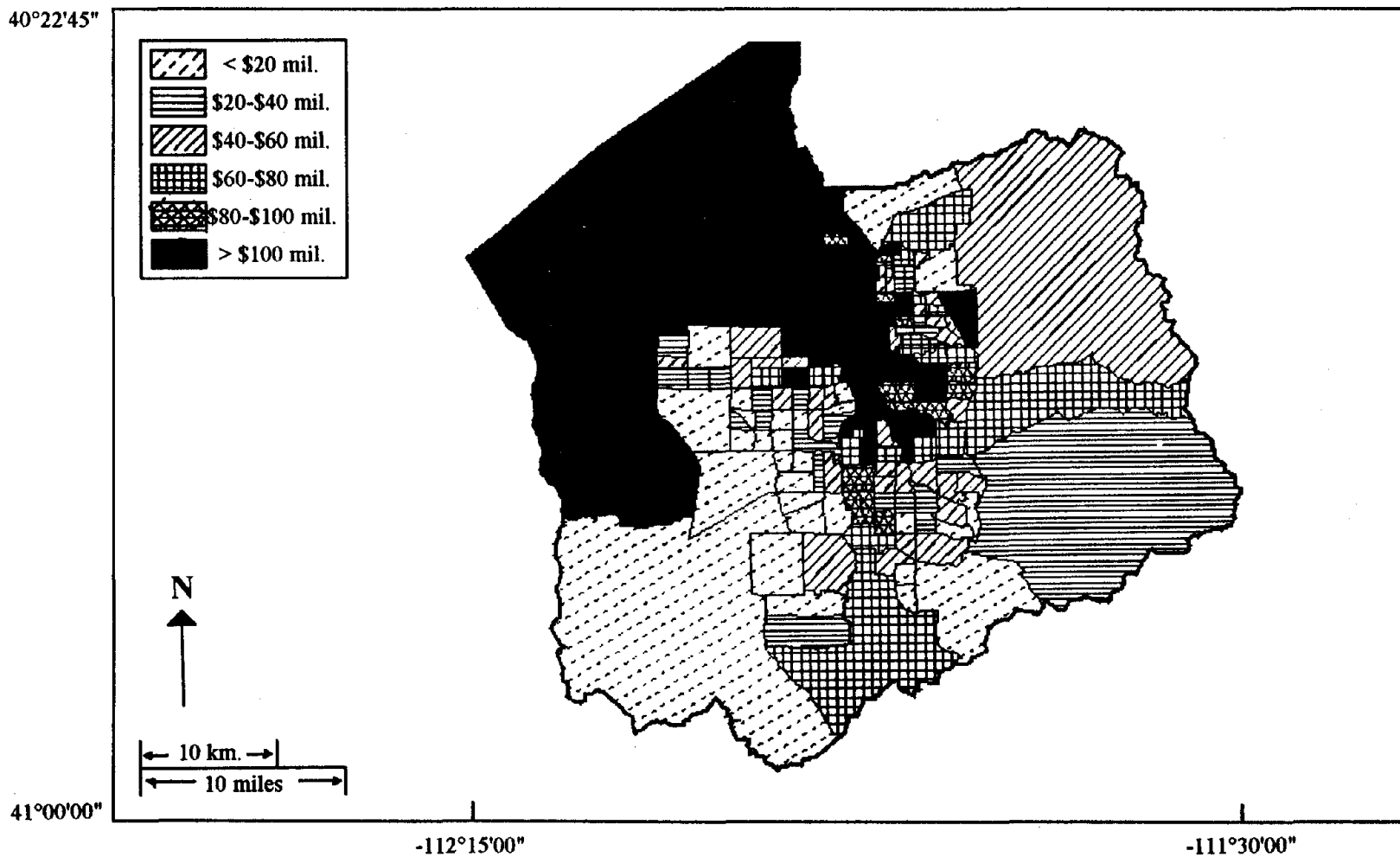
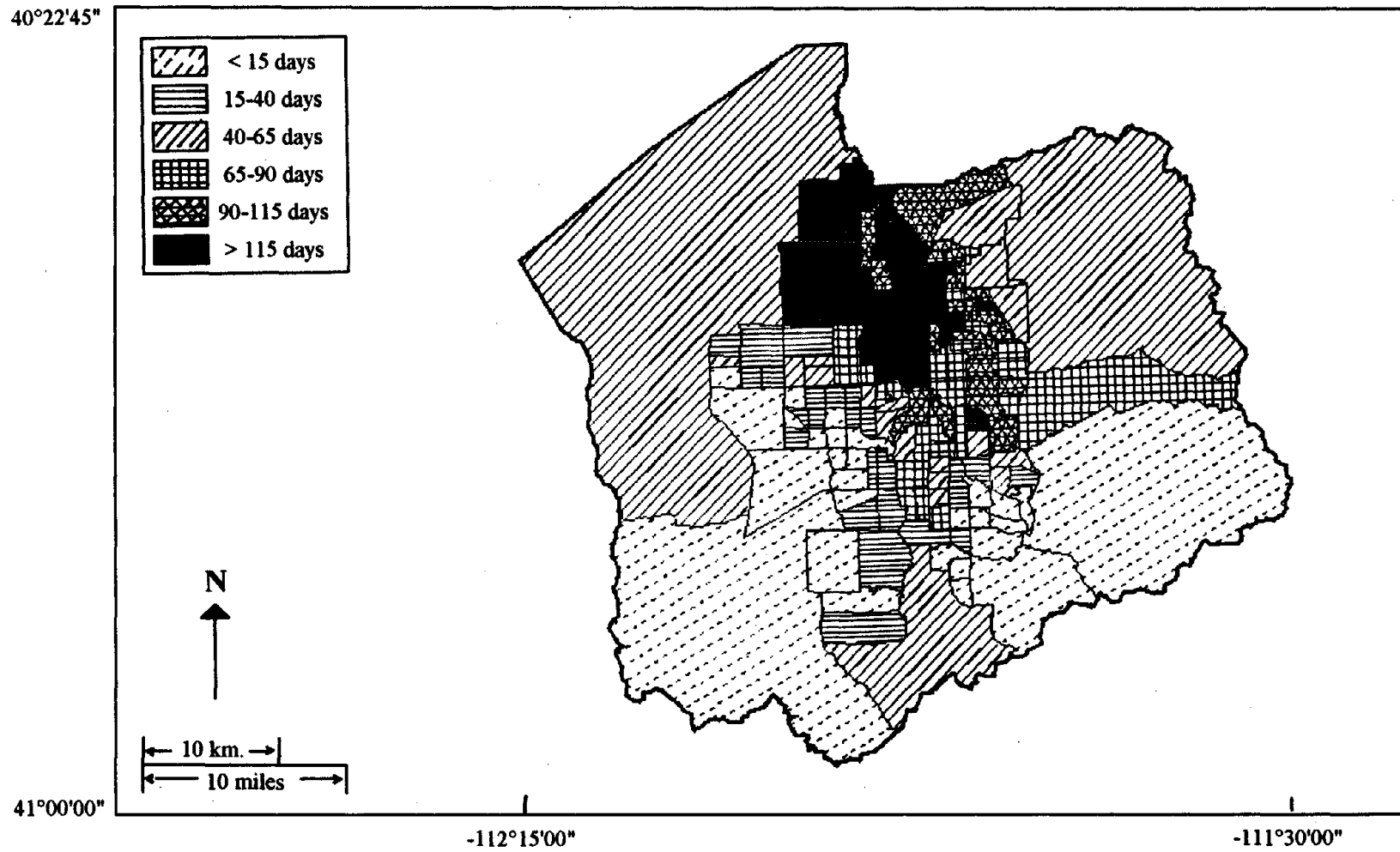
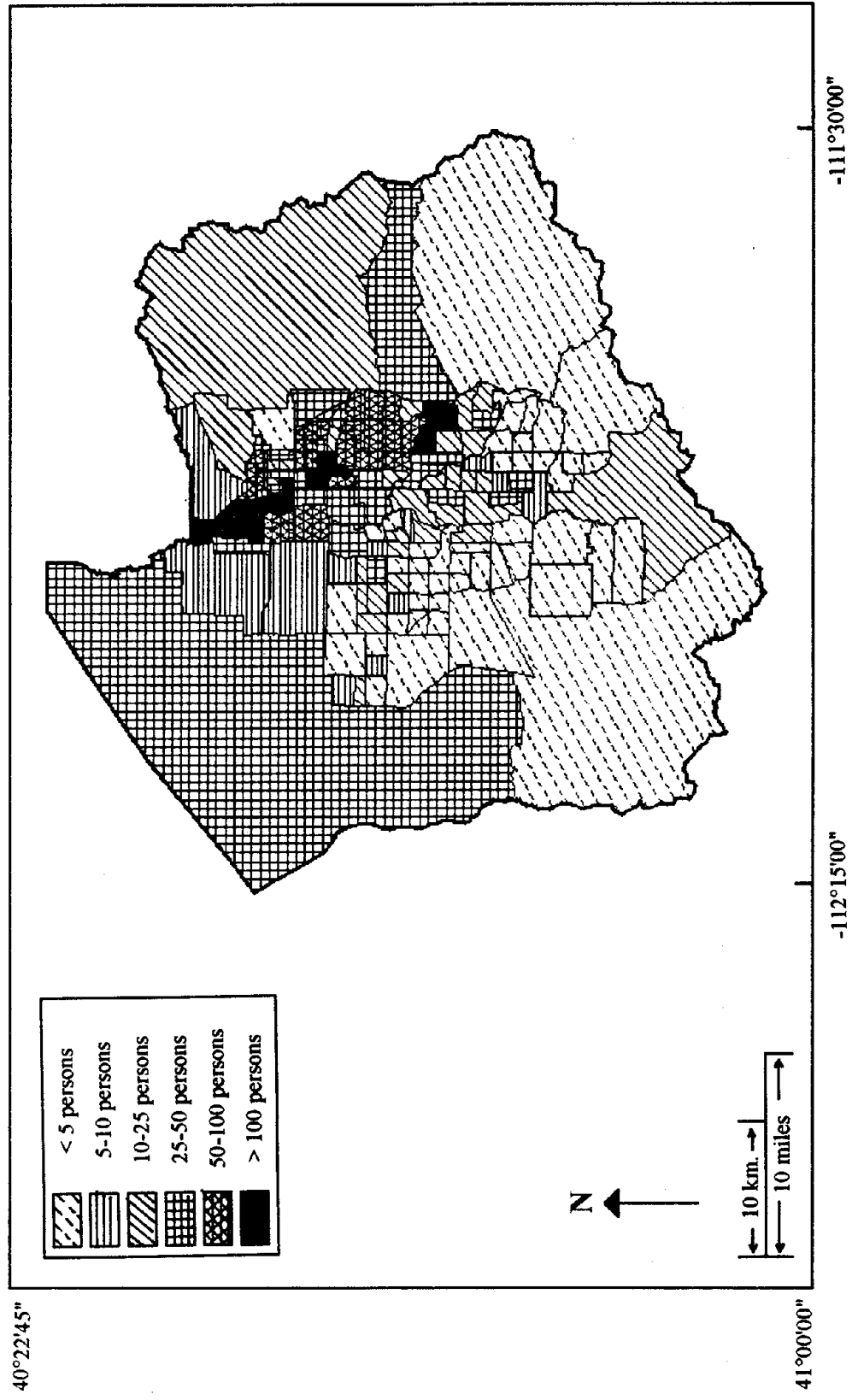


Figure 5.27. Map showing total expected loss due to combined seismic hazard ( $MMI_F$ ) in each Census tract in Salt Lake County, Utah.



**Figure 5.28.** Map showing average number of days to restore buildings to 100% functionality due to combined seismic hazard ( $MMI_F$ ) in each Census tract in Salt Lake County, Utah.



**Figure 5.29.** Map showing total number of deaths due to combined seismic hazard (MMI<sub>F</sub>) in each Census tract in Salt Lake County, Utah.

One last representation of the final results is by a summary table for the entire county. These results are shown in Tables 5.11 and 5.12 for buildings, and in Tables 5.13 and 5.14 bridges. In Table 5.12, the building results are separated by construction type and in Table 5.14, the bridge results are separated by both structural type and function. Summaries such as these allow for quick checks on the reasonableness of the results. For example, the total expected loss for buildings is about \$12.1 billion  $\pm$  \$2.9 billion, and for bridges is about \$1.7 billion  $\pm$  \$0.2 billion. Preliminary estimates of loss due to the magnitude 6.8 1994 Northridge earthquake are over \$15 billion, therefore the results estimated here appear reasonable. The number of deaths is estimated at over 7,500 in this case study. This seems very high when compared to recent previous earthquakes in the United States, indicating that the models used to estimate casualties need further investigation. Lastly, the expected damage factor estimated for the bridges in this case study is about 89%  $\pm$  11%. Although many of the bridges are located in the areas of high seismic hazard, these numbers appear to be too large, indicating a need for further research into the seismic behavior of highway bridges.

As discussed in Sections 4.2.3 and 4.3.3, the results for damage and loss in this case study are not intended to be used for site-specific analysis. They are based on simplified models and several assumptions, therefore they are meant to be used only for averages or summaries on a regional basis. Relative comparison of the results is intended to indicate areas that should be investigated in a more detailed analysis. The final results are also meant to help emergency managers and planners allocate resources and prepare hazard mitigation programs in a region.

**Table 5.11.** Summary of final results for all buildings in Salt Lake County, Utah.

Average design date	1960
Total square footage	593,088,274
Total number of buildings	195,785
Average replacement cost (\$)	160,466
Total replacement cost (\$)	31,416,939,684
Total night occupancy	1,354,363
Average E[DF] (shaking,%)	27.27
Average SD[DF] (shaking,%)	7.45
Average E[DF] (all haz.,%)	36.00
Average SD[DF] (all haz.,%)	8.60
# w/ E[DF] < 10% (all haz.)	53,600
% w/ E[DF] < 10% (all haz.)	27.38
# w/ E[DF] = 10-30% (all haz.)	49,415
% w/ E[DF] = 10-30% (all haz.)	25.24
# w/ E[DF] = 30-60% (all haz.)	42,028
% w/ E[DF] = 30-60% (all haz.)	21.47
# w/ E[DF] = 60-100% (all haz.)	47,459
% w/ E[DF] = 60-100% (all haz.)	24.24
# w/ E[DF] = 100% (all haz.)	3,283
% w/ E[DF] = 100% (all haz.)	1.68
Avg. E[\$ loss] (shaking,\$)	43,493
Avg. SD[\$ loss] (shaking,\$)	12,384
Avg. E[\$ loss] (all haz.,\$)	61,780
Avg. SD[\$ loss] (all haz.,\$)	14,756
Total E[\$ loss] (shaking,\$)	8,515,478,105
Total SD[\$ loss] (shaking,\$)	2,424,552,699
Total E[\$ loss] (all haz.,\$)	12,095,615,015
Total SD[\$ loss] (all haz.,\$)	2,889,010,346
Avg. days to 30% func. (all haz.)	20.73
Avg. days to 60% func. (all haz.)	37.48
Avg. days to 100% func. (all haz.)	68.90
Avg. 3-day func. (all haz.,%)	39.45
Total minor injuries (all haz.)	105,325
% w/ minor injuries (all haz.)	7.78
Total major injuries (all haz.)	44,171
% w/ major injuries (all haz.)	3.26
Total deaths (all haz.)	7,638
% dead (all haz.)	0.56
Computed E[DF] (shaking,%)	27.10
Computed SD[DF] (shaking,%)	7.72
Computed E[DF] (all haz.,%)	38.50
Computed SD[DF] (all haz.,%)	9.20

Table 5.12. Summary of final results for buildings in Salt Lake County, Utah by construction type.

	Wood Frame Construction Buildings	URM Construction Buildings	Steel Construction Buildings	Concrete Construction Buildings	Other/Mixed Construction Buildings
Total number of buildings	111,732	52,519	555	156	30,823
Average replacement cost (\$)	111,849	140,690	933,727	3,828,976	346,315
Total replacement cost (\$)	12,497,119,279	7,388,896,656	518,218,820	597,320,254	10,674,462,124
Average E[DF] (all haz.,%)	15.58	77.46	22.54	36.12	39.90
Average SD[DF] (all haz.,%)	12.41	1315.47	7.01	9.2	9.79
Avg. E[\$ loss] (all haz.,\$)	37,816	10,670,129	163,706	1,346,971	126,095
Avg. SD[\$ loss] (all haz.,\$)	14,082	1,842,328	48,184	349,391	33,925
Total E[\$ loss] (all haz.,\$)	1,986,051,797	5,921,911,812	90,857,308	210,127,496	3,886,666,602
Total SD[\$ loss] (all haz.,\$)	739,581,508	1,022,504,749	26,742,632	54,504,992	1,045,676,465
Total minor injuries (all haz.)	9,896	85,009	32	200	10,889
Total major injuries (all haz.)	3,147	36,599	12	53	4,360
Total deaths (all haz.)	188	7,130	1	4	317
Computed E[DF] (all haz.,%)	15.89	80.15	17.53	35.18	36.41
Computed SD[DF] (all haz.,%)	5.92	13.84	5.16	9.12	9.80



**Table 5.13.** Summary of final results for all highway bridges in Salt Lake County, Utah.

<b>Average design date</b>	1971
<b>Total number of bridges</b>	279
<b>Total replacement cost (\$)</b>	1,886,000,000
<b>Average E[DF] (shaking alone,%)</b>	69.06
<b>Average SD[DF] (shaking alone,%)</b>	8.72
<b>Average E[DF] (all hazards,%)</b>	89.26
<b>Average SD[DF] (all hazards,%)</b>	9.85
<b># bridges w/ E[DF] &lt; 10% (all hazards)</b>	4
<b>% bridges w/ E[DF] &lt; 10% (all hazards)</b>	1.43
<b># bridges w/ E[DF] = 10-30% (all haz.)</b>	0
<b>% bridges w/ E[DF] = 10-30% (all haz.)</b>	0
<b># bridges w/ E[DF] = 30-60% (all haz.)</b>	11
<b>% bridges w/ E[DF] = 30-60% (all haz.)</b>	3.94
<b># bridges w/ E[DF] = 60-100% (all haz.)</b>	152
<b>% bridges w/ E[DF] = 60-100% (all haz.)</b>	54.48
<b># bridges w/ E[DF] = 100% (all haz.)</b>	112
<b>% bridges w/ E[DF] = 100% (all haz.)</b>	40.14
<b>Avg. E[dollar loss] (shaking alone,\$)</b>	4,383,239
<b>Avg. SD[dollar loss] (shaking alone,\$)</b>	614,005
<b>Avg. E[dollar loss] (all hazards,\$)</b>	5,978,274
<b>Avg. SD[dollar loss] (all hazards,\$)</b>	732,672
<b>Total E[dolar loss] (shaking alone,\$)</b>	1,227,306,940
<b>Total SD[dollar loss] (shaking alone,\$)</b>	171,921,500
<b>Total E[dollar loss] (all hazards,\$)</b>	1,673,916,980
<b>Total SD[dollar loss] (all hazards,\$)</b>	205,148,320
<b>Computed E[DF] (shaking alone,%)</b>	65.07
<b>Computed SD[DF] (shaking alone,%)</b>	9.12
<b>Computed E[DF] (all hazards,%)</b>	88.75
<b>Computed SD[DF] (all hazards,%)</b>	10.88

**Table 5.14.** Summary of final results for highway bridges in Salt Lake County, Utah by structural type and function.

	<b>Conventional Bridges</b>	<b>Continuous Bridges</b>	<b>Interchange Bridges</b>	<b>Minor Bridges</b>
<b>Average design date</b>	1966	1977	1973	1969
<b>Total number of bridges</b>	172	107	102	177
<b>Total replacement cost (\$)</b>	968,000,000	918,000,000	1,530,000,000	356,000,000
<b>Average E[DF] (all hazards,%)</b>	96.84	77.2	88.54	89.67
<b>Average SD[DF] (all hazards,%)</b>	7.7	13.26	11.31	9.01
<b>Avg. E[dollar loss] (all hazards,\$)</b>	5,259,985	7,122,216	13,281,232	1,793,434
<b>Avg. SD[dollar loss] (all hazards,\$)</b>	438,323	1,201,450	1,696,820	180,183
<b>Total E[dollar loss] (all hazards,\$)</b>	904,717,580	769,199,400	1,354,685,700	319,231,280
<b>Total SD[dollar loss] (all hazards,\$)</b>	75,391,620	129,756,700	173,075,700	32,072,620
<b>Computed E[DF] (all hazards,%)</b>	93.46	83.79	88.54	89.67
<b>Computed SD[DF] (all hazards,%)</b>	7.79	14.13	11.31	9.01

## CHAPTER 6

# SUMMARY, CONCLUSIONS, AND FUTURE WORK

---

### 6.1 Summary

The purpose of this research was the development of a methodology for using geographic information system (GIS) technology to integrate the various components of a regional multi-hazard seismic risk analysis. In this dissertation, the seismic risk analysis included consideration of primary hazards due to ground shaking and to local site effects such as soil amplification, liquefaction, landslide, and surface fault rupture. The analysis incorporates structural inventories, motion-damage relationships, and loss modeling for estimating regional damage and loss distributions. In the GIS environment, maps representing regional geologic and geographic information are overlaid and their attributes are combined to produce intermediate maps of regional seismic hazards. These hazard maps are then overlaid and combined with structural inventory maps to produce maps predicting regional damage distributions. Combining the maps of damage distributions with maps of population distributions for the area results in final estimates of direct loss, indirect loss, and casualties.

The integrated GIS-based methodology presented in this dissertation was designed for seismic hazard and risk analysis on the regional, not site-specific level. The results are intended to give general estimates of damage and loss distributions and to indicate areas that require further detailed investigation. For this reason, the hazard and loss models that were chosen for use in this dissertation are fairly simplified and suitable for use with regional spatially-distributed data. The flexible framework of the GIS-based methodology allows the analysis system to be updated and expanded with new models and database information.

A detailed description of geographic information system technology was presented in Chapter 2. Graphic and non-graphic data types and the database management

capabilities of a GIS were discussed. The point, line, and polygon analysis, modeling, and display features of a GIS were covered, and the available computer software packages and hardware platforms were mentioned. Chapter 2 also presented a broad overview of regional seismic hazard and risk analysis. The various steps in the analysis were discussed, including seismic event characterization, regional hazard estimation, and prediction of final damage and loss estimates. A general background of each step was given, as well as a description of the implementation in the GIS environment.

Chapter 3 covered the effects of local site conditions on earthquake damage and loss potential. Soil amplification was discussed first, with a description of the various methods for estimating the dynamic behavior of soil deposits. A treatment of soil parameter uncertainty was also included in this section to account for the often large variations in the amount and type of spatial geologic data that are available in the analysis region. One of the soil amplification techniques was used to illustrate an example GIS-based regional estimation of surface ground shaking. Secondary site effects were covered next. They include the liquefaction, landslide, and surface fault rupture that typically accompany earthquake ground shaking. For each of these, an overview of the qualitative and quantitative models that are available for estimating the effects was presented.

The latter half of Chapter 3 was devoted to the development and illustration of a GIS-based methodology for integrating the seismic hazards associated with ground shaking and the local site effects of soil amplification, liquefaction, landslide, and surface fault rupture. The behavior of the local soil conditions, as well as the accuracy of the geologic and geotechnical information, can vary greatly from region to region. For this reason, the regional hazard combination methodology developed in this dissertation is based on a heuristic weighted average approach. The methodology is intended to be general enough so as to allow the application of more or less sophisticated models depending on the availability of information in the desired analysis region. A hypothetical example based on several simplifying assumptions was presented at the end of Chapter 3 to help illustrate the seismic hazard integration methodology.

Earthquake damage and loss estimation was the subject of Chapter 4. Regional structural inventories were covered in detail, including the required information, the potential sources of data, and the use of classification and inference schemes. An inventory compilation methodology that was developed as part of this research was also presented in this section. Damage distributions were discussed here, including the

different definitions of damage, the available motion-damage relationships, and the application of GIS technology to regional earthquake damage forecasting. Loss distributions were also covered, including both monetary and non-monetary losses, as well as the application of GIS technology to regional earthquake loss forecasting.

Chapter 5 presented a case study. A detailed seismic hazard and risk analysis utilizing many of the developments and ideas discussed in the previous four chapters was undertaken for Salt Lake County, Utah. The study is part of a larger project sponsored by the Federal Emergency Management Agency to estimate the damage and loss to this region due to a magnitude 7.5 earthquake on the Wasatch fault (see Applied Technology Council, ATC-36, in progress). The analysis included the estimation and integration of the various seismic hazards due to ground shaking, liquefaction, landslide, and surface fault rupture according to the methodology presented in Chapter 3. A detailed structural inventory of more than 195,000 buildings and about 275 highway bridges was compiled utilizing many of the ideas presented in Chapter 4. Dollar loss, loss-of-function, and casualties were estimated for each facility in the county and then summed at the Census tract level.

## 6.2 Conclusions

The primary objective of this research was the development of a GIS-based methodology for conducting a regional seismic hazard and risk analysis. As part of this overall methodology, two secondary objectives were identified. These included the development of a methodology for combining the various collateral hazards associated with earthquake ground shaking and the development of a methodology and an integrated database design for compiling a comprehensive structural inventory for a large region. In research such as this that involves methodology development, conclusions are typically drawn from the implementation of the methodology in a case study.

The case study in Chapter 5 illustrated the effectiveness of a geographic information system for use in conducting a large regional earthquake hazard and risk analysis. Numerous maps and tables were included in this chapter to show the different types of spatial and tabular data that are stored, manipulated, and displayed in the analysis. Several maps were used to illustrate the different types of summary information or results that can be displayed at various stages in the analysis. The entire analysis, from identifying

the potential seismic sources to computing the final loss estimates, was carried out in the GIS environment according to the various methodologies presented in the earlier chapters of this dissertation.

The hazard integration scheme for combining the secondary effects of liquefaction, landslide, and surface fault rupture proved to be very effective in the GIS environment. The flexibility of the combination methodology will allow improved hazard models, expanded geologic data, and enhanced weighting schemes to be included in future analyses. A structural inventory of about 195,00 buildings and 275 highway bridges was compiled for the study region according to the compilation methodology and integrated database table design developed in this research. These numbers account for roughly 95% of the total inventory of structures in Salt Lake County, Utah. The remaining 5% is comprised primarily of lifeline facilities and public buildings. It was found that the Salt Lake County Tax Assessor's datafile was the most useful source of inventory information as it contained the most accurate and complete data. The other sources should be used to augment the inventory in a minor way and to verify the accuracy of the compiled data.

Although the case study presented in Chapter 5 contained several simplifying assumptions, the final results for damage and loss in the county can be used to check the overall reasonableness of the models and methodologies. For example, the total direct loss for buildings was estimated at about \$12 billion  $\pm$  \$3 billion. This number seems reasonable when compared to previous large earthquakes in metropolitan areas. The expected damage factor for all buildings was estimated at about 38.5%. Wood frame buildings had an expected damage factor of about 16% and unreinforced masonry building had an expected damage factor of about 80%. The unreinforced masonry buildings comprise roughly 25% of the building stock in Salt Lake County. Expected damage of 80% is typically considered a total loss, therefore these results indicate that about 25% of the buildings in Salt Lake County would be destroyed in the assumed magnitude 7.5 earthquake.

The influence of collateral hazards was illustrated in this case study. The expected damage factor for all buildings decreases from about 38.5% to about 27% when the effects of liquefaction, landslide, and surface fault rupture are ignored in the analysis. The total direct loss for all buildings also decreases by about 30%, from \$12.1 billion to \$8.5 billion.

The only indirect loss estimates made in this study involved the time to restore facilities to their full functionality. Few conclusions can be drawn from these results as several factors were not included in the analysis. Loss-of-function is very difficult to estimate and can be influenced by factors such as the availability of natural resources, non-structural and contents damage, financing, and litigation. This case study illustrated how loss-of-function can be estimated in the GIS environment, provided that all of the influencing parameters are stored in the relevant database tables. As models in the area of in-direct losses improve, they can easily be added to the GIS-based seismic hazard and risk analysis.

Although the damage and loss estimates for the buildings in the study region seem reasonable, the results for the highway bridges appear to be too high when compared to those resulting from previous earthquakes in metropolitan areas. The expected damage factor for highway bridges was estimated at about  $90\% \pm 10\%$ . Even for a magnitude 7.5 event, it is unlikely that the majority of the highway bridges would sustain this high level of damage. These results indicate that improved damage and loss models are needed for highway bridges.

The only non-monetary loss considered in the case study was casualties. The total number of major injuries was estimated at about 44,000 and the total number of deaths was estimated at about 7,600. Although these numbers are much higher than those observed during any earthquake in the United States in recent history, they appear reasonable due to the expected amount of building damage. About 52,500 unreinforced masonry buildings were estimated to have a damage factor of about 80%, and over 3,200 buildings were estimated to have 100% damage. The models from which casualty estimates were computed are very simple, but are the only ones currently available due to the lack of empirical data. Improved models are needed that consider factors other than only the amount of damage to the structure. For example, structure type can influence the number of deaths and injuries because different structural systems have different failure modes. Some systems may fail suddenly and catastrophically, others may fail more slowly allowing time for evacuation of occupants.

Sections 6.1 and 6.2 have briefly summarized the main points or ideas contained in each of the previous five chapters of this dissertation. The first four chapters described geographic information system technology, detailed the steps in a regional seismic hazard and risk analysis, and developed the methodology for implementing this analysis in the

GIS environment. The fifth chapter presented a case study that applied this methodology to compute earthquake damage and loss estimates in a large region subject to a scenario event. As in most case studies that serve to illustrate a recently developed methodology, several areas of needed improvement and future research quickly became apparent in Chapter 5. Section 6.3 builds on the conclusions drawn in this study by presenting some recommendations for future work in the area of seismic hazard and risk analysis in the GIS environment.

## 6.3 Future Work

This dissertation covered a very broad topic, therefore several areas of future research can be identified. These areas can be divided into three general categories. The first category concerns the effects of local site conditions, including seismic hazard integration and the treatment of uncertainty. The second area deals with the definitions and models for earthquake damage and loss estimation. The final category concerns the utility of a regional seismic hazard and risk analysis. The remainder of this section is devoted to a discussion of these three areas.

### 6.3.1 Site Effects, Hazard Integration, and Uncertainty

The effects of local site conditions due to seismic excitation are still not well understood. In this dissertation, soil amplification was modeled by a simple multiplication factor, liquefaction and landslide were modeled with a qualitative description of 'high', 'moderate', 'low', or 'very low' potential, and surface fault rupture was characterized by a defined zone of rupture potential. More quantitative models for these site effects that can be applied over a large region are needed. Computational power and storage is becoming less of a concern, therefore models that require three-dimensional soil parameters can and should be implemented in the GIS environment.

A methodology for integrating the various seismic hazards in a GIS-based regional analysis was developed in this dissertation. The hazard models contained several simplifying assumptions in order to illustrate the methodology. Improvements are needed in the models themselves as discussed in the previous paragraph, as well as the quantification of the hazards, i.e., the estimation of the amount of damage to constructed facilities given a certain potential hazard level. The heuristic weighted average approach



to the hazard integration can also be improved. The analysis and modeling capabilities of the GIS provide an ideal environment to conduct sensitivity studies that will help to refine different hazard combination schemes.

Lastly, uncertainty was only briefly discussed in this dissertation. In Chapter 3, one method for treating the uncertainty in soil parameter data was illustrated in a study of soil amplification of ground motions. In dealing with local site effects, uncertainty is present in the spatially-varying soil properties, the models that estimate the potential of these effects to occur, and the models that estimate the resultant damage to structures. Further research is needed in each of these areas, especially to develop methods for treating uncertainty that can be applied over a large region.

### 6.3.2 Earthquake Damage and Loss

Every major earthquake illustrates the need for research in numerous areas dealing with earthquake damage and loss. A discussion of these could fill an entire chapter, however, only a few areas that pertain to the GIS-based regional analysis will be mentioned here. The definition of structural damage and the existing motion-damage relationships are greatly in need of improvement. Damage has typically been defined in terms of percent loss. Although this makes the computation of losses easier, a damage definition based on structural behavior or performance that can be used for all structural types in a large region is needed. The range of percent loss has typically been discretized into several damage states that are independent of engineering or social function class. Damage states should be dependent on the structure type because each structural system has different modes of failure, i.e., moderate damage to a wood frame structure will not be similar in percent loss or structural integrity as moderate damage to an unreinforced masonry structure.

The motion-damage relationships used in this dissertation are based on expert opinion and use Modified Mercalli Intensity (MMI) as the ground motion parameter. Clearly, new relationships are needed that estimate damage as a function of an instrumented ground motion parameter or measured structural response. These relationships are needed not only for buildings, but also for all types of lifeline and non-building facilities, as well as non-structural components such as partition walls.

Dollar loss due to direct structural damage, days to restore to various levels of full functionality, and casualties were the only losses considered in this dissertation. Current loss models are typically based on the damage state or amount of damage to the structure as well as the social function class of the structure. Improved loss models should consider the engineering class of the facility because the type of structural system can often influence the direct, in-direct, and non-monetary losses of the facility. Loss of functionality and other in-direct losses such as clean-up and financing of repairs are very hard to estimate, but each new earthquake provides more empirical data for model development. Improvements to these types of loss models are best made by economists and business managers rather than structural engineers. There are very few models for non-monetary losses such as casualties, unemployment and homelessness. As with indirect loss models, improvements to the non-monetary loss models are best made by sociologists and socio-economists rather than structural engineers.

### 6.3.3 Utility of Regional Analysis

The purpose of the GIS-based regional seismic hazard and risk analysis discussed in this dissertation is to estimate the potential earthquake damage and loss in a given region. Although the focus of this research has been on earthquakes, the GIS-based methodology can be easily applied to other natural and man-made hazards such as hurricanes, tornadoes, flooding, fires, and hazardous material accidents. An analysis such as this is intended to be used for indicating areas or facilities that have the potential for large damage and loss in future events, for allocating emergency resources, for planning locations and construction of future facilities, and for analyzing and comparing regional effects of various retrofit schemes. Microzone maps are typically used as a means of transferring information from the scientific community to the professional community involved in hazard and risk mitigation.

Improvements are needed in the overall regional analysis to make it more beneficial to the intended users. Particularly in the area of emergency management and planning, communication between the end-users and those developing the GIS-based analysis will help define the types of needed results, how the results should be displayed, the speed at which they should be available, the level of desired detail, and other system design specifications. The accuracy and completeness of the results of the analysis depend on the underlying geologic, geographic, and structural databases. Improvements can be made in

the manner that future regional database information is collected by the various government agencies. Here again, improved communication would help to define industry standards for data compilation and storage. Lastly, improved awareness by the political decision makers, as well as the general public, of the utility of a GIS-based regional seismic hazard and risk analysis cannot help but improve the hazard mitigation and emergency response efforts in seismically active regions.

## REFERENCES

---

Agbabian, M. and G. V. Chilingarian (1991). "Earthquakes of the Armenia Highlands (Seismic Setting)." *University of Southern California Report*. Los Angeles, California.

Aki, K. (1988). "Local Site Effects on Strong Ground Motion." *Proceedings of the ASCE Conference on Earthquake Engineering and Soil Dynamics II*. Rolla, Missouri, pages 103-155.

Algermissen, S. T. and K. Steinbrugge (1984). "Seismic Hazard and Risk Assessment: Some Case Studies." *The Geneva Papers on Risk and Insurance*. Volume 9, Number 30.

Anagnos, T. and A. S. Kiremidjian (1984). "Stochastic Time-Predictable Models for Earthquake Occurrences." *Bulletin of the Seismological Society of America*. Volume 74, Number 6, pages 2593-2611.

Anagnos, T. and A. S. Kiremidjian (1988). "A Review of Earthquake Occurrence Models for Seismic Hazard Analysis." *Probabilistic Engineering Mechanics*. Volume 3, Number 1, pages 3-11.

Antenucci, J. C., K. Brown, P. L. Crosswell, M. J. Kevany, and H. Archer (1991). *Geographic Information Systems: A Guide to the Technology*. Van Nostrand Reinhold, New York.

Applied Technology Council (1985). *Earthquake Damage Evaluation Data for California, ATC-13*. Redwood City, California.

Applied Technology Council (1991). *Seismic Vulnerability and Impact of Disruption of Lifelines in the Coterminous United States, ATC-25*. Redwood City, California.

Applied Technology Council (in progress). *Earthquake Losses Evaluation Methodology and Databases for Utah, ATC-36*. Redwood City, California.

Association of Bay Area Governments (ABAG) (1991). "Macroeconomic Effects of the Loma Prieta Earthquake." *ABAG Report*. Oakland, California.

- Boore, D. M., Joyner, W. B., and T. E. Fumal (1993). "Estimation of Response Spectra and Peak Accelerations From Western North American Earthquakes: An Interim Report." *Open File Report 93-509*. United States Geological Survey. Menlo Park, California.
- Borcherdt, R. D. (1990). "Influence of Local Geology in the San Francisco Bay Region, California on Ground Motions Generated by the Loma Prieta Earthquake of October 17, 1989." *Proceedings of the International Symposium on Safety of Urban Life and Facilities*. Tokyo, Japan. November 1-2, 1990, pages 1-35.
- Borcherdt, R., C. M. Wentworth, A. Janssen, T. Fumal, and J. Gibbs (1991). "Methodology for Predictive GIS Mapping of Special Study Zones for Strong Ground Shaking in the San Francisco Bay Region, CA." *Proceedings of the Fourth International Conference on Seismic Zonation*. Stanford, California. August 25-29, 1991. Volume III, pages 545-552.
- Borcherdt, R. D. and G. Glassmoyer (1992). "On the Characteristics of Local Geology and Their Influence on Ground Motions Generated by the Loma Prieta Earthquake in the San Francisco Bay Region, California." *Bulletin of the Seismological Society of America*. Volume 82, Number 2, pages 603-641.
- Boyle, R. and W. Dong (1991). "Using Geographic Information Systems with Embedded Expert Systems and a Coupled Dynamic Database to Perform Seismic Hazard Evaluation." *Proceedings of the Fourth International Conference on Seismic Zonation*. Stanford, California. August 25-29, 1991. Volume III, pages 569-584.
- Campbell, K. W. (1985). "Strong Ground Motion Attenuation Relations: A Ten-Year Perspective." *Earthquake Spectra*. Volume 1, Number 4, pages 759-804.
- Chang, T. S., P. S. Tang, C. S. Lee, and H. Hwang (1991). "Liquefaction Potential in the Memphis Area." *Proceedings of the Fourth International Conference on Seismic Zonation*. Stanford, California. August 25-29, 1991. Volume II, pages 459-466.
- Christian, J. (1980). "Probabilistic Soil Dynamics: State-of-the-Art" *ASCE Journal of Geotechnical Engineering*. Volume 106, Number GT4, pages 385-397.
- Chung, Y. S., C. Meyer, and M. Shinozuka (1987). "Seismic Damage Assessment of Reinforced Concrete Members." *Technical Report NCEER-87-0022*. State University of New York at Buffalo, New York.
- Clough, G. W., J. R. Martin II, and J. L. Chameau (1993). "Lessons Learned from the 1989 Loma Prieta Earthquake: The Geotechnical Aspects." *Proceedings from the Symposium on Practical Lessons from the Loma Prieta Earthquake*. San Francisco, California. March 22-23, 1993.

Dobry, R., I. Oweis, and A. Urzua (1976). "Simplified Procedures for Estimating the Fundamental Period of a Soil Profile." *Bulletin of the Seismological Society of America*. Volume 66, Number 4, pages 1293-1321.

Emmi, P. C. and C. A. Horton (1993). "A GIS-Based Assessment of Earthquake Property Damage and Casualty Risk: Salt Lake County, Utah." *Earthquake Spectra*. Volume 9, Number 1, pages 11-33.

Environmental Systems Research Institute (ESRI) (1992). *Understanding GIS: The Arc/Info Method*. Redlands, California.

Faccioli, E. (1972). "A Stochastic Model for Predicting Seismic Failure in a Soil Deposit." *Earthquake Engineering and Structural Dynamics*. Volume 1, pages 293-307.

Faccioli, E. (1976). "A Stochastic Approach to Soil Amplification." *Bulletin of the Seismological Society of America*. Volume 66, Number 4, pages 1277-1291.

Fenton, G. A. and E. H. Vanmarcke (1991). "Liquefaction Risk Assessment: 3-D Modeling." *Proceedings of the Fourth International Conference on Seismic Zonation*. Stanford, California. August 25-29, 1991. Volume II, pages 669-676.

FICCDC Technology Working Group (1988). "A Process For Evaluating Geographic Information Systems." *Technical Report 1, Open-File Report 88-105*. United States Geological Survey. Washington, DC.

French, S. P., J. C. Castanon, and A. Hanson (1991). "A Knowledge-Base Approach to Using Existing Data for Seismic Risk Assessment." *Department of City and Regional Planning Report*. California Polytechnic State University, San Luis Obispo, California. December, 1991.

Frost, J., J. Chameau, and R. Luna (1992). "Geographic Information Systems in Earthquake Hazard Analyses." *Proceedings of the ASCE Specialty Conference on Computing in Civil Engineering*. Dallas, Texas. June, 1992. pages 452-459.

Hansen, A. and C. A. M. Franks (1991). "Characteristics and Mapping of Earthquake Triggered Landslides for Seismic Zonation." *Proceedings of the Fourth International Conference on Seismic Zonation*. Stanford, California. August 25-29, 1991. Volume I, pages 149-195.

Ho, C. L., K. Kornher, and G. Tsiatas (1991). "Ground Motion Model for Puget Sound Cohesionless Soil Sites." *Earthquake Spectra*. Volume 7, Number 2, pages 237-266.

Hong, H. P. and E. Rosenblueth (1987). "Seismic Spectra on Soil with Uncertain Properties." *Earthquake Engineering and Structural Dynamics*. Volume 15, pages 911-920.

Hryciw, R. D., K. M. Rollins, M. Homolka, S. E. Shrewbridge, and M. McHood (1991). "Soil Amplification at Treasure Island During the Loma Prieta Earthquake." *Proceedings of the Second International Conference on Recent Advances in Geotechnical Earthquake Engineering and Soil Dynamics*. St. Louis, Missouri. March 11-15, 1991.

Idriss, I. M. (1990). "Response of Soft Soil Sites During Earthquakes." *Proceedings of the Memorial Symposium to Honor Professor H. Bolton Seed*. Berkeley, California. May 10-11, 1990.

Iwasaki, T., K. Tokida, F. Tatsuoka, S. Watanabe, S. Yasuda, and H. Sato. (1982). "Microzonation for Soil Liquefaction Using Simplified Methods." *Proceedings of the Third International Earthquake Microzonation Conference*. Seattle, Washington. Volume 3, pages 1319-1330.

Jensen, J. R. and E. J. Christensen (1986). "Solid and Hazardous Waste Disposal Site Selection Using Digital Geographic Information System Techniques." *The Science of the Total Environment*. Volume 56, pages 265-276.

Joyner, W. B. and D. Boore (1988). "Measurement, Characterization, and Prediction of Strong ground Motion." *Proceedings of the ASCE Conference on Earthquake Engineering and Soil Dynamics II*. Rolla, Missouri. pages 43-102.

Joyner, W. B. and A. T. F. Chen (1975). "Calculation of Nonlinear Ground Response in Earthquakes." *Bulletin of the Seismological Society of America*. Volume 65, Number 5, pages 1315-1336.

Journel, A. G. (1989). "Fundamentals of Geostatistics in Five Lessons." *American Geophysical Union Short Course in Geology: Volume 8*. Washington, DC.

Journel, A. and Huijbregts, C. (1978). *Mining Geostatistics*. Academic Press. London, U. K.

Juang, C. H. and D. J. Elton (1991). "Use of Fuzzy Sets for Liquefaction Susceptibility Zonation." *Proceedings of the Fourth International Conference on Seismic Zonation*. Stanford, California. August 25-29, 1991. Volume II, pages 629-636.

Kanai, K. (1957). "Semi-Empirical Formula for the Seismic Characteristics of the Ground." *Bulletin of the Earthquake Research Institute, University of Tokyo*. Volume 32, Number 2, pages 309-325.

Kausel, E. and J. M. Roësset (1984). "Soil Amplification: Some Refinements." *Soil Dynamics and Earthquake Engineering*. Volume 3, Number 3, pages 116-123.

Kim, S. H., M. P. Gaus, G. Lee, and K. C. Chang (1992). "A GIS-Based Regional Risk Approach for Bridges Subjected to Earthquakes." *Proceedings of the ASCE Specialty*

*Conference on Computing in Civil Engineering*. Dallas, Texas. June, 1992. pages 460-467.

King, S. A. and A. S. Kiremidjian (1993). "GIS for Regional Seismic Hazard and Risk Analyses." *Proceedings of the NSF workshop on Geographic Information Systems and their Application in Geotechnical Earthquake Engineering*. Atlanta, Georgia. January 28-29, 1993, pages 56-60.

King, S. A. and A. S. Kiremidjian (1993). "Uncertainties in the Dynamic Response of Soils in the San Francisco Bay Region." *Proceedings of the Sixth International Conference on Structural Safety and Reliability*. Innsbruck, Austria. August 9-13, 1993.

King, S. A., A. S. Kiremidjian, R. D. Borcherdt, and C. M. Wentworth (1993). "GIS Mapping of Earthquake Ground Shaking in San Francisco, California." *Proceedings of the ASCE Structures Congress '93*. Irvine, California. April 19-21, 1993. Volume I, pages 259-264.

Kircher, C. A. and M. W. McCann (1983). "Appendix A: Development of Seismic Fragility Curves For Sixteen Types of Structures Common to Cities of the Mississippi Valley Region." *Jack Benjamin and Associates Report*. Mountain View, California.

Kiremidjian, A. S. (1984). "Reliability of Structures Subjected to Differential Fault Slip." *Earthquake Engineering and Structural Dynamics*. Volume 12, pages 603-618.

Kiremidjian, A. S. (1992). "Methods for Regional Damage Estimation." *Proceedings of the 10th World Conference on Earthquake Engineering*. Madrid, Spain. July 19-24, 1992. Invited paper.

Kiremidjian, A. S. and T. Anagnos (1984). "Stochastic Slip-Predictable Model for Earthquake Occurrences." *Bulletin of the Seismological Society of America*. Volume 74, Number 2, pages 739-755.

Kiremidjian, A. S., S. A. King, M. Sugito, and H. C. Shah (1991). "Simple Site-Dependent Ground Motion Parameters for the San Francisco Bay Region." *The John A. Blume Earthquake Engineering Center Report No. 97*. Department of Civil Engineering, Stanford University. Stanford, California.

Kurt, C. E., K. Mohyuddin, and B. Guo (1992). "A Comparison of Geographical Information Systems." *Proceedings of the ASCE Specialty Conference on Computing in Civil Engineering*. Dallas, Texas. June, 1992. pages 17-24.

Luna, R. (1993). "Liquefaction Analysis in a GIS Environment." *Proceedings of the NSF workshop on Geographic Information Systems and their Application in Geotechnical Earthquake Engineering*. Atlanta, Georgia. January 28-29, 1993. pages 65-71.



Lutz, K. A. and A. S. Kiremidjian (1993). "A Generalized Semi-Markov Process for Modeling Spatially and Temporally Dependent Earthquakes." *The John A. Blume Earthquake Engineering Center Report No. 104*. Department of Civil Engineering, Stanford University. Stanford, California.

Martel, R. R. (1964). "Earthquake Damage to Type III Buildings in Long Beach, 1933." *Earthquake Investigations in the Western United States, 1931-1964. Publication 41-2*. U.S. Department of Commerce, Coast and Geodetic Survey. Washington, DC.

Martin, P. P. and H. B. Seed (1978). "MASH - A Computer Program for the Non-Linear Analysis of Vertically Propagating Shear Waves in Horizontally Layered Deposits." *Earthquake Engineering Research Center Report 78-23*. University of California, Berkeley.

Massachusetts Civil Defense Agency (1989). *Metropolitan Boston Area Earthquake Loss Study*. URS/Blume Report. San Francisco, California.

McLaren, M. (1992). "GIS Prepares Utilities for Earthquakes." *GIS World*. Volume 5, Number 4, pages 60-64.

Mohraz, B. (1976). "A Study of Earthquake Response Spectra for Different Geological Conditions." *Bulletin of the Seismological Society of America*. Volume 66, Number 3, pages 915-935.

Newmark, N. M. and E. Rosenblueth (1971). *Fundamentals of Earthquake Engineering*. Prentice-Hall, Inc. Englewood Cliffs, New Jersey.

Ohsaki, Y. (1982). "Dynamic Characteristics and One-Dimensional Linear Amplification Theories of Soil Deposits." *Department of Architecture Research Report 82-01*. University of Tokyo. Tokyo, Japan.

Parent, P. and R. Church (1987). "Evolution of Geographic Information Systems as Decision Making Tools." *Proceedings of the GIS '87 Conference*. San Francisco, CA. October, 1987.

Park, Y.-J., and A. H.-S. Ang (1985). "Seismic Damage Analysis of Reinforced Concrete Buildings." *ASCE Journal of Structural Engineering*. Volume 111, Number 4, pages 740-757.

Pyke, R. M. (1979). "Nonlinear Soil Models for Irregular Cyclic Loadings." *ASCE Journal of the Geotechnical Engineering Division*. Volume 105, Number GT6, pages 715-726.

Reitherman, R. (1985). "A Review of Earthquake Damage Estimation Methods." *Earthquake Spectra*. Volume 1, Number 4, pages 805-847.

Rentzis, D. N., A. S. Kiremidjian, and H. C. Howard (1992). "Identification of High Risk Areas Through Integrated Building Inventories." *The John A. Blume Earthquake Engineering Center Report No. 98*. Department of Civil Engineering, Stanford University. Stanford, California.

Ripple, W. J., editor (1989). *Fundamentals of Geographic Information Systems: A Compendium*. American Society for Photogrammetry and Remote Sensing and American Congress on Surveying and Mapping, Maryland.

Rojahn, Christopher (1993). Estimation of Earthquake Damage to Buildings and Other Structures in Large Urban Areas. *Proceedings of the Geohazards International / Oyo Pacific Workshop*. Istanbul, Turkey. October 8-11, 1993.

Schnabel, P. B., J. Lysmer, and H. B. Seed (1972). "SHAKE - A Computer Program for Earthquake Response Analysis of Horizontally Layered Sites." *Earthquake Engineering Research Center Report 72-12*. University of California, Berkeley.

Seale, S. H. and R. J. Archuleta (1989). "Site Amplification and Attenuation of Strong Ground Motion." *Bulletin of the Seismological Society of America*. Volume 79, Number 6, pages 1673-1696.

Seed, H. B. and I. M. Idriss (1971). "Simplified Procedure for Evaluating Liquefaction Potential." *ASCE Journal of the Soil Mechanics and Foundation Division*. Volume SM9, pages 1249-1273.

Seed, H. B., C. Ugas, and J. Lysmer (1976). "Site-Dependent Spectra for Earthquake Resistant Design." *Bulletin of the Seismological Society of America*. Volume 66, Number 1, pages 221-243.

Seed, R. B., S. E. Dickenson, M. F. Riemer, J. D. Bray, N. Sitar, J. K. Mitchell, I. M. Idriss, R. E. Kayen, A. Kropp, L. F. Harder Jr., and M. S. Power (1990). "Preliminary Report on the Principal Geotechnical Aspects of the October 17, 1989 Loma Prieta Earthquake." *Earthquake Engineering Research Center Report 90-05*. University of California, Berkeley.

Shah, H. C. (1993). *Personal communication*.

Smith, T. R., S. Menon, J. L. Star, and J. E. Estes (1987). "Requirements and Principles for the Implementation and Construction of Large-scale Geographic Information Systems." *International Journal of Geographic Information Systems*. Volume 1, Number 1, pages 13-31.

Steinbrugge, K. V., S. T. Algermissen, H. J. Lagorio, L. S. Cluff, and H. J. Degenkolb (1981). "Metropolitan San Francisco and Los Angeles Earthquake Loss Studies: 1980 Assessment." *Open File Report 81-113*. United States Geological Survey. Menlo Park, California.

Susuki, S. and A. S. Kiremidjian (1988). "A Stochastic Ground Motion Forecast Model with Geophysical Considerations." *The John A. Blume Earthquake Engineering Center Report No. 88*. Department of Civil Engineering, Stanford University. Stanford, California.

Thomson, W. T. (1950). "Transmission of Elastic Waves Through a Stratified Solid Medium." *Journal of Applied Physics*. Volume 21.

Trifunac, M. D. (1976). "Preliminary Analysis of the Peaks of Earthquake Strong Ground Motion - Dependence of Earthquake Peaks on Earthquake Magnitude, Epicentral Distance, and Recording Site Conditions." *Bulletin of the Seismological Society of America*. Volume 66, Number 1, pages 189-219.

Trifunac, M. D. and Brady, A. G. (1975). "On the Correlation of Seismic Intensity with Peaks of Recorded Strong Ground Motion." *Bulletin of the Seismological Society of America*. Volume 65, Number 1, pages 139-162.

Tsai, N. C. and G. W. Housner (1970). "Calculations of Surface Motions of a Layered Half-Space." *Bulletin of the Seismological Society of America*. Volume 60, Number 5, pages 590-616.

Usery, E. L., P. Altheide, R. R. P. Deister, and D. J. Barr (1988). "Knowledge-Based GIS Techniques Applied to Geological Engineering." *Photogrammetry Engineering and Remote Sensing*. Volume 54, Number 11, pages 1623-1628.

Vanmarcke, E. H. (1977). "Probabilistic Modeling of Soil Profiles." *ASCE Journal of Geotechnical Engineering*. Volume 103, Number GT11, pages 1227-1246.

Vasudevan, R., A. S. Kiremidjian, and H. C. Howard (1992). "An Integrated Inventory Methodology for Seismic Damage Assessment." *The John A. Blume Earthquake Engineering Center Report No. 102*. Department of Civil Engineering, Stanford University. Stanford, California.

Wieczorek, G. F., R. C. Wilson, and E. L. Harp (1985). "Map Showing Slope Stability During Earthquakes in San Mateo County, California." *Map I-1257-E*. United States Geological Survey. Menlo Park, California.

Whitman, R. V. (1973). "Damage Probability Matrices for Prototype Buildings." *Department of Civil Engineering Research Report R73-57*. Massachusetts Institute of Technology. Cambridge, Massachusetts.

Whitman, R. V., editor (1992). Proceedings from the Site Effects Workshop, October 24-25, 1991. *Technical Report NCEER-92-0006*. State University of New York at Buffalo, New York.

Wilson, R. C. and D. K. Keefer (1985). "Predicting Areal Limits of Earthquake Induced Landsliding." *Evaluating Earthquake Hazards in the Los Angeles Region, Professional Paper 1360*. United States Geological Survey. Pasadena, California, pages 317-493.

Youd, T. L. (1991). "Mapping of Earthquake-Induced Liquefaction for Seismic Zonation." *Proceedings of the Fourth International Conference on Seismic Zonation*. Stanford, California. August 25-29, 1991. Volume I, pages 111-147.